

REMOVAL OF SELECTED PHARMACEUTICALS FROM AQUEOUS MATRICES WITH ACTIVATED CARBON

PhD dissertation

Mohammed Elabadsa

Supervisor: Dr. Viktor G. Mihucz, associate professor

Department of Analytical Chemistry

Eötvös Loránd University



Doctoral School of Environmental Science

Head of the School: Prof. Dr. Imre Jánosi

Environmental Chemistry Doctoral Program

Head of the Program: Prof. Dr. Tamás Turányi

Eötvös Loránd University

Cooperative Research Center for Environmental Sciences

Budapest

2020

Table of contents

List of abbreviations	5
Chapter 1. Introduction	8
Chapter 2. Objectives	8
Chapter 3. Literature overview	11
3.1 Chemical structure and properties of the investigated three pharmaceutical compounds	11
3.1.1 Carbamazepine	11
3.1.2 Diclofenac	12
3.1.3 Naproxen	12
3.2 Emerging contaminants, pharmaceuticals and personal care products in the aquatic environment	14
3.3 Occurrence of the three target compounds in living organisms	26
3.4 Methods for the determination of pharmaceutical compounds	29
3.5 Removal of pharmaceutical compounds from aqueous environment by adsorption	31
3.5.1 Conventional adsorption materials	36
3.5.1.1 Activated carbon	36
3.5.1.2 Polymeric adsorbents	41
3.5.1.3 Zeolites	42
3.5.2 Adsorption modeling in batch condition	42
3.5.2.1 Linear isotherm	43
3.5.2.2 Freundlich isotherm model	43
3.5.2.3 Langmuir isotherm model	44
3.5.2.4 Temkin isotherm model	44
3.5.2.5 Dubinin-Radushkevich isotherm model	44
3.5.2.6 Redlich-Peterson model	45
3.5.3 Adsorption kinetics	45
3.5.3.1 Pseudo first order kinetics	46
3.5.3.2 Pseudo second order kinetics	46

3.5.3.3	Elovich model	46
3.5.3.4	Intra-particle diffusion model	47
3.5.4	Adsorption thermodynamics	47
3.5.5	Removal of PPCPs from aqueous environment in flow condition	48
3.5.6	Modeling of fixed-bed adsorption	50
3.5.6.1	Thomas model	50
3.5.6.2	Yoon-Nelson model	50
3.5.6.3	Adams-Bohart model	51
Chapter 4. Removal of selected pharmaceuticals from aqueous matrices with activated carbon under batch conditions		52
4.1.	Experimental part	52
4.1.1	Chemicals	52
4.1.2	Characterization of GAC	52
4.1.3	Adsorption equilibrium experiments and HPLC analysis	54
4.1.4	Thermodynamic experiments and modeling	54
4.1.5	Experimental conditions of kinetic analyses	57
4.1.6	Study of model solutions and secondary sewage water in semi open system	57
4.2	Result and discussion	59
4.2.1	Characterization of charcoal	59
4.2.2	Adsorption isotherms studies and modeling	63
4.2.3	Thermodynamic studies and modeling	64
4.2.4	Kinetic studies and modeling	68
4.2.5	Model solutions and secondary sewage water in semi open system	72
4.2.6	Adsorption mechanism	77
4.3	Conclusions	80
Chapter 5. Removal of selected pharmaceuticals from aqueous matrices with activated carbon under flow conditions		81
5.1	Experimental part	81
5.1.1	Chemicals	81
5.1.2	Set-up of the flow system	81
5.1.3	Sampling of test solutions and model sewage water for HPLC-UV analysis	84

5.1.4	Investigation of secondary sewage water	84
5.1.5	HPLC-UV and UHPLC-MS method performance	86
5.2	Results and discussion	87
5.2.1	HPLC method performance	87
5.2.2	Results obtained for model solutions	87
5.2.3	Comparison of adsorption for sewage water with model solutions	89
5.2.4	Modeling of fixed-bed experiments	95
5.3	Conclusions	98
Chapter 6. Summary		99
Chapter 7. New results		100
	SCI publications constituting the basis of the present dissertation	102
	Acknowledgements	103
	References	104

List of abbreviations

AC	activated carbon
APIs	active pharmaceutical ingredients
ATR FT-IR	attenuated total reflection -Fourier-transform infrared
BET	Brunauer-Emmett-Teller
BJH	Barrett, Joyner and Halenda
BSE	back scattered electron
C	outlet concentration
C ₀	inlet concentration
C _{max}	maximum concentration
C C ₀ ⁻¹	outlet-to-inlet concentration ratio
COX	cyclooxygenase
CRB	carbamazepine
d	inner diameter of column
DAD	diode-array detector
DCL	diclofenac
DLLME	dispersive liquid-liquid microextraction
DR	Dubinini-Radushkevich
d.w.	dry weight
ECs	emerging contaminants
FPSE	fabric phase sorptive extraction
GAC	granulated activated carbon
GC-MS	gas chromatography mass spectrometry
GO	graphene oxide
h	height of fixed-bed
HLB	hydrophilic-lipophilic balance
HPLC	high performance liquid chromatography

HRMS	high-resolution mass spectrometry
i.d.	internal diameter
IPD	intra-particle diffusion
IUPAC	International Union of Pure and Applied Chemistry
K_a	dissociation constant
K_{ow}	octanol/water partition coefficient
LC	liquid chromatography
LC ₅₀	lethal dose at 50% (median lethal dose)
LC-MS	liquid chromatography mass spectrometry
LC-MS/MS	liquid chromatography tandem mass spectrometry
LLE	liquid liquid extraction
LOEC	lowest observed effect concentration
LOQ	limits of quantification
LSV	linear sweep voltammetry
MDL	method detection limit
MSW	model sewage water
MTZ	mass transfer zone
n.d.	not detected
NOEC	no observed effect concentration
NSAIDs	non-steroidal anti-inflammatory drugs
NPR	naproxen
OECD	Organisation for Economic Co-operation and Development
PAC	powdered activated carbon
PFO	pseudo first order
PPCPs	pharmaceuticals and personal care products
PSO	pseudo second order
q_m	maximal adsorbed amount

QuEChERS	A quick, easy, cheap, effective, rugged, and safe approach
Q-TOF-MS	quadrupole–time of flight mass spectrometer
R–P	Redlich–Peterson
RP-HPLC	reverse-phase high performance liquid chromatography
RQs	risk quotients
RSD	relative standard deviation
SAC	saturation adsorption capacity
SEM	scanning electron microscopy
SEM-EPMA	scanning electron microscope–electron probe microanalysis
SBSE	stir bar sportive extraction
SMX	sulfamethoxazole
SPE	solid phase extraction
SPME	solid phase microextraction
SSW	secondary sewage water
STPs	sewage treatment plants
t_b	breakthrough time
t_{ex}	exhaustion time
TN	total nitrogen
TOC	total organic carbon
TVFM	theory of volume filling of micropores
UAE-SPME	ultrasound-assisted extraction combined with solid-phase microextraction
UHPLC	ultra-high performance liquid chromatography
US EPA	United States Environmental Protection Agency
UV	ultraviolet
WW	wastewater
WWTPs	wastewater treatment plants

Chapter 1

Introduction

Globally, more than 100,000 tons of pharmaceuticals are consumed every year [1]. In the European Union, consumption of pharmaceuticals per capita has tripled between 2000 and 2014, their production reached 258,000 tons in 2017 [2-3]. The main part of the consumed pharmaceuticals is discharged into wastewater (WW). Effluents from wastewater treatment plants (WWTPs) have been identified as the major sources of these pharmaceuticals in the environment due to their limited removal efficiencies, depending on the physico-chemical characteristics of the drugs and type of WW treatment technologies [4-7]. Consequently, their residues can be transported into the environment. Because of their low biodegradability, continuous release, stability, high persistence in nature, facile bioaccumulation and ecotoxicological effects on terrestrial and aquatic organisms [6, 8] pharmaceuticals have been categorized as hazardous pollutants [4, 9-11]. The presence of these emerging contaminants in the aquatic environment has become a serious concern in recent years [5, 12-13]. Accordingly, in the European Union, four active pharmaceutical ingredients had been included into the Watch List of substances for Union wide monitoring in the field of water policy established by 2015/495 Commission implementing decision (EU) [14-15].

Many studies reported the presence of pharmaceutical compounds in different aquatic systems [4, 16-18]. The environmental levels of pharmaceuticals varied from the ng L^{-1} to $\mu\text{g L}^{-1}$ concentration level according to their media and discharge patterns and their usage pattern [19-20]. Lately, antibiotics, antidepressants, beta blockers, hormones, lipid regulators, diagnostic contrast media, antineoplastic, non-steroidal anti-inflammatory drugs (NSAIDs) such as naproxen (NPR) and diclofenac (DCL), as well as the anticonvulsant carbamazepine (CRB) - among other compounds, have been detected in surface water, groundwater, WW, and even in drinking water at concentrations ranging from ng L^{-1} to $\mu\text{g L}^{-1}$ [4, 6]. Among the 71 PPCPs in African and European freshwater samples determined by Fekadu et al., the top ten most frequently quantified compounds were sulfamethoxazole (SMX), CRB, DCL, trimethoprim, ibuprofen, NPR, paracetamol, ketoprofen, venlafaxine and clarithromycin [4]. Among these drugs, CRB deserves special attention because of its very poor removal efficiency and high concentrations in WWTP effluents [6, 21]. That is why CRB can be determined even in tap water in Budapest [22]. The NSAID DCL included in the Watch List of substances for which Union-wide monitoring data are to be gathered

[15] is also of great importance together with NPR, this latter being one of the pharmaceuticals having the highest reported concentrations in aquatic environment and WW [4]. In Hungary, the most frequently prescribed NSAIDs were DCL and NPR in 2018 [23]. The three aforementioned drugs are very widely used in EU, and often occurred in higher concentrations than their ecotoxicological levels all over the world [4].

A great variety of technologies has been developed for the removal of these contaminants in water such as biological degradation, advanced oxidation and physical adsorption processes. One of the most effective methods to eliminate contaminants from the aqueous phase is adsorption onto different sorbent materials. Several novel adsorbents such as graphene, graphene oxide (GO), carbon nanotubes [24-28] have been developed for removal of different hazardous materials. Nevertheless, adsorption onto granulated activated carbon (GAC) has been preferred for removal of pharmaceutical from aqueous matrices [24, 29-31].

Chapter 2

Objectives

The primary aim of this dissertation was to study the relationship between adsorption properties of GAC and physicochemical characteristics of pharmaceuticals under batch conditions. Another objective was to study the breakthrough curves for the target pharmaceuticals to approach operating conditions closer to the industrial application. Thus, study of adsorption of diclofenac (DCL), naproxen (NPR) and carbamazepine (CRB) from aqueous matrices onto a commercially available granulated activated carbon under both batch and continuous conditions was aimed as follows:

For batch conditions:

1. Study of the relationship between the adsorption properties (i.e. pore size and availability) of GAC and chemical characteristics of pharmaceuticals having different physico-chemical characteristics.
2. Study of the adsorption isotherms experimentally and by modeling.
3. Study of the kinetic behaviour of adsorption experimentally and by modeling.
4. Study of the temperature dependence of the adsorption process experimentally and by modelling.
5. Method proposal (i.e. semi-open system) to investigate adsorption of low-water soluble compounds (i.e. CRB) and potential interferences among the target compounds in model aqueous solutions.

For flow conditions:

1. Investigation of the effect of the initial pharmaceutical concentration, adsorbent dosage and volumetric flow rate.
2. Study of the breakthrough curves for the three pharmaceuticals using GAC in a fixed-bed column system at conditions similar to industrial application.
3. Study of the effect of flow rate and GAC mass, as well as GAC particle size on the breakthrough curve.
4. Comparison of adsorption from model solutions with secondary sewage water (SSW) using the designed fixed-bed technique.
5. Optimization of the adsorption parameters by application of a mathematical model for both model solutions and SSW.

Chapter 3

Literature overview

3.1 Chemical structure and properties of the investigated three pharmaceutical compounds

Two of the target compounds to be tested in sewage samples, i.e. DCL and NPR, are the two most frequently prescribed NSAIDs in Hungary, while CRB is used mostly in psychiatry. The NSAIDs are anti-inflammatory agents, which do not act on receptors for steroid hormones. The structure and physical parameters of the investigated compounds are summarized in Table 3.1.

3.1.1 Carbamazepine

Carbamazepine is widely used for the treatment of various types of seizures and pain resulting from trigeminal neuralgia. It is used to treat patients with acute mania, partial onset seizure epilepsy, partial seizures with secondary generalization, mixed manic depressive episodes, generalized tonic alcohol withdrawal syndrome and restless legs syndrome [32].

The structural formula of CRB is shown in Table 3.1 [33]. It belongs to the class of dibenzazepines and in its molecule two benzene rings are connected by an azepine ring. Its IUPAC name is benzo[b][1]benzazepine-11-carboxamide. The molecular weight of CRB is 236.269 g mol⁻¹. Its formulations are called Epitol, Finlepsin, Neurotol, Tegretol and Amizepine [32].

Carbamazepine is a white to off-white powder. It is very poorly soluble in water, the water solubility data available in the literature are between 0.112 mg L⁻¹ – 35 mg L⁻¹. This is an apolar compound, its acid dissociation constant is pK_a= 7.0. It does not hydrolyze under environmental conditions. This compound is only slightly soluble in ethanol or glacial acetic acid but soluble in methanol, chloroform, dimethylformamide and ethylene glycol monomethyl ether.

Presumably, CRB inhibits the voltage-dependent Na⁺ channels in the membrane of nerve cells [34]. In the case of overdose, neuromuscular disturbances, mild cardiovascular disorders, respiratory depression and vomiting are observable [32].

3.1.2 Diclofenac

Diclofenac is a NSAID. It is used for treatment of acute and chronic pain and inflammation. It has also analgesic, antipyretic, and platelet-inhibitory actions. It is used also to treat patients with inflammatory reaction, operation site inflammation, inflammatory disease of the oral cavity or throat, ocular inflammatory conditions, conjunctivitis, acute musculoskeletal injury, localized soft tissue rheumatism, rheumatoid arthritis, acute gouty arthritis, acute migraine [32].

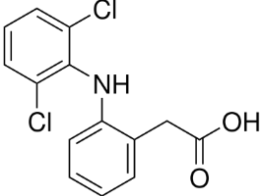
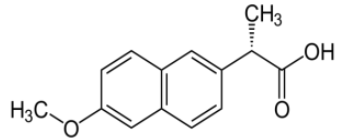
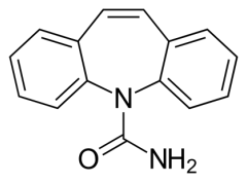
The chemical structure of DCL is shown in Table 3.1 [33]. Diclofenac is a phenyl acetic acid derivative. It belongs to the class of dichlorobenzenes, its UPAC name is 2-[2-(2,6-dichloroanilino) phenyl] acetic acid. The molecular weight of diclofenac is $296.148 \text{ g mol}^{-1}$. It is sold under several trade names such as Diclofenaco, Diclofenacum, Feloran, Novapirina, Orthofen, Orthophen, Ortofen, Voltaren and Voltarol [32]. Diclofenac is used in medicines in the form of sodium (Pennsaid, Solaraze), or potassium (Cataflam) salts or as DCL diethylamine or diclofenac epolamine.

The NSAIDs act in a similar way by binding and chelating both isomorphs (COX-1 and COX-2) of the enzyme cyclooxygenase (COX). Diclofenac is a COX inhibitor; it combines with COX preventing its substrate-enzyme combination with arachidonic acid and formation of pro-inflammatory-prostaglandins. This may be the explanation of its analgesic, antipyretic, and platelet-inhibitory actions. Symptoms of overdose are respiratory depression, vomiting, chest pain, gastrointestinal bleeding, rarely hypertension and acute renal failure [32].

3.1.3 Naproxen

Naproxen is a non-selective NSAID. It can effectively treat acute pain for example related to rheumatic diseases. This medicine is used in the case of headaches, migraine, toothache, backache, fevers, arthritis, ankylosing spondylitis, dysmenorrhea, bursitis, tendinitis, etc. [32]. The molecular weight of NPR is $230.259 \text{ g mol}^{-1}$. Its UPAC name is (2S)-2-(6-methoxynaphthalen-2-yl)propionic acid. The chemical structure of NPR can be seen in the Table 3.1 [33].

Table 3.1 Structural formula and chemical/physical characteristics of DCL, NPR and CRB

Compound	Chemical structure	Water solubility	Molecular mass	Acidity	Vapor pressure	Henry's law constant	Polarity
		[Ref]		[Ref]	[Ref]	[Ref]	[Ref]
		mg L ⁻¹	g mol ⁻¹	pK _a	mm Hg at 25 °C	atm·m ³ mol ⁻¹	lgP
Diclofenac		2.37 [37]	296.148	3.99 [42]	6.14·10 ⁻⁸ [38]	4.73·10 ⁻¹² [38]	4.51 [33]
Naproxen		15.9 [39]	230.259	4.19 [44]	1.89·10 ⁻⁶ [40]	3.39·10 ⁻¹⁰ [40]	3.18 [44]
Carbamazepine		18.0 [41]	236.269	7.00 [33]	1.84·10 ⁻⁷ [43]	1.08·10 ⁻⁷ [43]	2.20 [33]

It belongs to the class of naphthalenes. Its main trade marks are Aprolag, Naproxène, Naproxeno, Naproxenum, Aleve, Anaprox, Methoxypropioicin, Naprosin, Naprosyn, Naproxen Sodium, Proxen, Sodium Naproxenate and Synflex [32].

Naproxen is a white to off-white crystalline powder. Its melting point is 153 °C. Its solubility in water is low, 15.9 mg mL⁻¹ at 25 °C. It is slightly soluble in ether, soluble in methanol and chloroform. It has acidic character, its dissociation constant is pK_a = 4.19. It is optically active [35], its specific optical rotation: +66 deg at 25 °C/D (in chloroform). In the vapor phase, this compound is degraded by reaction with photochemically produced hydroxyl radicals with 0.8 - 4 hours half-life [36].

The explanation of its therapeutic effect is that NPR also inhibits COX-1 and COX-2 enzymes, resulting in decreased formation of precursors of prostaglandins and thromboxanes.

3.2 Emerging contaminants, pharmaceuticals and personal care products in the aquatic environment

Emerging contaminants (ECs) are synthetic or naturally occurring chemicals or any microorganisms that are not commonly monitored in the environment [45]. Emerging contaminants include pharmaceuticals, personal care products (PPCPs), pesticides, herbicides, endocrine disrupting compounds, surfactants, flame-retardants and industrial additives. Pharmaceuticals are used primarily to prevent or treat human and animal disease, whereas personal care products are used to improve quality of daily life and include products such as moisturizers, lipsticks, shampoos, hair colors, deodorants and toothpastes [46]. Pharmaceutical industry produces annually large amounts of these active pharmaceutical ingredients (APIs).

These APIs are absorbed by human body through drug consumption or through skin by externally applied products. A significant part of the active ingredient of drugs consumed is excreted into faeces and urine together with their by-products [47] and finally into WW. There are three main pathways by which APIs can be released into environment. The main pathways are manufacturing (pharmaceutical and cosmetic industries), consumption and, finally waste management (e.g. expired medicine, hospitals, animal waste, research activities). The major pathway for APIs and their metabolites to enter the WW is through municipal sewage.

Effluents from WWTPs, hospital WW discharges have been identified as major sources for these pharmaceuticals in the environment [48-61]. For example, 559 APIs or their metabolites have

been identified in WW influent, effluent and sludge [49] because PPCPs are not completely removed during conventional WW treatment processes, and consequently, they are ubiquitously present in water at trace concentration levels ranging from a few ng L^{-1} to several $\mu\text{g L}^{-1}$ [6, 62-65]. Composition of WWTP influent and effluent depends on consumption of medicines, their prices, seasonal variations [66], choice of the individual medicine, prescription rates in the given country [4]. Concentration of drugs measured downstream of a WWTP also depends on the different consumption rates of these medicines in the given settlement [67]. Direct discharge of animal farm WW is also an important contamination source [4]. Discharge of drug manufacturers also causes environmental contamination [68]. Occupational exposure is also possible through inhalation and dermal contact at the sites where these compounds are produced or used.

Removal efficiencies of PPCPs are highly variable, ranging from 12.5 to 100% depending on properties of the drug in question and operating conditions of WWTP [7, 69]. Conventional treatments have been reported to be ineffective in removal of several pharmaceuticals [70-71] with an efficiency of <40%, or negative efficiency values can also be found in the literature [6, 69, 72-73]. For example, in the case of CRB and NPR, negative removal efficiency values are due to metabolite reversal to parent compound or desorption from organic matter [18, 74-75].

In recent years, many papers reported on occurrence of PPCPs in the aquatic environment such as groundwater [76], rivers [77-79] lakes [80] and sea [81-82]. Deo et al. found 93 different PPCPs that have been reported to contaminate surface waters in the USA according to a metadata analysis. The most frequently detected drugs were antibiotics and antidepressants [83]. According to their results, maximal detected concentrations in surface water in USA for DCL, NPR and CRB were 42 ng L^{-1} and 107 ng L^{-1} and 1238 ng L^{-1} , respectively. Wang et al. evaluated occurrence of 36 PPCPs in urban river water samples in China, the median concentration of the 28 detected PPCPs were in the range of $0.16 - 164 \text{ ng L}^{-1}$ [84]. Antibiotic was the predominant class detected. Naproxen and CRB median concentrations were 1.04 and 5.11 ng L^{-1} in river water samples, while maximal measured values were 3.5 ng L^{-1} and 21.3 ng L^{-1} , respectively. In another study, occurrence of 34 PPCPs in the aquatic environment of Pearl River Delta in China was studied. Thus, 9, 21, 14, and 28 PPCPs were detected in water, sediments, aquatic organisms and fish feeds, respectively [17]. In water samples, six antibiotics, two anti-inflammatory drugs (paracetamol and ketoprofen) and one antihistaminic were detected. Diclofenac, NPR and CRB were not detected in those samples. Also in China, a separate study was conducted in a drinking water treatment plant

to detect occurrence of 39 PPCPs in source water and drinking water. Twenty-four out of 39 PPCPs were detected in raw water, and 12 PPCPs were detected in the treated water [18]. Concentration range of DCL, NPR and CRB in the raw water samples were 1.929-3.707 ng L⁻¹ and 0.366-0.458 ng L⁻¹ and 0.827-0.994 ng L⁻¹, respectively. In treated water, DCL was not detected, NPR and CRB concentration ranged between 0.471 and 0.522 ng L⁻¹ as well as between 0.833 and 0.968 ng L⁻¹, respectively. DCL removal was practically complete, while CRB was removed in 4.1%. For NPR removal efficiency, a negative number was obtained. In Tables 3.2-3.4 DCL, NPR and CRB concentration data are given in different water samples according to publications from 2017 to 2019. Pharmaceuticals could be detected also in soils irrigated with reclaimed water [295].

Recently, there are many concerns on the presence of APIs in the aquatic environment due to their potential toxicity and persistency [87-90]. Studies have shown direct effects on wildlife from some APIs [90-91]. In a separate study, 2986 different pharmaceuticals have been listed as toxic substances for aquatic organisms [92]. In addition, the permanent presence of antibiotics in aquatic systems produces antibiotic resistant and harmful bacteria [57, 93] and it can affect bacterial communities responsible for biological degradation [94]. Da Silva Santos et al. reported that chronic exposure of zebrafish to CRB led to altered feeding behaviour and reduced egg viability [95]. Different organisms absorb hazardous pollutants to varying extent and the biomagnification of different active substances varies, as well [80, 91, 96]. Level of toxicity can be characterized with ecotoxicity endpoint [74] and risk quotient values (determined environmental concentration divided by ecotoxicity endpoints) [97]. In the case of CRB, no observed effect concentration (NOEC) value was determined as 230 ng L⁻¹ according to the experiment dealing with *Dreissena polymorpha* as test organism [4]. The NOEC in the case of DCL for brown trout was found to be 500 ng L⁻¹ [98], and its lowest observed effect concentration (LOEC) for thyroid hormone level decrease of Indian major carp (*Cirrhinus mrigala*) was 1000 ng L⁻¹ [99]. The LOEC of NPR was found to be 10000 ng L⁻¹, according to hatching, developmental rate, morphology and histopathology [13]. In Table 3.5, the ecotoxicity endpoints and corresponding risk quotients (RQs) are given for DCL, NPR and CRB according to the river water concentration data listed in Tables 3.2-3.4. It can be stated that in some cases DCL and CRB maximal concentrations (C_{max}) were higher than ecotoxicity endpoints. Moreover, the corresponding risk quotients (RQs) were higher than the unit. In seawater samples, the maximal concentrations of

DCL, NPR and CRB were in the 0.021 - 3.99 ng L⁻¹ and n.d. - 177.7 ng L⁻¹ and n.d. - 28.3 ng L⁻¹ concentrations ranges, the calculated RQs were 0.004, 0.018 and 0.123.

In Table 3.6, the ecotoxicity endpoints and corresponding risk quotients (RQs) are given for DCL, NPR and CRB according to the WWTP effluent concentration data listed in Tables 3.2-3.4. It can be stated that DCL and CRB risk quotients (RQs) in most cases exceeded the acceptable value (i.e. 1). This means that the emitted effluent in most cases posed an environmental threat. That is increasingly complex because of micropollutants interaction [100-101]. These drugs also pose a risk to population because they eventually enter human body *via* contaminated drinking water [102-103], consumption of fish [104-107] and mussels [108]. Due to the harmful effects of these substances, the 2015/495 Commission implementing decision (EU) included some pharmaceuticals into the Watch List for Union wide monitoring in the field of water policy [89, 15].

Table 3.2 Diclofenac concentration data (ng L⁻¹) in different water samples according to scientific papers published between 2017 and 2019

DCL, ng L ⁻¹									
River water	Lake	Reservoir	WWT influent	WWT effluent	Coastal water	Estuary	Sea water	Reference	Country
258-1398			560-2470	466-2180				[75]	Mexico
19000-193000								[78]	Brazil
		n.d. - 50						[109]	Brazil
n.d.*			n.d.*	n.d.*			n.d.-3.99	[110]	Portugal, Atlantic Ocean
98- 3224								[15]	Portugal
canal with WW 1900-2100	n.d.		540-6300	910- 4000				[111]	Germany
			186-195	172-277	n.d.-31.9		n.d-2.5	[85]	Spain, Cadiz Bay
							n.d.- 0.021	[81]	Italy, Western Mediterranean Sea
0.0649-4.62				113-812				[112]	Slovenia, Croatia
13.3-20.3								[113]	Hungary
400-880				2500-3350				[114]	Germany
						n.d.-250.8		[79]	United Kingdom

continued

						1.60-51.8		[115]	Portugal
				8-1932		1-650		[116]	Basque Country
5.9-380								[117]	United Kingdom
			1038-3429	811-3697				[118]	Italy
4-3560								[67]	Ukraine
33 -46				3291-3842				[22]	Hungary
514-1080**								[119]	Czech Republic
n.d.-111								[103]	India
					n.d.-26.9			[120]	Saudi Arabia, Red sea
			142-245	152-561				[121]	New Zealand
	n.d.-26							[80]	China
			n.d. - 836000					[122]	Pakistan
n.d.-1010			n.d.-10200	n.d.				[66]	South Africa
467.4- 1461.5								[70]	South Africa
	n.d.			77-15087***				[123]	Antarctica

n.d.=not detected; *veterinarian usage prohibited; **after WWTP treatment; ***wastewater discharge into the sea

Table 3.3 Naproxen concentration data (ng L⁻¹) in different water samples according to scientific papers published between 2017 and 2019

River	Ponds	Groundwater	Reservoir	WWT influent	WWT effluent	Coastal water	Sea water	Reference	Country
		3220 - 98390		50 -2063840 median: 28700	50 – 34718990 median:33680*			[124]	USA
					5760–253000			[68]	Canada
732-4880				825-4210	49-392			[75]	Mexico
			n.d.- 100					[109]	Brazil
n.d.				533.3-2078.7	n.d.-110.7		n.d.-177.7	[110]	Portugal, Atlantic Ocean
				12883-16774	75-124	n.d.-95.8	n.d.	[85]	Spain, Cadiz Bay
n.d.-333	n.d.				96-333**			[123]	Antarctica
2.67-20.4					81.6-2190			[112]	Slovenia, Croatia
270								[54]	Italy
					n.d.-1375			[22]	Hungary
LOQ-929.8***								[119]	Czech Republic

continued

				414-7976	<LOQ			[121]	New Zealand
	n.d.-22							[80]	China
LOQ-43.2								[125]	China
12.6-527								[53]	Republic of Korea
					n.d.- 464000			[122]	Pakistan
							n.d.-1.70	[81]	Mediterranean Sea
224.3-1112.8								[70]	South Africa
133-355							126-147	[126]	South Africa
n.d.				n.d.- 59300	n.d.			[66]	South Africa
				22000 -67000				[127]	Colombia

LOQ = limit of quantification; n.d.=not detected; *Naproxen was removed to a lesser extent because of negative removal potentially due to metabolite reversal to parent compound or desorption from organic matter; **wastewater discharge into the sea , ***after WWTP

Table 3.4 Carbamazepine concentration data (ng L⁻¹) in different water samples according to scientific papers published between 2017 and 2019

Bottled water	Tap water	River water	Lake	Ground water	WWT influent	WWT effluent	Coastal water	Estuary	Sea	Reference	Country
		52-276			85-380	165-476				[75]	Mexico
					323-338	214-329	n.d.-31.1		n.d.-0.1	[85]	Spain, Cadiz Bay
									Baltic 1.9	[82]	Sweden, Baltic sea
n.d.-22.1	20.0-22.3	32.9-34.4			66.2-110.9	98.5-244.9			n.d.-28.3	[110]	Portugal, Atlantic Ocean
		2.69-18.4				86.2-5320				[112]	Slovenia, Croatia
						2-390		1-93		[116]	Basque Country
					87-375	129-847				[118]	Italy
	22-27	23-37				2917-3726				[22]	Hungary
		280-730				640-1000				[114]	Germany
		n.d.-779								[103]	India
					2-11500	3-6880				[128]	Republic of Korea
					53.8	61.9				[129]	Japan

continued

					435-725	595-793				[121]	New Zealand
			1-6.6							[80]	China
		12.6-527.9								[53]	Republic of Korea
									0.0038-0.0133	[81]	Mediterranean Sea
		157.1-279.5								[70]	South Africa

n.d.=not detected

Table 3.5 Ecotoxicity endpoints and corresponding risk quotients (RQs) for pharmaceutical compounds in river water

River water	DCL			NPR			CRB		
	$c_{max,ng L^{-1}}$	RQ	Ref.	$c_{max,ng L^{-1}}$	RQ	Ref.	$c_{max,ng L^{-1}}$	RQ	Ref.
Portugal	n.d.	-	[110]	n.d.	-	[110]	34.4	0.150	[110]
Portugal	3224	3.224	[15]						
Italy				270	0.027	[54]			
Ukraina	3560	3.560	[67]						
Croatia	4.62	0.005	[112]	20.4	0.002	[112]	18.4	0.080	[112]
Hungary	20.3	0.020	[113]						
Hungary	46	0.046	[22]				37	0.161	[22]
Germany	880	0.880	[114]				730	3.174	[114]
United Kingdom	380	0.380	[117]						
Czech	1080	1.080*	[119]	929.8	0.093	[119]			
Antarctica				333	0.033	[123]			
India	111	0.111	[103]				779	3.386	[103]
Korea				527	0.053	[53]	527.9	2.295	[53]
China				43.2	0.004	[125]			
Mexico	1398	1.398	[75]	4880	0.488	[75]	276	1.200	[75]
Brazil	193000	193**	[78]						
South Africa	1010	1.010	[66]	355	0.036	[126]			
South Africa	1461	1.461	[70]	1112.8	0.111	[70]	279.5	1.215	[70]

Endpoint (LOEC) conc. ng/L DCL 1000; NPR: 10000; CRB: 230; n.d.=not detected; *after WWTP; **sewage from city

Table 3.6 Ecotoxicity endpoints and corresponding risk quotients (RQs) for pharmaceutical compounds in WWTP effluents

Effluent	DCL			NPR			CRB		
	$c_{max,ng L^{-1}}$	RQ	Ref.	$c_{max,ng L^{-1}}$	RQ	Ref.	$c_{max,ng L^{-1}}$	RQ	Ref.
USA				33680	3.368	[124]			
Canada				253000*	25.30*	[68]	575000*	2500*	[68]
Mexico	2180	2.180	[75]	392	0.039	[75]	476	2.069	[75]
Portugal	n.d	-	[110]	110.7	0.011	[110]	244.9	1.065	[110]
Spain	277	0.277	[85]	124	0.012	[85]	329	1.430	[85]
Italy	3697	3.697	[118]				847	3.683	[118]
Slovenia	812	0.812	[112]	2190	0.219	[112]	5320	23.13	[112]
Hungary	3842	3.842	[22]	1375	0.138	[22]	3726	16.20	[22]
Germany	4000	4.000	[111]						
Germany	3350	3.350	[114]				1000	4.348	[114]
Antarctica	15087**	15.09**	[123]	333	0.033	[123]			
Basque	1932	1.932	[116]				390	1.695	[116]
Pakistan				464000	46.40	[122]			
Korea							6880	29.91	[128]
Japan							61.9	0.269	[129]
New Zealand	561	0.561	[121]	n.d	-	[121]	793	3.448	[121]

Endpoint (LOEC) conc. ng/L DCL: 1000; NPR: 10000; CRB: 230; n.d.=not detected; * direct effluent at pharmaceutical facilities.; ** wastewater discharge into the sea .

3.3 Occurrence of the three target compounds in living organisms

Vapor pressures of the target compounds (DCL, NPR, CRB) are between 6.1×10^{-8} and 1.9×10^{-6} mm Hg at 25 °C. These values indicate that they are present in the atmosphere in both solid and vapor phases and do not volatilize from dry soil surfaces. Their octanol-water partition coefficient (K_{oc}) values ranging between 245 and 510 indicate that they are likely to have only moderate mobility [130] in soil water. Moreover, they are adsorbed onto sediment in the aquatic environment. Based on the corresponding Henry's Law constants, their volatilization from wet soil and water is not expected. In the case of DCL and NPR, it is also important to mention that they have acidic character and are in anionic form at the pH values between 5 and 9 ($pK_a = 4.0$ and 4.2). In the vapor phase, these compounds are degraded with 0.8 - 4 hours half-life by photochemically produced hydroxyl radicals [36]. The active compounds in solid phase are released from the atmosphere by wet and dry deposition. Thus, CRB [131], NPR and DCL [132] may be susceptible to direct photolysis in water by sunlight.

Several authors investigated the bioconcentration, accumulation of these harmful compounds in living organisms. Carbamazepine is a noteworthy anthropogenic pollutant, as its removal during wastewater treatment is relatively inefficient and is very common in aquatic environments [133]. Vernouillet et al. investigated bioaccumulation of CRB preparing an experimental trophic chain consisting of a green algae (*Pseudokirchneriella subcapitata*), a crustacean (*Thamnocephalus platyurus*) and a cnidarian (*Hydra attenuata*). As a first step of the experiment, the first trophic level was contaminated, green algae were exposed to 150 mg L^{-1} CRB for 24 h in triplicate. After this step, the CRB-contaminated (or control) algae were added as food to 250 specimen of adult *T. platyurus* and incubated in triplicate for 24 h. Then, *H. attenuata* were fed during 6 h with *T. platyurus*. According to their results, the bioaccumulation factor was found 2.2 and 12.6 in algae and crustaceans, respectively. In the case of *Hydra attenuate* significant bioaccumulation was not observable, but the enzymatic activity was altered. This work indicates the ability of CRB to bioaccumulate in aquatic organisms through food contamination [134].

Oliveira et al. investigated the effects of the active ingredient on mussel (*Mytilus galloprovincialis*), both short and long terms. Similar size *M. galloprovincialis* specimens were taken from the Ilhavo channel (from Northwest Atlantic coast of Portugal). After depuration and acclimation, they were exposed to 0.0; 0.3; 3.0; 6.0; and $9.0 \text{ } \mu\text{g L}^{-1}$ CRB concentrations for 96 h or 28 days. Six organisms were placed in 3 L of medium, which was supplied by continuous aeration

and photoperiod of 12 : 12 h. During the experiment, water was renewed once a week, after which CRB concentrations were reestablished. Carbamazepine was taken up by the mussel *M. galloprovincialis* despite the low bioaccumulation factor (maximum average of 2.2). It was stated that the uptake was very rapid, so it is possible to use these organisms as indicators of CRB contamination. Research has shown that CRB did not induce oxidative stress but the physiological parameters were negatively affected, thus causing problems for population sustainability [135]. A similar result was obtained in the experiments conducted by Boillot et al. on the same mussel species at a concentration of 10 µg L⁻¹ CRB and 10-hydroxy-10,11-dihydro-carbamazepine (100H) for one week. They reached 3.9 and 4.5 L kg⁻¹ dry weight bioconcentration factors and 29.3 ± 4.8 ng g⁻¹ dry weight (d.w.) CRB and 40.9 ± 4.6 ng g⁻¹dw 100H mean concentrations were determined in the tissues within one week. Their results showed that the compounds were uptaken by the mussel [136].

Gomes et al. investigated the effect of CRB and clonazepam on oxidative stress biomarkers and essential metal homeostasis in *Danio rerio* fish specimens. Reduced glutathione, metallothionein, catalase and glutathione S-transferase as well as essential metal concentrations in fish liver, kidney and brains were determined. Dishomeostasis of several essential elements in all analyzed organs and significant oxidative stress effects were observed, with brain GST activity being the most altered [137].

The adverse effects of DCL on the environment have been previously observed. Ericson et al. for exposed Baltic Sea blue mussels, *Mytilus edulis trossulus* to 1 to 10,000 µg L⁻¹ DCL, ibuprofen and propranolol concentrations. The active ingredients were tested both individually and simultaneously. Mussels exposed to high-concentrations had smaller growth rates; mussel silk produced by them was weaker thus limiting the ability of the mussel to attach to various surfaces. Shells exposed to lower concentrations also showed these tendencies. According to this experiment, it can be stated that the drugs were taken up by the investigated species. The concentration of DCL and propranolol determined reached concentrations of two orders of magnitudes larger than found in sewage treatment plant effluents [138]. Oviedo-Gomez et al. (2010) studied the effects of DCL on a North American Bolar crab (*Hyalella azteca*). The experiments were carried out on artificial sediments with high DCL content. The artificial sediment consisted of 70% sand, 20% kaolin and 10% organic matter. The source of the organic material was compost, which was inactivated by heating at 55-60 °C for 3 days. The aim of this work was

to evaluate toxicity of DCL on *Hyalella Azteca*, using oxidative stress biomarkers. According to their results, the LC₅₀ in the acute toxicity assay was 0.467 mg kg⁻¹ for DCL at 72 h. This acute toxicity value is much higher than the usual DCL concentrations in the aquatic environment, but lower concentration may lead to chronic exposure due to its constant release into the environment. It has been observed that DCL induces oxidative stress on *H. azteca*, which can lead to cell damage. Set of the tests used represents a suitable early damage biomarker to estimate toxicity of DCL in aquatic species [139].

According to experiments of Cunha et al., mussels can be used as bioindicators in coastal environment. Mussels from eight sites in Portugal coast were taken. They found that DCL concentration in mussels were closely related to the environmental contamination. Diclofenac was detected in 7 out of 8 sites and the determined concentrations were in the range of 0.5 to 4.5 mg/kg (d.w.). The highest levels of DCL in mussels were found in areas characterized by higher population density [140]. Lee et al. observed the long-term effects of DCL on two species of crabs (*Daphnia magna*; *Moina macrocopa*) and one species of fish (*Oryzias latipes*). In the study involving crabs, DCL concentrations of 25 and 50 mg L⁻¹, resulted in a reduction in the number of crabs *Daphnia magna* and *Moina macrocopa*, respectively, within 3 months. In fish, DCL concentrations of 0.001 to 10 mg L⁻¹ increased the time required for hatching and reduced the rate of successful hatching from eggs. No effect concentration of DCL was estimated at 0.1 mg L⁻¹ [141].

Naproxen has been detected at varying concentrations in various freshwater lakes and rivers of the Earth and deserves special attention due to its side effects and frequency. Thibaut et al. investigated, among other drugs, the effect of NPR on the liver processes of carp and found that they could increase the catalytic activity of various enzymes, thereby affecting liver function [142]. Isidori et al. investigated acute and chronic effects of NPR in a species of algae (*Selenastrum capricornutum*), wheelworms (*B. Calyciflorus*) and micro-sized shellfish (*C. dubia*; *T. platyurus*). In addition, effects of degradation products resulting from photolytic decomposition have also been investigated. The results indicated that these products were more toxic than NPR itself. Their chronic effect was observed in decrease of growth and reproduction [143].

3.4 Methods for the determination of pharmaceutical compounds

Even though the concentration of pharmaceuticals found in the environment is at a trace level (from ng L^{-1} to several $\mu\text{g L}^{-1}$), identification and quantification of PPCs is possible by using different advanced instrumental analytical techniques such as liquid chromatography mass spectrometry (LC-MS), gas chromatography mass spectrometry (GC-MS), liquid chromatography tandem mass spectrometry (LC-MS/MS) and gas chromatography tandem mass spectrometry (GC-MS/MS). Applying these methods, ng/L level of method detection limits (MDL) can be achieved.

Sample pretreatment and preparation are very important steps prior to GC and HPLC determination of PPCs. The type of sample preparation used depends on the complexity of the sample matrix, analyte concentration, MDL and limit of quantification (LOQ). The most common sample preparation techniques are filtration, extraction, clean up and concentration of aqueous media in the case of HPLC and GC. In addition, derivatization may also be required in the case of GC [144].

The main goal for the extraction processes is to transfer the analytes from an aqueous phase to an organic one. Recently, liquid liquid extraction (LLE), solid phase extraction (SPE) and solid phase microextraction (SPME) could be successfully coupled online to LC for automated analysis. Moreover, these are the most common techniques for extraction of the aqueous samples [145-148]. Identification and quantitation of PPCs are most often accomplished by LC and GC. In recent years, LC has been used predominantly (in 70% of the cases) for determination of the three target compounds. The LC is more favorable than GC [149] for these analytical tasks due to the polar nature of these PPCs. Moreover, derivatization is not necessary when LC is applied. Among the scientific papers published in the last three years dealing with the determination of DCL, NPR and/or CRB in different water matrices, the number of publications applying ultra-high performance liquid chromatography tandem mass spectrometry (UHPLC-MS/MS), or LC-MS/MS, or GC-MS methods is approximately the same. However, high selectivity and sensitivity detectors are required for determination of PPCs by applying LC and GC. Mass spectrometers coupled to GC or LC are highly sensitive and selective even for very complex matrices. Therefore, LC-MS technique is frequently applied to PPCs quantification. The analytical performance parameters of LC-MS methods are far better than those involving conventional HPLC equipment with diode-array detector (DAD). However, the much lower operation cost of the HPLC-DAD equipment renders it suitable to get preliminary information prior to LC-MS determination [150].

According to literature data for determination of the three target APIs, reverse-phase high performance liquid chromatography (RP-HPLC) methods are mainly used. Some of the publications deal with the determination of only one active ingredient [151]. Depending on the analytical task, simultaneous determination of several drugs has also been reported [152]. Gul et al. developed a RP-HPLC analytical method using methanol / water mixture (90 : 10 V/V) as eluent to determine the concentration of six NSAIDs, including DCL and NPR in drug formulations and human plasma [152]. Roscher et al. investigated the degradation products of DCL from aqueous samples. In this study, aqueous solutions were irradiated by light in the wavelength range of 220 to 500 nm, which resulted in the degradation of DCL in less than 4 minutes. Eleven degradation products were detected by LC-MS, from which seven have not been reported in the literature yet [153].

Nowadays, using hyphenated techniques like high-resolution mass spectrometry (HRMS) coupled to ultra-high performance liquid chromatography (UHPLC) or GC is becoming increasingly popular for detection and determination of PPCs at trace levels (e.g. ng L^{-1}) [154-156]. Krakkó D. et al. developed a method for ultra trace analysis of ten APIs including CRB, DCL and NPR in Hungarian drinking, river and waste water samples using UHPLC-HRMS. The lower LOQ was achieved by pre-concentration by SPE. The recovery rates for the investigated APIs ranged between 20% and 80% [22]. There are several advantages when SPE is coupled to the LC-MS equipment. Tran et al. coupled SPE with UHPLC-MS/MS to detect and quantify 20 antibiotics in different environmental water matrices [65]. In this study, the MDL values ranged between 0.02 and 15 ng L^{-1} as well as 0.05 and 25 ng L^{-1} and, finally, 0.1 and 40 ng L^{-1} in surface waters, treated effluents and raw influent, respectively. Kim et al. developed a novel and reliable method for determination of 18 antibiotics in different environmental water matrices using on-line SPE HPLC-HRMS [147]. Also in another study, Lee et al. developed a highly sensitive analysis method for the determination of nine nitrosamines at ng L^{-1} concentration level in the influent and effluent of WWTPs and in rivers using an automated SPE-LC-MS/MS equipment [157]. Aparicio et al. used stir bar sportive extraction (SBSE) combined with LC-MS for determination of different polar and nonpolar emerging micropollutants, 14 pharmaceutical compounds including DCL and NPR in surface water and tap water samples [158].

In the study by Togola and Budzinski, a GC-MS method was reported for the determination of different PPCs including CRB, DCL, ketoprofen, NPR in wastewater and surface water matrices.

The authors indicated that the MDL varied from 0.4 to 2.5 ng L⁻¹ [159]. In a separate study, linear sweep voltammetry (LSV) and GC-MS were used for determination of DCL with LOQs of 4.8 and 0.15 µg mL⁻¹ for LSV and GC-MS, respectively [160].

In Table 3.7, analytical methods and performance parameters are summarized reporting on DCL, NPR or CRB determinations according to the literature search based on recent years.

3.5 Removal of pharmaceutical compounds from aqueous environment by adsorption

Due to the increasing concern on human health risks posed by pharmaceutical compounds in aquatic environment, control and removal of these emerging contaminants are required. Furthermore, it is necessary to search for alternative WW treatment methods to possibly reuse treated WW for agricultural purposes. In recent decades, a wide spectrum of technologies have been developed for the treatment of these contaminants of water sources through transformation or sorption involving physical adsorption processes (activated carbon, graphene and graphene oxide, carbon nanotubes), biological degradation processes (pure cultures, mixed cultures, activated sludge process), chemical advanced oxidation processes (ozonation, fenton oxidation, UV treatment, ionizing irradiation), combined chemical and biological methods [176-179]. Among the aforementioned treatment methods, adsorption has shown to be a promising technology as tertiary process with high removal efficiency for micropollutants [180].

Adsorption is a phase transfer process that occurs when a gas or liquid solute accumulates on the surface of a solid sorbent. Adsorption technologies are widely used to remove several organic micro-contaminants from fluid phases at low cost and with high efficiency [181]. In water treatment, adsorption can be used as a reliable, cost effective, flexible, simple designed method based on the application of various adsorbents [182-214].

Table 3.7 Summary of methods for determination of diclofenac, naproxen and carbamazepine by LC and GC

Sample matrix	Sample enrichment method	Quantification	LOD	LOQ	Drug (acronym)	Reference
River-, seawater and treated wastewater	SPE	LC-MS/MS	-	1.2-28 ng L ⁻¹ and 5.0-160 ng L ⁻¹	DCL, CRB, NPR	[161]
Water, soil, sediment and fish	SPE	UHPLC-MS/MS		0.3-26 ng L ⁻¹	DCL, CRB, NPR	[162]
Wastewater	SPE	HPLC-HRMS	-	0.01-0.1 ng L ⁻¹	DCL, CRB, NPR	[163]
Tap-, bottled-, sea- and river water, WWTP effluent and influent	SPE	UHPLC-MS/MS	-	-	DCL, CRB, NPR	[110]
Sludge of STPs and livestock WWTPs.	SPE	LC-MS/MS	-	0.001 to 0.122 mg g ⁻¹	DCL, CRB, NPR	[128]
Surface water, groundwater and WWTP effluent	SPE	LC-MS/MS	0.5-2.5 ng L ⁻¹	1.7-8.5 ng L ⁻¹	DCL, CRB	[164]
Surface water and tap water	SPE	LC-MS/MS	-	7.0 ng L ⁻¹ - 177 ng L ⁻¹	DCL, NPR	[158]
Drinking-, river- and wastewater	SPE	UHPLC-HRMS	-	0.05 - 0.01 µg L ⁻¹	DCL, CRB, NPR	[22]

continued

Wastewater	SPE	HPLC-DAD	-	0.1 $\mu\text{g L}^{-1}$ - 0.4 $\mu\text{g L}^{-1}$	NPR, DCL and ibuprofen	[165]
Seawater and river water	SPE	HPLC-DAD	-	0.025, 0.036 and 0.035 $\mu\text{g L}^{-1}$,	NPR, DCL and ibuprofen	[126]
Bile of two wild fish species	SPE	LC-MS/MS	-	1.1–76.6 ng mL^{-1}	DCL, NPR and ibuprofen	[166]
Model solution	-	HPLC-DAD	0.361 $\mu\text{g ml}^{-1}$	0.975 $\mu\text{g ml}^{-1}$	DCL	[167]
Soil samples	ultrasonic solvent extraction- SPE	LC-MS/MS	0.03 to 1 ng g^{-1}	0.09 to 3.3 ng g^{-1}	DCL, CRB	[168]
Sediment samples	dispersive SPE	LC-MS/MS UHPLC-MS/MS	-	0.002 and 1.93 $\mu\text{g kg}^{-1}$	DCL, CRB, NPR	[169]
Wastewater influent and effluent	SPE	LC-MS/MS	-	0.05-0.01 $\mu\text{g L}^{-1}$	CRB and its metabolites	[129]
Wastewater	SPE	LC-MS/MS	0.011 to 188 ng L^{-1}	0.033 to 628 ng L^{-1}	23 PCP, DCL, CRB, NPR	[64]
Estuarine waters-, influent and effluent WWTP	SPE	LC-MS/MS	0.001 and 25 pg	0.01 to 30.3 ng L^{-1}	DCL, CRB	[170]

continued

Wastewater	SPE	UHPLC-MS/MS	2 ng L ⁻¹	10 ng L ⁻¹	CRB, NPR	[171]
Human plasma	LLE, derivatization.	GC-MS	-	0.03 and 0.10 µg mL ⁻¹	NPR	[172]
Wastewater influent and effluent	ultrasound-assisted emulsification-microextraction	GC-MS	0.002–0.121 µg L ⁻¹ influent / 0.002–0.828 µg L ⁻¹ effluent	0.005–0.403 µg L ⁻¹ influent / 0.006–2.758 µg L ⁻¹ effluent	DCL, NPR	[173]
Clams (<i>Ruditapes decussatus</i>)	QuEChERS	LC-MS/MS	0.73-5.65 µg g ⁻¹	2.4-18.2 µg g ⁻¹	DCL, CRB, NPR	[174]
Groundwater and river water	SPE	LC-HRMS	0.2-11.9 ng L ⁻¹		18 popular antibiotics	[147]
Surface water samples	SD-DLLME	LC-MS/MS		0.0125-1.25 mg L ⁻¹	58 PPCPs and pesticides	[154]
Wastewater effluents	molecularly imprinted-SPE	HPLC with fluorescence detector	0.18-0.45 ng·mL ⁻¹	-	estrogens and their metabolites	[155]
Environmental water samples	FPSE	LC-MS/MS	1–50 ng L ⁻¹		CRB, DCL	[156]
River sediment	UAE-SPME	GC-MS	<0.25 ng g ⁻¹	<0.8 ng g ⁻¹	NPR, DCL	[175]

Adsorption onto different sorbent materials is one of the most effective methods to eliminate hazardous micropollutants such as PPCPs from aqueous phase [24, 44]. According to adsorbents origin, there are two different types of adsorbents used in water treatment, namely natural and manufactured adsorbents. Usage of adsorbents of natural origin such as clay [182-183], natural zeolites [185], oxides and biopolymers has become less widespread lately. Manufactured adsorbents as carbon based ones (e.g. activated carbon, AC) [184], polymeric adsorbents [186], oxidic adsorbents, and zeolite molecular sieves [187] have a larger pore volume and finer pores, which make its internal surface area much larger than their external one [187].

Several novel carbonaceous adsorbents, graphene, graphene oxide [25-26, 188-192], carbon nanotubes [27-28, 193] have been developed for removal of different hazardous materials. Nam et al. investigated the adsorption behaviors of DCL and sulfamethoxazole on graphene oxide at an initial concentration of $10 \mu\text{mol L}^{-1}$. Both DCL and sulfamethoxazole were removed from solution up to 35% and 12%, respectively, within 6 h and maximum adsorbed amount of DCL 1.69 mmol g^{-1} was achieved [188]. Also in the study by Hiew et al., adsorption of DCL was investigated using graphene oxide at initial concentration of 400 mg L^{-1} . Results showed that graphene oxide exhibited a maximum adsorption capacity of 2.20 mmol g^{-1} for DCL [199]. In another study by Nodeh et al., adsorption of NPR on silica and magnetic nanoparticle-decorated graphene oxide were studied. Initial concentration was varied in the range of $10\text{--}200 \text{ mg L}^{-1}$. The q_m of maximum adsorption capacity for NPR was $0.135 \text{ mmol g}^{-1}$ [190]. Ncibi et al. investigated the efficiency of mesoporous activated carbons and assynthesized multi-walled carbon nanotubes to remove CRB and Dorzolamide from artificially contaminated waters. The highest removal capacities were registered at initial concentration in the range of $5 \text{ to } 75 \text{ mg L}^{-1}$ using assynthesized multi-walled carbon nanotubes (0.95 mmol g^{-1} for CRB) [193].

However, separation from aqueous phase, reduced dispersibility, and small particle size are still existing problems for usage of carbon nanotubes for wastewater treatment [24]. Nevertheless, adsorption onto granulated activated carbon (GAC) [24, 29, 194-198, 201-207] and biochar [30-31, 208-209] has been preferred for removal of pharmaceuticals from aqueous matrices due to their outstanding advantages (simple and cheap application, avoidance of undesirable by-products, high effectiveness, etc.) [210]. On the other hand, it is necessary to mention that the cost of using AC is

increased by its difficult regeneration [206]. Adsorption of pharmaceutical compounds onto GAC has been extensively studied both under batch and flow conditions [211].

Adsorption mechanism of micropollutants depends on the physicochemical properties of both adsorbent and adsorbate (molecular size, solubility in water, acid dissociation constant (K_a), K_{ow} and nature of the substituent in the benzene ring [197]. Adsorption can be achieved by different mechanisms such as hydrogen bonding, surface complexation, cation exchange and cation bridging [151].

There are various types of operating modes in adsorption studies, for example batch, continuous moving bed, continuous fixed bed (upflow or downflow), continuous fluidized bed and pulsed bed [212]. Generally, the batch and fixed bed modes are the most commonly used to understand adsorption processes. Batch conditions are used to clarify theoretical background (adsorption capacity, adsorption kinetic, mathematical model, etc.) of adsorption processes. At the same time, parameters applicable for industrial operation (flow rate, parameters of fixed-bed, etc.) are usually investigated in flow systems. Nevertheless, adsorption can be used during water cleaning technologies applied at STPs in both aforementioned operation modes. However, depending on certain parameter sets, batch operation mode can be preferred to the flow one [213]. Study of kinetics, adsorption equilibrium, and isotherm modeling is essential in supplying basic information required for the design and operation of adsorption processes for wastewater treatment plant [214].

3.5.1. Conventional adsorption materials

3.5.1.1 Activated carbon

Activated carbon is a microcrystalline form of carbon, which can be made from carbonaceous source materials such as petroleum residue, natural coal, wood and peat by chemical activation or gas activation [215]. Recently, ACs are derived from agro-industrial wastes such as nutshells, date stones, piassava fibers, leather shaving waste, coffee husks, tobacco residues for a lower adsorption system cost [216]. The carbonaceous source materials are pyrolyzed at temperatures ranging from 600 to 900°C in the absence of oxygen. The ACs have been widely used for organic micropollutants removal from water because of its high porosity, high surface area, inert nature and stability over a wide pH range, suitable pore size and functional groups [151]. Using GAC, more than 90%

removal efficiency of PPCP compounds can be achieved [217]. For the removal of NSAIDs, commercially available powdered activated carbon (PAC) and GAC are widely used. The main difference between the two adsorbents is that GAC has larger particles and smaller external surface area [44].

Surface area plays a very important role in the adsorption process. The external surface area has a strong influence on the rate of mass transfer during adsorption, while the internal surface area controls adsorption capacity. In addition, the internal surface area affects the adsorption of organic molecules onto the inner surface. Therefore, the pores should not be too small to make the adsorption of large molecules possible [151]. In general, the major characteristics of AC used in water treatment are the following: pore diameter <1 nm, specific surface area up to 3000 m² g⁻¹ and internal surface area in range of 800–1,000 m² g⁻¹ [151, 218]. Several studies investigated the removal efficiencies of the three target compounds, DCL, NPR and CRB onto activated carbon under batch conditions [188, 194, 211, 217, 219-220, 221-225].

Adsorption of 22 organic micropollutants (including DCL and CRB) typical to the given region and WWTPs, was studied using different types of GAC and PAC at three Swedish municipal wastewater treatment plants that differed in plant configuration and in wastewater characteristics [224]. A mobile pilot plant was applied at the three WWTPs consisting of three treatment lines for GAC application, three for PAC, and other lines either for ozonation or using biofilm and finally one line with sand filtration after ozonation. The GAC was placed in two connected columns; the operation was performed in down-flow configuration. In this way, it was possible its regeneration and reactivation. The larger specific surface of PAC resulted in faster adsorption kinetics, but specific measures were required for its application. Lines used for PAC treatment consisted of an initial tank for mixing of wastewater and dosed PAC, followed by three sequential aerated contact tanks, a sedimentation tank and a final sand filter. The aim of the study was to achieve 95% removal of the emerging micropollutants in relation to the effluent of the WWTP plants. The GAC and PAC were shown to be efficient for removal of pharmaceutically active compounds in the effluents and the goal of the 95% removal was reached for almost all tested substances by the applied purification system. The PAC system achieved the planned 95% removal efficiency applying a fresh dose of 15-20 mg L⁻¹ PAC, while carbon usage rates for the GAC application were much broader and ranged from 28 to 203 mg L⁻¹ depending on the carbon product [224]. No considerable differences were observable regarding pharmaceutical removal in the three chosen WWTPs.

Efficiency of the adsorption of the drug depends on contact time, dose, the physico-chemical parameters of the substance, as well as pH [44]. Increasing the contact time results in increased removal efficiency. The increased dose of sorbent results in increase of activation sites, so increase of the removal efficiency. Pharmaceuticals with higher $\log K_{ow}$ values showed a stronger trend to be adsorbed onto ACs [220]. The pK_a of the drug to be removed and pH of water determine the electric charge of the molecules. Diclofenac and NPR are in anionic form below the normal environmental pH conditions, thus being protonated at low pHs. As surface of AC is negatively charged, the low pH values are optimal for the removal of these NSAIDs [226]. In the case of CRB, pH has no effect on the electric charge of the molecules. Adsorption is influenced by van der Waals interactions, hydrogen bond and $\pi - \pi$ interactions. Increase of ionic strength decreases electrostatic interactions between activated carbon and pharmaceuticals [227]. As an example, Larous and Meniai investigated adsorption of DCL onto AC prepared from olive stones. Different parameters were studied such as contact time, pH, initial concentration of DCL and adsorbent dose (from 2 to 7 g L⁻¹). The adsorbed amount of DCL onto AC increased with the increase of contact time. Maximum adsorption was reached at pH=2, where DCL molecules are in protonated form. Results showed that adsorption was fast during the first 20 min and then slowed down to reach equilibrium after 30 min. Contact time needed to reach equilibrium was 3 h in the case of higher DCL initial concentrations. An increase of initial DCL concentration resulted in increased DCL uptake. By increasing adsorbent dose, adsorption efficiency increased because the number of available adsorption sites increased. The adsorption kinetics fitted resulted to be pseudo second order controlled by the intraparticle diffusion [228]. Investigating the removal of NPR by adsorption onto two different ACs from aqueous solutions, Lach and Szymonik found lower adsorption efficiency at higher pH. Moreover, increase of temperature enhanced removal of NPR [226]. Furthermore, they found that the adsorption process followed a pseudo second order reaction and the Elovich model. On the contrary, Baccar et al. found that the increase of temperature in the range 4–40 °C had no perceptible effect on the adsorption process of NPR and DCL [194]. Adsorption of DCL, NPR and CRB from ultrapure water, unfiltered and filtered effluents was investigated applying GAC made of coconut shell by Gao et.al. The maximal adsorbed amounts of CRB, NPR and DCL were 0.013, 0.012 and 0.009 mmol g⁻¹ respectively, at a carbon dosage of 133 mg L⁻¹. Adsorption kinetics were best described by a pseudo second order kinetic model and the Freundlich isotherm model. Removal of the target compounds was affected by the ionic strength

of wastewater because the increase of ionic strength decreases the electrostatic interactions between the AC and pharmaceuticals [227].

Competitive adsorption of acetaminophen, DCL, and SMX onto GAC was investigated by Chang et al. [229]. In binary systems, adsorbate with the smaller K_{ow} was replaced by the one with larger K_{ow} , DCL. Only the small target molecules, acetaminophen and SMX could occupy the portion of the micropores. Therefore, in multiple-component systems, the competitive adsorption might significantly be affected by macropores. They reported the increase of diffusion with decrease in particle size of GAC, but this was not related to the molecular weight of the adsorbate. In another work, Bo et al. also studied the competitive adsorption of four pharmaceutical compounds including DCL, NPR and CRB onto GAC from ultrapure water and secondary effluent. The target drugs were removed completely at initial concentration of $500 \mu\text{g L}^{-1}$ from the ultrapure water when 250 mg L^{-1} carbon dosage was used. In the effluent from a WWTP, the removal efficiencies of DCL, NPR and CRB were 57.9, 44.7, and 31.0%, respectively, with carbon dosage of 250 mg L^{-1} . It was found that filtration of the secondary effluent by $0.22 \mu\text{m}$ hydrophilic membrane increased the removal efficiencies of DCL, NPR and CRB, which could be recovered up to 67.1, 53.4, and 48.1% by using the same carbon mass [230]. Sotelo et al. studied adsorption of caffeine and DCL onto GAC. It was concluded that single adsorbate interactions were altered by the presence of other adsorbates due to competition for the binding sites. In competitive adsorption, lower adsorption amounts for caffeine and DCL were found (0.98 and 0.79 mmol g^{-1} , respectively). Compared to the single adsorption system, a decrease of about 30% was registered. The equilibrium adsorption data were best adjusted to the extended Freundlich model [231].

Modification of commercial AC can improve efficiency of adsorption. Comparing the removal efficiency of DCL onto the surface of a modified/oxidized AC to that of the commercial unmodified one, Bradha et al. found a six times increase [232]. Application of two types of AC (N-biochar or O-biochar) was studied in single- and multi-solute adsorption experiments for removal of DCL, NPR by Jung et al. Biochars were produced by pyrolyzing pine chip at $300 \text{ }^\circ\text{C}$ for 15 min with pure nitrogen (N-biochar) or 7% oxygen with 93% nitrogen gas (O-biochar). Both biochars were activated by NaOH to increase the surface area and pore volume of the products. The maximum adsorbed amounts for DCL and NPR were 1.26 and 1.26 mmol g^{-1} respectively, for N-biochar and 0.723 and $0.991 \text{ mmol g}^{-1}$ respectively for O-biochar [202]. The strongest interaction

was found between DCL and the adsorbent. This is the explanation of the occupation of effective adsorption sites as compared to other solutes [202].

According to literature data, the maximal adsorption capacities depend on characteristics of the investigated adsorbates and the adsorbent. Hiew et al. compared the maximal adsorption capacity (q_m) of DCL onto various other adsorbents reported in the literature with own graphene oxide results (reduced graphene oxide aerogel: 2.01 mmol g^{-1} and GO suspension: 2.21 mmol g^{-1}). The q_m varied in the range of 0.091 and 3.12 mmol g^{-1} [199]. In decreasing order of their q_m values, the reported non-graphene oxide sorbents were the following: amine groups functionalized mesoporous silica (3.12 mmol g^{-1}), oxidized activated carbon (1.64 mmol g^{-1}) and granular CNT/alumina hybrid adsorbent ($0.091 \text{ mmol g}^{-1}$). Husein et al. also summarized the q_m of NPR and DCL for different adsorbents. Results showed that q_m of DCL and NPR were in the range of 0.065 and 1.68 mmol g^{-1} as well as 0.077 and 1.28 mmol g^{-1} , respectively [200]. The highest q_m values for NPR were found when AC fibers (made of textile waste) were used (1.28 mmol g^{-1}); then, for N-biochar (1.26 mmol g^{-1}), O-biochar ($0.991 \text{ mmol g}^{-1}$), AC from apricot waste ($0.463 \text{ mmol g}^{-1}$), micelle-clay complex ($0.311 \text{ mmol g}^{-1}$) and copper nanoparticles ($0.147 \text{ mmol g}^{-1}$). The highest q_m values for DCL were obtained when montmorillonite clay (1.68 mmol g^{-1}) was applied; then, for N-biochar (1.26 mmol g^{-1}), O-biochar ($0.723 \text{ mmol g}^{-1}$), sawdust– polyaniline ($0.302 \text{ mmol g}^{-1}$) and copper nanoparticles ($0.122 \text{ mmol g}^{-1}$). According to the review by Ahmed, q_m of NPR and DCL for different ACs from various aqueous solutions were in the range of 0.172 and 1.26 mmol g^{-1} as well as 0.037 and 1.26 mmol g^{-1} , respectively [233]. The q_m according to Jung et al. for NPR and DCL were the same (i.e. 1.26 mmol g^{-1}) using AC made of pine chips by chemical activation with NaOH [202]. Baccar et al. investigated adsorption of NPR and DCL onto a low-cost AC derived from olive waste-cake. According to Langmuir isotherm curves, the q_m values for NPR and DCL were 0.172 and $0.190 \text{ mmol g}^{-1}$, respectively [194]. The maximal adsorption capacities for four PACs including DCL-Na onto three different commercial ACs (one GAC and two PACs possessing ~ 650 and 900 or $1500 \text{ m}^2 \text{ g}^{-1}$ surface areas) were studied by Rakić et al. Under batch adsorption conditions, the q_m values were about $0.010 \text{ mmol g}^{-1}$ [184]. Surface concentrations of the investigated drugs on ACs were found to be between 0.1 and 0.4 mmol g^{-1} . Authors underlined the importance of the surface chemistry of ACs, tunable by surface modification in order to improve their adsorptive characteristics.

Stoykova et al. found that q_m of CRB was larger by increasing the activation temperature of AC. The applied charcoals had been activated with water steam at different temperatures (480 – 740 °C; 360 – 630 °C and 650 – 700 °C); q_m values of CRB (0.061 mmol g⁻¹; 0.059 mmol g⁻¹ and 0.050 mmol g⁻¹, respectively) were reported [203]. In another study, Delgado et al. investigated the adsorption of three emergent contaminants, methylparaben, CRB and sildenafil citrate onto GAC in aqueous solutions. Adsorption capacity for methyl paraben and CRB were 1.97, 1.27 mmol g⁻¹ respectively, while this value was much lower, about 0.225 mmol g⁻¹ for sildenafil citrate. The slow adsorption kinetics required at least 168 h average adsorption time [223]. Similar results were reported for adsorption of CRB with q_m of 1.42 mmol g⁻¹ onto GAC obtained from peach seeds [205]. Peach stones were chemically activated with H₃PO₄, then oxidation and gas phase treatments were applied in order to obtain mesoporous and high surface area of AC. Adsorption of caffeine, DCL and CRB was studied in batch and flow systems. Results indicated aqueous solution components competed with adsorbates. Carbamazepine adsorption capacity was higher than that for caffeine and DCL [205]. Chen et al. investigated adsorption of CRB onto activated biochars. A q_m up to 1.21 mmol g⁻¹ [236] was reported in the aforementioned work. In the study by Cai and Larese-Casanova, the q_m of CRB onto GAC at an initial concentration of 0.5 mg L⁻¹ was investigated. Results showed a q_m of 0.847 mmol g⁻¹ [189]. Lower adsorption affinity of 1 mg g⁻¹ CRB was achieved by using low initial concentration of 500 ng L⁻¹ [237]. Similar results were observed by Fallou H et al. According to their investigations, adsorption capacities of DCL and CRB onto AC fiber cloths were significantly influenced by the nature of the adsorbed molecule when the concentration was decreased [235].

3.5.1.2 Polymeric adsorbents

Polymeric adsorbents also referred to as synthetic resins are porous solids with considerable surface areas, high adsorption capacities, high mechanical strength and uniform pore size distribution [187, 238]. Polymeric adsorbents have the ability to be regenerated easily because the binding forces are relatively weak in comparison to the binding forces in case of the adsorption on AC [239].

Polymeric sorbents are classified based on the charge properties as neutral, ionic or hydrophobic. Recently, several studies have been proposed on the surface modification of the polymer sorbents for the removal of polar and nonpolar pharmaceuticals from water [240-241]. A

number of studies have been undertaken to investigate the adsorption of PPCPs onto polymeric adsorbents [186, 242].

3.5.1.3 Zeolites

Zeolites are a group of porous minerals (crystalline) of aluminosilicates with the general formula of $(\text{MeII}, \text{MeI}_2)\text{O} \cdot x \cdot \text{Al}_2\text{O}_3 \cdot y \cdot n\text{SiO}_2 \cdot z \cdot p\text{H}_2\text{O}$ (where n and p are stoichiometric coefficients), also known as molecular sieves. For adsorption, microporous solids of this family are used. Zeolites have internal and external surface areas of up to several hundred square meters per gram and cation exchange capacities of up to several milliequivalents per kg [243]. Zeolites have a porous structure (cage-like structures) characterized by defined pore sizes, which can be selected in the range of the desired molecular diameters. Thus, zeolites can adsorb molecules of a certain size very well because of the very regular pore structure [185, 244].

Zeolites have high adsorption capacity, catalyzing action, they are stable in wide ranges of temperature (thermal treatments) and acidic conditions [245]. Their high stability under radiative and thermal treatments, which induces complete degradation of adsorbates, enhances the regeneration of the exhausted zeolites [246]. Both natural and synthetic zeolites are used in the industry as adsorbents, ion exchangers and molecular sieves [243, 247]. It has been proven that zeolites are efficient in removing of different pharmaceuticals from WW [185, 248-258].

Faud et al. studied removal of selected pharmaceuticals including ibuprofen, DCL sodium, indomethacin, chlorpheniramine maleate, and paracetamol from water using natural Jordanian zeolite at initial concentration varied in the range of 10.0 and 50.0 mg L⁻¹. Results showed that the highest removal was found to be 30.1% for DCL-Na with adsorption capacity of 0.016 mmol g⁻¹ [296].

3.5.2 Adsorption modeling in batch condition

Adsorption is generally described by isotherms that provide all the information needed to study the equilibrium. In addition, each adsorption equilibrium state is uniquely defined by the change in amount of adsorbate (adsorbate concentration) on the adsorbent as a function of pressure (for gases) or concentration (for liquids) at a constant temperature. The concentration of the adsorbate changes until the equilibrium is reached [259]. At equilibrium, when the adsorption rate equals to the

desorption rate, the remaining amount of adsorbate is measured in the solution. The mass of the adsorbate that has been adsorbed can then be calculated.

The adsorption capacity of adsorbent is determined by using the adsorption isotherm models. So far, no universal isotherm equation was found that would describe all of the experimental isotherm curves with the same accuracy [162]. Several isotherm equations are available for application in adsorption studies, which enhance understanding the theory of adsorption equilibrium. The most important models are attributed to Langmuir, Freundlich, Temkin, Redlich-Peterson, and Dubinin-Radushkevich.

3.5.2.1 Linear isotherm

The linear isotherm is the simplest adsorption isotherm. It is used when a linear relationship is assumed between a given component concentration in solid phase (c_s) and concentration in the solution (c), according to the Eq. (3.1).

$$c_s = K_d \times c \quad \text{Eq. (3.1)}$$

The adsorption coefficient, K_d ($L\ m^{-2}$) can be determined from the experimental data as the slope of the linear fitting. K_d can also be expressed in $L\ kg^{-1}$ using the specific surface area ($m^2\ kg^{-1}$) of the solid.

3.5.2.2 Freundlich isotherm model

The Freundlich isotherm (1906) is an empirical model based on adsorption on a heterogeneous surface (surface with varying properties). This model describes the relationship between the concentration of adsorbates in a solution and the amount that has been adsorbed. It is also applicable to non-ideal sorptions as well as multilayer sorption processes. The Freundlich isotherm model has been widely used to fit experimental data for liquid-phase adsorption. The Freundlich equation is given as Eq. (3.2)

$$\ln q_e = \ln K_F + n^{-1} \ln C_e \quad \text{Eq. (3.2)}$$

Where C_e is the equilibrium concentration of adsorbate ($mg\ L^{-1}$), q_e is the amount of the compound adsorbed by the adsorbent at equilibrium ($mg\ g^{-1}$), K_F ($mg\ g^{-1}$) ($dm^3\ mg^{-1}$), $1/n$ and n are indicators of adsorption capacity and adsorption intensity, respectively. The K_F and n can be determined from the linear plot of $\ln q_e$ versus $\ln C_e$.

3.5.2.3 Langmuir isotherm model

The Langmuir isotherm model (1918) is widely used to describe adsorption of molecules or a solute (amount of adsorbate adsorbed) from a liquid solution of different concentration values on the solid surface (adsorbent) and its equilibrium concentration in aqueous solution at a fixed temperature. The Langmuir isotherms are based on three assumptions: (1) adsorption is limited to monolayer coverage, (2) adsorbent surface is in contact with a solution containing an adsorbate, which is strongly attracted to the surface; (3) all surface sites are alike and they can only accommodate one adsorbed atom as well as the ability of a molecule to be adsorbed on a given site is independent of its neighboring site occupancy [259]. The Langmuir equation can be written in the following form:

$$\frac{C_e}{q_e} = \frac{C_e}{q_m} + \frac{1}{K_L q_m} \quad \text{Eq. (3.3)}$$

Where q_e (mmol g^{-1}) is equilibrium adsorption capacity, C_e is equilibrium concentration (mg L^{-1}), q_m is maximum adsorption capacity (mg g^{-1}), and K_L (L mg^{-1}) is the Langmuir's constant.

3.5.2.4 Temkin isotherm model

The Temkin model is based on the assumption that heat of adsorption (as a function of temperature) of all the molecules in the layer would decrease linearly as a result of increased surface coverage [257]. The Temkin isotherm is valid only for an intermediate range of ion concentrations [259]. The linear Temkin equation can be written in the following form

$$q_e = B_T \ln K_T + B_T \ln C_e \quad \text{Eq. (3.4)}$$

Where B_T is Temkin constant which is related to heat of sorption (J mol^{-1}) and K_T (L g^{-1}) is Temkin isotherm constant.

3.5.2.5 Dubinin-Radushkevich isotherm model

The Dubinin-Radushkevich (DR) model (1960) is an empirical equation generally applied to express adsorption of sub-critical vapours in microporous solids such as ACs and zeolites. The DR model, based on the theory of volume filling of micropores, was developed for vapor adsorption onto microporous adsorbents [260]. The DR model is widely used to describe the adsorption mechanism with Gaussian energy distribution onto heterogeneous surfaces [263] based on the assumptions of a change in the potential energy between the gas and adsorbed phases and a characteristic energy of a given solid.

In the modified form for solutes, equilibrium and saturation pressure of the vapor in the original isotherm equation are substituted by the concentration and saturated concentration of the solute [162]. The linear DR equation can be expressed in the following form

$$\ln q_e = \ln q_{m,DR} - \frac{R^2 T^2}{E^2} \left[\ln \left(1 + \frac{1}{C_e} \right) \right]^2 \quad \text{Eq. (3.5)}$$

The Dubinin-Radushkevich equation (Eq. (3.5)) gives information on the thermodynamic parameters of the adsorption process. From the linearized form, q_m (mol g⁻¹) and activation energy [E, (kJ mol⁻¹)] can be obtained, R (J K⁻¹ mol⁻¹) is the universal gas constant and T (K) is the absolute temperature.

3.5.2.6 Redlich-Peterson model

Three-parameter isotherms can be derived from the Redlich-Paterson (R-P) model, capable to represent adsorption equilibria over a wide concentration range. This model is widely used as compromise between the Langmuir and Freundlich isotherm systems. It incorporates the advantageous significance of both models [214]. The (R-P) model can be represented as follows

$$q_e = \frac{K_{RP} C_e}{1 + \alpha_{RP} C_e^\beta} \quad \text{Eq. (3.6)}$$

Where K_{RP} (L g⁻¹) and α_{RP} (L mg⁻¹) are Redlich-Peterson isotherm constants and β is the exponent that can be between 0 and 1. The R-P model unifies the features of the Langmuir and Freundlich isotherms. In the case of $\beta=1$, the R-P equation results in the Langmuir equation, whereas when $\beta = 0$, the Redlich-Peterson isotherm equation transforms to Henry's law equation.

3.5.3 Adsorption kinetics

The adsorption kinetics describe the time dependence of adsorption processes, change of adsorbed amounts in time [187]. Knowledge of adsorption kinetics is very important to clarify the rate-limiting mass transfer mechanisms and to evaluate the characteristic mass transfer parameters. Different kinetic models have been employed to study adsorption of micropollutants from aqueous phases. For the design and optimization of effluent treatment models, information is needed on the kinetic performance of the adsorbent, indicating the solute uptake rate, which, in return, determines the residence time required for completion of adsorption. This latter is needed to determine the performance of fixed-bed or any other flow-through systems [264].

So far, several kinetic models have been widely proposed or employed under batch conditions to describe the kinetic process of pollutants adsorption from aqueous solutions. These models can be generally classified as adsorption reaction models (pseudo first order, pseudo second order) and adsorption diffusion models (i.e. Elovich and intra-particle diffusion models).

3.5.3.1 Pseudo first order kinetics

Pseudo first order kinetics is a reaction based model which was first proposed by Lagergren (1898). It is generally used in the linear form proposed by Ho and McKay [265].

$$\ln(q_e - q_t) = \ln q_e - k_1 q_t \quad \text{Eq. (3.7)}$$

Where q_t is the amount of adsorbed solute in time (mg g^{-1}), q_e is its value at equilibrium, k_1 is the pseudo first order rate constant and t is the time.

Pseudo first order reaction is a reaction that should actually happen by order higher than the unit. Its explanation is that the concentration difference between the two reactants is very high. Pseudo first order does not fit well for the whole range of contact time and it is applicable over the initial 20 to 30 min of the adsorption process [266].

3.5.3.2 Pseudo second order kinetics

Pseudo second order model is based on the adsorption equilibrium capacity of the solid phase.

This model is usually represented by its linear form as shown

$$\frac{t}{q_t} = \frac{t}{q_e} + \frac{1}{k_2 q_e^2} \quad \text{Eq. (3.8)}$$

where q_e , (mmol g^{-1}) represents equilibrium adsorption capacity, q_t (mmol g^{-1}) is adsorption capacity at time t , and k_2 is the second order rate constant ($\text{g mg}^{-1} \text{min}^{-1}$). The pseudo second order rate constants can be determined experimentally by plotting t/q versus t .

Recently, for adsorption of DCL, NPR and CRB from aqueous matrices applying pseudo second order adsorption kinetic has been widely reported [264, 267-272].

3.5.3.3 Elovich model

The Elovich equation, first proposed in 1939, describes chemical adsorption processes. It is suitable for systems with heterogeneous adsorbing surfaces [273]. The Elovich equation assumes that the actual solid surfaces are energetically heterogeneous and the adsorption sites increase

exponentially with progressing adsorption process. This implies a multilayer adsorption [274], represented by its linear form as shown in Eq. (3.9)

$$q_t = \beta \ln (\alpha \beta) + \beta \ln t \quad \text{Eq. (3.9)}$$

where q_t (mmol/g) is the amount of gas adsorbed at time t , β is the desorption constant, and α is the initial adsorption rate [265]; β can be directly obtained from the slope of the plot of q_t versus $\ln(t)$ and α can be calculated from the intercept of the same plot once β is known.

The Elovich equation has been widely used to study the kinetics of chemisorption of gases onto heterogeneous solids [275]. Recently, this model has been also successfully applied to the adsorption of DCL, NPR and CRB from aqueous solution [194, 275-278].

3.5.3.4 Intra-particle diffusion model

Intra-particle diffusion is a model, appropriate to describe the diffusion mechanism inside the porous adsorbents [276]. The adsorption rate depends on the diffusion towards the porous adsorbents [277]. The IPD model does not depend on the hydrodynamic conditions and, therefore are transferable to other process conditions. The IPD model is also known as Weber and Morris sorption kinetic model. The model is usually represented by its linear form (Eq. (3.10)):

$$q_t = K_{ip}t^{0.5} + C_{ip} \quad \text{Eq. (3.10)}$$

where q_t is the amount adsorbed at time t , K_{ip} is the intraparticle diffusion rate constant and C_{ip} is the liquid phase concentration of sorbate in the inner pore of sorbent at time t .

3.5.4 Adsorption thermodynamics

Adsorption is a surface process and adsorbate-adsorbent system is always evaluated by thermodynamic parameters such as Gibbs free energy (ΔG), change in enthalpy (ΔH), and change in entropy (ΔS) [214, 278]. The Van't Hoof equation is widely used to explore changes in a thermodynamic system, which relates to the change in the equilibrium constant, K_{eq} to the variations of the temperature.

$$\Delta G = - RT \ln K_{eq} \quad \text{Eq. (3.11)}$$

where R is the universal gas constant ($8.314 \text{ J K}^{-1} \text{ mol}^{-1}$), T is the absolute temperature (K), and K_{eq} is the thermodynamic equilibrium constant.

Enthalpy and entropy changes are also related to the Langmuir equilibrium constant by the following expression:

$$\ln K_{eq} = \frac{\Delta G}{R} - \frac{\Delta H}{RT} \quad \text{Eq. (3.12)}$$

Thus, by plotting $\ln K_{eq}$ as a function of $1/T$, it is possible to calculate the change in enthalpy (ΔH°) from the slope. The standard free energy can be derived from the intercept. The entropy change (ΔS°) can be calculated by using the following equation [234]:

$$\Delta G = \Delta H - T\Delta S \quad \text{Eq. (3.13)}$$

3.5.5 Removal of PPCPs from aqueous environment in flow condition

Adsorption onto fixed-bed (percolation) has become a frequently used industrial application in wastewater treatment. In this operating mode, the equilibration process proceeds successively, layer by layer, from the column inlet to the column outlet.

The adsorbent particles are arranged in a bed. Consequently, adsorption takes place in a particular region of the adsorbent bed, known as the mass transfer zone, or adsorption zone which moves through the bed [187].

By applying flow systems, fixed-bed columns usually packed with GAC are usually used. The most important parameters necessary to be optimized for such packed-bed systems are as follows: i) flow rate; ii) inlet concentration; and iii) bed height (or mass of GAC). The flow rate influences the contact time between the adsorbate and the adsorbent, while the removal capacity of the system depends on the contact time. The inlet concentration is an important factor because it can influence the adsorbed amounts on the column. Furthermore, the bed height has a primary effect on the adsorption efficiency. The data obtained during the optimization process are demonstrated with the so-called breakthrough curve, which is the outlet-to-inlet concentration ratio (C/C_0^{-1}) as a function of time (or throughput volume). Breakthrough is defined as the contact time (t_b) at 2 or 5 C/C_0^{-1} %, while the exhaustion time (t_{ex}) is the time at 90 or 95% C/C_0^{-1} %. A further parameter that characterizes the adsorption properties on fixed-bed columns is the saturation adsorption capacity (SAC) determined at t_{ex} [180].

Further interpretation of the experimentally determined data can be obtained by modeling adsorption. To achieve this, several mathematical models have been proposed [212, 279-281] — based on different assumptions — capable of describing the distinct parts of the breakthrough curve. The most commonly applied approaches in environmental research are the Adams-Bohart and Thomas kinetic sorption models. The former describes mostly the initial part of the breakthrough curve. Moreover, it can be used in the case of negligible mass transfer or axial dispersion, as well.

Applicability of Thomas model is more restricted because some prerequisites have to be fulfilled such as: i) it assumes a Langmuir isotherm; ii) the adsorption process should follow pseudo second order kinetics and iii) axial dispersion cannot occur [180]. Both models can be properly applied for optimization of fixed-bed column systems because the parameter values for fulfillment of these prerequisites can be calculated or experimentally measured. There are several publications on fixed-bed column applications using GAC for removal of inorganic contaminants and dyes but there are only few ones for pharmaceuticals by applying this approach [212].

Concerning adsorption of pharmaceuticals, determination of the breakthrough curves has been reported under circumstances that are far different than the industrially applicable ones, i.e. flow rate ($1-10 \text{ mL min}^{-1}$), inlet concentration ($10-500 \text{ mg L}^{-1}$) and bed height ($1-15 \text{ cm}$) [180]. Sotelo et al. [282] studied adsorption of caffeine and DCL on AC in fixed bed column at $10-15 \text{ mg L}^{-1}$ initial concentration using $0.4-1 \text{ g}$ commercial GAC and $2-3 \text{ mL min}^{-1}$ flow rate. The column design parameters were estimated by the linearized form of the Adams-Bohart model. It was found that GAC was not an efficient adsorbent for DCL. The same research group reported on adsorption of CRB at $1.2-2.5 \text{ mg L}^{-1}$ initial concentration, $0.4-0.8 \text{ cm}$ column length and $1-3 \text{ mL min}^{-1}$ flow rate [283]. By using the Thomas model, the experimental and predicted data were in good agreement. De Franco et al. [211] studied adsorption of DCL on GAC through a full factorial two-level experimental design involving three variables: initial pollutant concentration ($20 - 100 \text{ mg L}^{-1}$), adsorbent weight ($0.5 - 1.0 \text{ g}$) and volumetric feed flow rate ($3 - 5 \text{ mL min}^{-1}$). The breakthrough curve experimental data were fitted by three different models among them the Thomas and Adams-Bohart ones. The experimentally determined S-shaped curve was modeled properly with the applied mathematical models. Marzbali and Esmaili [284] investigated adsorption of tetracycline on mesoporous AC under the following conditions: 50 mg L^{-1} initial influent concentration, 4 cm bed height and 4 mL min^{-1} flow rate. For modeling, the Adams-Bohart and Yoon-Nelson models were used. Due to the poor data fitting, a specially adapted mathematical model for prediction of the proper parameters to the design of fixed bed was developed and applied.

Meta-analysis calculation based on 44 studies has been provided on the performance of fixed-bed column packed with GAC for the removal of organic micropollutants from municipal wastewater applying realistic parameterization [285]. Nevertheless, it is problematic to prove experimentally the calculated optimal conditions. The main difficulties of the experimentally determined breakthrough curves at realistic pollutant concentrations ($\mu\text{g L}^{-1}$ or ng L^{-1}) are that the

quantitative determination requires very sensitive analytical techniques (e.g. UHPLC-MS) that cannot be applied without sample purification and analyte pre-concentration (e.g. SPE). First of all, these increase dramatically the cost of the research due to the large sample throughput. Furthermore, the sample volume should be increased so that a 100-2000-fold analyte pre-concentration rate is obtained. The samples taken provide only a mean concentration assignable to certain time (effluent volume) intervals. Therefore, the determination of the complete breakthrough curve is not only expensive but also not accurate enough. Due to the aforementioned reasons, adaptation of the laboratory-scale results to the treatment of real SW using fixed-bed column has not been properly demonstrated yet.

3.5.6 Modeling of fixed-bed adsorption

3.5.6.1 Thomas model

The Thomas model (TM) is one of the most general and widely used model in fixed bed columns studies. The TM assume that the adsorption process follows a Langmuir isotherm and a pseudo second order with no axial dispersion in the adsorption column [286]. Using this model, the maximum solid-phase concentration of adsorbate on adsorbent and rate constant is determined [82]. This model can be described with the following expression (Eq. (3.14)):

$$C/C_0 = 1/[1+\exp(k_T q_0 M/Q - k_T C_0 t)] \quad \text{Eq. (3.14)}$$

where C and C_0 are the outlet and inlet concentration (mg L^{-1}), respectively; k_T ($\text{L mg}^{-1} \text{min}^{-1}$) is the rate parameter; q_0 (mg g^{-1}) - adsorbate uptake of the adsorbent; M (g) - quantity of adsorbent bed; Q (L min^{-1}) - flow rate; t (min) - time [180]. The Eq. (3.14) is used in the linearized form as well (Eq. (3.15)):

$$\ln [(C_0-C)/C] = -k_T C_0 t + k_T q_0 M/Q \quad \text{Eq. (3.15)}$$

where $k_T C_0$ is the slope and $k_T q_0 M/Q$ is the intercept of the linear equation.

3.5.6.2 Yoon–Nelson model

The relatively simple Yoon–Nelson model (YNM) (1984) is based on the assumption that the decreasing rate of adsorption for each molecule is favorably proportional to the adsorbate adsorption and breakthrough within the bed [287]. This model does not focus on the adsorbent type, adsorbate characteristics, and the physical properties of adsorption bed [82].

This model can be described using the linear form of the following equation:

$$\ln C_t / (C_0 - C_t) = k_{YN} t - k_{YN} \tau \quad \text{Eq. (3.16)}$$

where t is the breakthrough time, C_0 and C_t are the breakthrough (effluent) concentration and inlet concentration, respectively, τ is the time required for 50% adsorbate breakthrough, k_{YN} - rate constant, and k - a proportionality constant. These parameters can be easily determined from the slope and intercept of linear plots of $\ln C_t / (C_0 - C_t)$ versus t [288].

3.5.6.3 Adams-Bohart model

The Adams-Bohart model (1920) is based on the assumption that the adsorption rate is favorable depending on both the residual capacity of the adsorbent and the concentration of the adsorbing species [78]. The Adams-Bohart model established the fundamental equation describing the relationship between C/C_0 and time. This model mainly clarifies the first region of the breakthrough curve ($C/C_0 < 0.5$) and focused on the estimation of characteristic parameters such as q_m .

The Adams-Bohart model can be described in the following way (Eq. (3.17)):

$$C/C_0 = \exp(k_A C_0 t - k_A N_0 H/u) \quad \text{Eq. (3.17)}$$

where C and C_0 are the outlet and inlet concentration (mg L^{-1}), respectively; k_A ($\text{L mg}^{-1} \text{min}^{-1}$) is the kinetic parameter; N_0 (mg L^{-1}) - saturation concentration, H (cm) - bed length, u (cmmin^{-1}) - superficial velocity, t (min) - time. At the same time,

the Thomas model can be described as follows (Eq. (3.18)):

$$C/C_0 = 1/[1 + \exp(k_T q_0 M/Q - k_T C_0 t)] \quad \text{Eq. (3.18)}$$

where C and C_0 are the outlet and inlet concentration (mg L^{-1}), respectively; k_T ($\text{L mg}^{-1} \text{min}^{-1}$) - rate parameter; q_0 (mg g^{-1}) - adsorbate uptake of the adsorbent; M (g) - quantity of adsorbent bed; Q (L min^{-1}) - flow rate; t (min) - time [180]. The Eq. (3.18) is used in the linearized form as well (Eq. (3.19)):

$$\ln [(C_0 - C)/C] = -k_T C_0 t + k_T q_0 M/Q \quad \text{Eq. (3.19)}$$

where $k_T C_0$ is the slope and $k_T q_0 M/Q$ - intercept of the linear equation.

Chapter 4

Removal of selected pharmaceuticals from aqueous matrices with activated carbon under batch conditions

4.1 Experimental part

4.1.1. Chemicals

All chemicals used throughout this study were of analytical grade. Diclofenac sodium ($C_{14}H_{10}Cl_2NNaO_2$), naproxen sodium ($C_{14}H_{13}NaO_3$) and CRB ($C_{15}H_{12}N_2O$) were purchased from Molar Chemicals Ltd. (Hungary) and they were applied without any further purification. From DCL and NPR, a 1000 mg L^{-1} stock solution, while from CRB a 5 mg L^{-1} one was prepared with deionized water. DCL and NPR stock solutions were further properly diluted to prepare working solutions. The pH of all solutions was set to 6 ± 0.1 before addition of GAC using 0.1 mol L^{-1} NaOH or 0.1 mol L^{-1} HCl solutions. Granulated carbon (i.e. Organosorb10, Organosorb11 and Organosorb10 AA) were obtained from Desotec HQ (Belgium). Organosorb10 and Organosorb11 are GACs produced by steam activation of selected grades of coal. Moreover, Organosorb11 is an acid washed version of Organosorb10. The Organosorb10 AA is an agglomerated GAC made of a pulverized blend of selected grades of coal. All of them are recommended for removal of impurities from water and different industrial processes. Acetonitrile and methanol (each purchased from Scharlau S.L., Spain) were of HPLC gradient grade. Glacial acetic acid of HPLC grade was purchased from Sigma–Aldrich Co. (USA).

4.1.2 Characterization of GAC

Granulated activated carbon was characterized by using the procedures listed below. Nitrogen physisorption measurements were carried out at $-196\text{ }^\circ\text{C}$ using Thermo Scientific Surfer (Germany) automatic volumetric adsorption analyzer. Before use, AC samples were outgassed under high vacuum ($< 10^{-6}$ mbar) at $200\text{ }^\circ\text{C}$ for 2 h. Specific surface area was calculated by the BET equation at 0.01–0.2 relative pressure. Pore size distribution was evaluated from the adsorption branch according to the BJH method. Micropore volume was calculated by the α_s plot method. Mesopore

volume was calculated as difference between the total pore volume and micropore one. This measurement was performed before and after GAC use.

Attenuated total reflection Fourier transform infrared (ATR-FT-IR) spectra were recorded on a Varian Scimitar (USA) 2000 FT-IR spectrometer equipped with a MCT (mercury-cadmium-tellurium) detector and a Golden Gate™ single reflection diamond ATR system (Specac, UK). In general, 128 scans and 4 cm⁻¹ resolutions were applied. For all spectra, ATR correction was performed (Varian ResPro 4.0 software).

Scanning electron microscopy (SEM) measurements were performed on a Quanta 3D scanning electron microscope (FEI, USA) equipped with secondary (Everhart-Thornley detector) and back scattered electron detectors together with silicon drift energy dispersive spectrometer. The local elemental composition of GAC was determined by SEM-EPMA technique (scanning electron microscope-electron probe microanalysis) at two points selected on the specimen. For the measurements, 20 kV high voltage, 4 nA probe current and 50 s as lifetime were used.

The point of zero charge (pzc) of GAC was determined in 0.05 mol L⁻¹ NaCl as electrolyte in a total volume of 25 mL by using the pH drift method. Thus, pH of the samples was adjusted between 1 and 12 (n=10) using proper amounts of NaOH or HCl solutions. Two series of measurements applying different amounts of GAC were performed. Thus, 0.2 g and 0.05 g GAC were added to the solutions for the first and second series of measurements, respectively. Then, each suspension was stoppered and shaken on an orbital shaker OS-20 (Biotech, Czech Republic). After 24 h of shaking, filtration was applied and pH of the filtrates was also recorded. The pzc value was determined by plotting the Δ pH (final pH–initial pH) vs. initial pH [289].

According to the specifications provided by Desotec HQ, the particle size (d) of GAC was $d < 1.7$ mm and $d > 0.42$ mm for the 90% and 93% of the particles, respectively.

4.1.3 Adsorption equilibrium experiments and HPLC analysis

The q_m were determined for DCL and NPR in a batch system. The mass of carbon, the initial concentration of pharmaceuticals and the volume of aqueous phase were varied between 0.05 and 0.25 g, 5 and 300 mg L⁻¹ as well as 50 and 500 mL, respectively. Equilibrium measurements with DCL and NPR were performed using GAC in the original presentation form, while for another set of experiments, GAC was pulverized and sieved through a 0.1 mm mesh size. The resulted pulverized activated carbon will be referred to as PAC ($d < 0.1$ mm) hereafter. The reactor was continuously stirred at 800 rpm, temperature was kept constant at 25 °C. After 1 h, when equilibrium was achieved, suspensions were filtered through glass microfiber filter papers of 0.8 µm pore size and the active ingredient concentration in the filtrates was determined by HPLC. The HPLC instrument consisted of an LC 1150 (GBC Scientific Equipment Pty Ltd., Australia) quaternary gradient pump, LC1460 online degasser, LC1120/1150 column oven, LC 1445 system organizer, DI 510 D interface and SPD-M20A (Shimadzu, Japan) photodiode array detector. For evaluation of the acquired data, EZ Chrom Elite Client/ Server software (Version 3.1.7) was used. The chromatographic separation was achieved on a ZORBAX Extend C18 analytical column (150×4.6 mm, 5 µm) equipped with a same type of guard column (12.5×4.6 mm, 5 µm) purchased from Agilent Technologies (USA). Twenty microliter of the samples was injected onto the column using a Rheodyne injector. For separation, isocratic elution was applied. The flow rate was 0.8 mL min⁻¹. The mobile phase consisting of 50% (v/v) acetonitrile and 0.1% acetic acid (v/v) was filtered through 0.22 µm pore size membrane filters and sonicated for 10 min before use in a Bransonic B-3200 ultrasonic bath (Branson Ultrasonics, USA). The UV spectra of the analytes were registered by a HALO RB-10 UV-VIS spectrometer (Dynamica Scientific Ltd, UK).

4.1.4 Thermodynamic experiments and modeling

Thermodynamic studies were performed at three different temperatures (25; 35; 45 ± 0.1 °C) in 100 mL of total volume using 0.1 g GAC ($d=0.8-1.0$ mm) for the three-component solutions (i.e., DCL, NPR and CRB). The initial concentrations were varied between 50 and 300 mg L⁻¹ for each pharmaceutical. For these experiments, CRB was dissolved in methanol in a concentration of 1000 mg L⁻¹. Then, suitable aliquots of this methanolic stock solution were added to prepare the three component solutions. Thus, the methanol content of the three-component solutions varied between 5 and 30% (v/v). Further sample manipulation was performed in the same way as described at

Section 4.1.3. Except for this type of measurements, all other experiments were performed in the aqueous phase.

The experimental data were evaluated by different isotherm models [289-291] after linearization (Table 4.1). In the case of the Langmuir model [Table 4.1, Eq. (4.1)] q_m is the maximum adsorption capacity of the adsorbed pharmaceuticals per unit weight of carbon (mg g^{-1}) forming a complete monolayer on the surface; b - Langmuir constant (L mg^{-1}) corresponding to $k_a k_d^{-1}$ (where k_a and k_d are rate constants for adsorption and desorption processes, respectively), and C_e (mg L^{-1}) and q_e (mg g^{-1}) are equilibrium concentrations in liquid and solid phases, respectively. From the Langmuir model, a dimensionless equilibrium parameter (R_L) considered as a separation factor can be derived cf. Eq. (4.2):

$$R_L = \frac{1}{1+bC_e} \quad \text{Eq. (4.2)}$$

The Freundlich constant (KF , $\text{mg g}^{-1} (\text{L mg})^{-n}$) and the dimensionless exponent (n) can be calculated from the Freundlich equation [Table 4.1, Eq. (4.3)] while KT , the dimensionless Temkin constant and BT (mg g^{-1}) can be derived from the Temkin equation [Table 4.1, Eq. (4.4)]. The latter can be considered as q_m . The Dubinin-Radushkevich equation with its corresponding isotherm constant, ϵ [Table 4.1, Eq. (4.5)] was also applied. Data evaluation was also performed by the Redlich–Peterson (R–P) model, as well [Table 4.1, Eq. (4.6)]. The constants of R–P isotherm can be calculated by a parameter estimation program.

Table 4.1 Isotherm and kinetic models used for evaluation of adsorption process

Models	Equation	Linear equation	Plot
Isotherm models			
Langmuir	$q_e = \frac{q_{m,L}K_L C_e}{1 + K_L C_e}$	$\frac{C_e}{q_e} = \frac{C_e}{q_m} + \frac{1}{K_L q_m}$ (4.1)	$\frac{C_e}{q_e}$ vs. C_e
Freundlich	$q_e = K_F C_e^{1/n}$	$\ln q_e = \ln K_F + n^{-1} \ln C_e$ (4.3)	$\ln q_e$ vs. $\ln C_e$
Temkin	$q_e = B_T \ln (K_T C_e)$	$q_e = B_T \ln K_T + B_T \ln C_e$ (4.4)	q_e vs. $\ln C_e$
Dubinin-Radushkevich	$q_e = q_{m,DR} e^{-(B\varepsilon^2)}$	$\ln q_e = \ln q_{m,DR} - \frac{R^2 T^2}{E^2} \left[\ln \left(1 + \frac{1}{C_e} \right) \right]^2$ (4.5)	$\ln q_e$ vs. $\left[\ln \left(1 + \frac{1}{C_e} \right) \right]^2$
Redlich-Peterson	$q_e = \frac{K_{RP} C_e}{1 + \alpha_{RP} C_e^\beta}$ (4.6)		
Kinetic models			
Pseudo first order	$\frac{dq_t}{dt} = K_1 (q_e - q_t)$	$\ln (q_e - q_t) = \ln q_e - K_1 t$ (4.7)	$\ln (q_e - q_t)$ vs. t
Pseudo second order	$\frac{dq_t}{dt} = k_2 (q_e - q_t)^2$	$\frac{t}{q_t} = \frac{t}{q_e} + \frac{1}{k_2 q_e^2}$ (4.8)	$\frac{t}{q_t}$ vs. t
Elovich	$q_t = \beta \ln (\alpha \beta t)$	$q_t = \beta \ln (\alpha \beta) + \beta \ln t$ (4.9)	q_t vs. $\ln t$
Intra-particle diffusion	$q_t = k_{ip} t^{0.5} + C_{ip}$	$q_t = k_{ip} t^{0.5} + C_{ip}$ (4.10)	q_t vs. $t^{0.5}$

4.1.5 Experimental conditions of kinetic analyses

For the kinetic experiments, the amounts of carbon, the total volume of the suspensions and concentration of each compound were 0.5 g, 200 mL and 5 mg L⁻¹, respectively. Larger GAC granules (0.8 < d < 1.0 mm) were applied by studying the individual solutions.

Smaller granule size fractions (0.42 < d < 0.8 mm) were also used to study adsorption from the three-component systems. The kinetic experiments were performed using PAC, as well. Temperature was kept at 25 °C ± 0.1. Sampling was performed for 1 h at varying intervals and the sampled volume was 1 mL. Samples were filtered immediately and analyzed by HPLC in the same way as described at Section 4.1.3. Data were evaluated using pseudo-first order (PFO), pseudo-second order (PSO), Elovich and intra-particle diffusion (IPD) models [289-291]. The kinetic equations and their linearized forms are summarized in Table 4.1.

4.1.6 Study of model solutions and secondary sewage water in semi open system

The SSW bulk sample originated from the effluent stream of a wastewater treatment plant (with GPS coordinates 46°53'46.9"N, 18°05'04.4"E) of a settlement with 70,000 inhabitants, located near the capital city of Hungary. In this plant, conversion of wastewater into an effluent is achieved through a cyclic activated sludge treatment technology.

For the quantitative determination of the background values of the target active ingredients in SSW, effluent wastewater samples were filtered subsequently through Whatman™ 0.45 and 0.2 µm pore size nylon membrane filters. For pre-concentration of the investigated drugs, SPE was used according to Tylová et al. [292]. For SPE, 200 mg Waters Oasis HLB cartridges were applied (Waters Ltd., Hungary). Prior to SPE, sample pH was adjusted to 4 with formic acid. The SPE cartridges were conditioned with 3 mL of methanol and 3 mL of ultra-pure water. Aliquots of 500 mL were loaded onto the cartridges with a flow rate of 3–4 mL min⁻¹. Then, cartridges were washed with 5 mL of ultra-pure water and dried under vacuum for 5 min. Elution of the retained analytes was achieved with 2 × 2 mL of methanol. Eluates were evaporated to dryness and reconstituted in 0.4 mL of methanol.

Quantitative analysis of the compounds was achieved on a Bruker Elute ultra-high performance liquid chromatography equipped with binary pump, autosampler and column oven – coupled to a Bruker Compact quadrupole–time of flight mass spectrometer (Bruker Daltonik GmbH, Bremen, Germany). For the chromatographic separation, Zorbax Eclipse XDB-C18 (50 ×

4.6mm i.d., 1.8 μm particle size) column was used, equipped with a 5 mm long guard column of the same type (Agilent Technologies Inc., USA). Mobile phase consisted of 0.2% (v/v) formic acid in ultra-pure water (eluent A) and acetonitrile (eluent B). The following gradient elution program was used: 10% B (initial conditions); 2 min, 10% B; 5 min, 50% B; 11 min, 99% B, 14 min, 99% B; 4 min post-run equilibration. The gradient elution method applied was similar to that reported by Campos-Mañas et al. [293]. Experiments performed in semi-open system were applied to individual and three-component model solutions of the target analytes, then to three-component model sewage water (MSW) and secondary sewage water (SSW) under continuous stirring at 800 rpm. In order to increase reproducibility of the measurements in the batch system, the particle size range of GAC was limited to $0.8 < d < 1.0$ mm after proper sieving. Concentration of all investigated analytes in the solutions was 5 mg L^{-1} . Moreover, the SSW sample was spiked with the target analytes to obtain the same concentration. For comparison of the individual and three-component model solutions, 0.1 g of GAC was used, while 1.0 and 5.0 g GAC were applied for the experiments performed on MSW and SSW, respectively. The pH and specific electrical conductivity of MSW were set to be the same as those for SSW (i.e., 7.72 and $900 \mu\text{S cm}^{-1}$, with NaHCO_3 and Na_2HPO_4 , respectively). Stirring was stopped for 30 s after 30 min and half of the 400 mL of the liquid phase was sampled without removal the carbon particles. Then, the reactor was replenished with 200 mL of 5 mg L^{-1} individual or three-component standard solutions. Sampling was repeated every 30 min for a total of 4 or 6 h. Then, samples were filtered and analyzed in the same way as described at Section 4.1.3. After finishing the experiments, the exhausted GAC was filtered and leaching experiments were performed in 25 mL of deionized water using 0.25 g of GAC at three different pHs (i.e., 4, 6 and 12) applying shaking for 3 h. Then, solutions were filtered and analyzed in the same way as described at Section 4.1.3.

4.2 Result and discussion

4.2.1 Characterization of charcoal

Surface characteristics of the studied GAC are summarized in Table 4.2. All studied GAC samples showed a high specific surface. The main difference among the commercial GACs was that Organosorb10 AA had a large mesopore volume besides the large micropore one. Data of Table 4.2 demonstrates that adsorption decreased the specific surface area and the mesopore volume, while there was no considerable difference in the micropore one. Since the investigated pharmaceuticals penetrated into mesopores, the mesoporous structure is advantageous to achieve a greater adsorption capacity. Thus, Organosorb10 AA was chosen for the adsorption experiments.

Further results for characterization of GACs by using an ATR FT-IR spectrometer can be seen in Fig. 4.1. In the spectra, absorption bands of surface carboxylic groups (at 1568, 1567, 1553 cm^{-1}), as well as the $-\text{Si}-\text{O}-\text{Si}-$ (at 1077, 1067, 1066 cm^{-1}), the $\text{Si}-\text{OH}$ (at 798 cm^{-1}) and $-\text{C}-\text{O}-\text{C}-$ or $-\text{C}-\text{OH}$ ones (at 1199, 1223 cm^{-1}) are clearly visible. Oxygen containing functional groups can be generated during steam activation, while the silicon content can be traced back to the silicate containing clays used for granulation aiming to improve mechanical strength and flexibility.

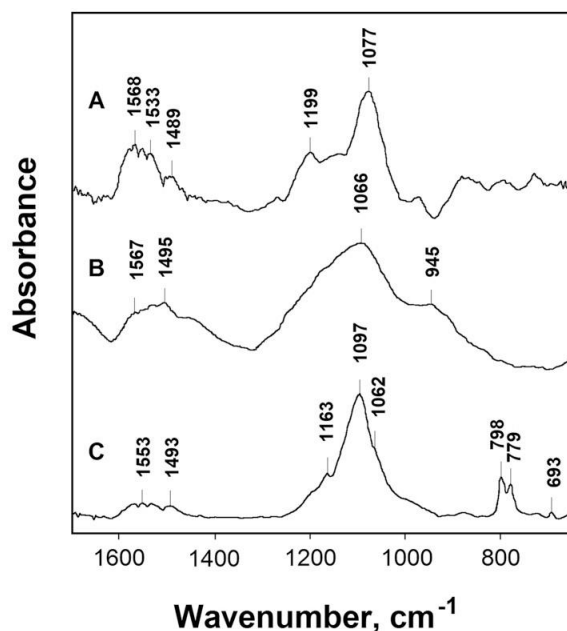


Fig. 4.1. ATR FT-IR spectra of studied GACs: A) Organosorb10 AA, B) Organosorb10, C) Organosorb11

The porous structure of the GAC is clearly visible in the SEM images recorded at different magnifications (Fig. 4.2). Its chemical structure and composition are not homogenous. Thus, lighter areas [Fig. 4. 2C (a)] have a greater silicon content while darker ones [Fig. 4.2C (b)] are richer in carbon according to the SEM-EPMA spectra. The X-ray fluorescence spectra of two points selected on the specimen can be seen in Fig. 4.3. Other elements than silicon were detectable only in traces (in all cases <1%) in the carbon matrix.

The conventional method for determination of pzc is plotting the ΔpH caused by the effect of solid particles on the liquid phase as a function of pH. When ΔpH is zero, the investigated surface can be considered electrically neutral. Results of pzc studies of GAC can be seen in Fig. 4.4. From this figure, it can be concluded that surface is electrically neutral at $\text{pH} < 1.0$ and $\text{pH} > 11$. Between these two pH values, there are charged functional groups on the surface. This effect is due to simultaneous presence of protonated and non-protonated carboxylic ($-\text{COOH}$, $-\text{COO}^-$) and silanol ($\equiv\text{Si}-\text{OH}$, $\equiv\text{Si}-\text{O}^-$) groups. These two functional groups act as a buffer system and compensate the pH of the original solution. At the usual mass (of GAC) – volume (of liquid) ratio applied in this work, pH of treated solution increased to 8–9. Therefore, there was no reason to study the effect of the initial pH on the adsorption processes.

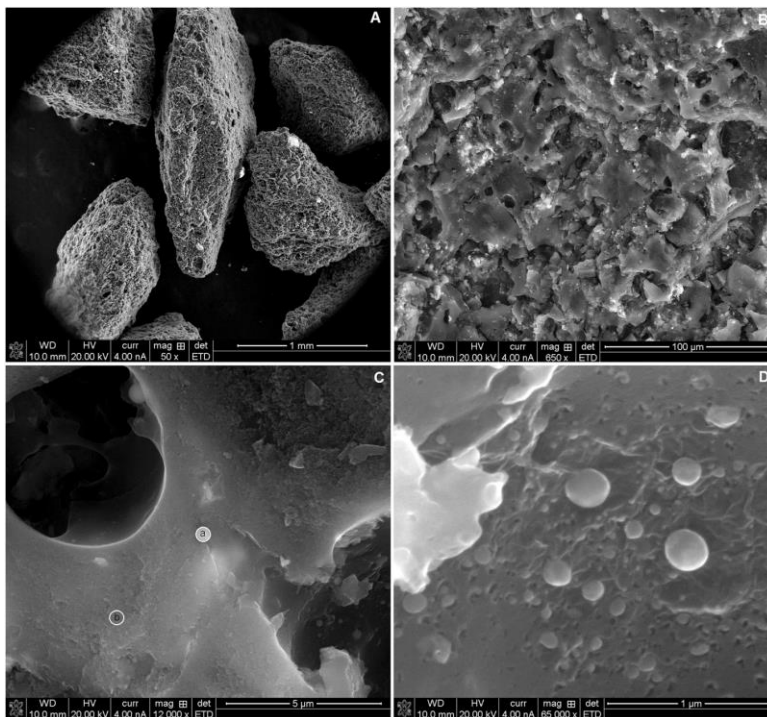


Fig. 4.2. SEM images of Organosorb10 AA at A) 50 \times , B) 650 \times , C) 12,000 \times and D) 65,000 \times magnifications

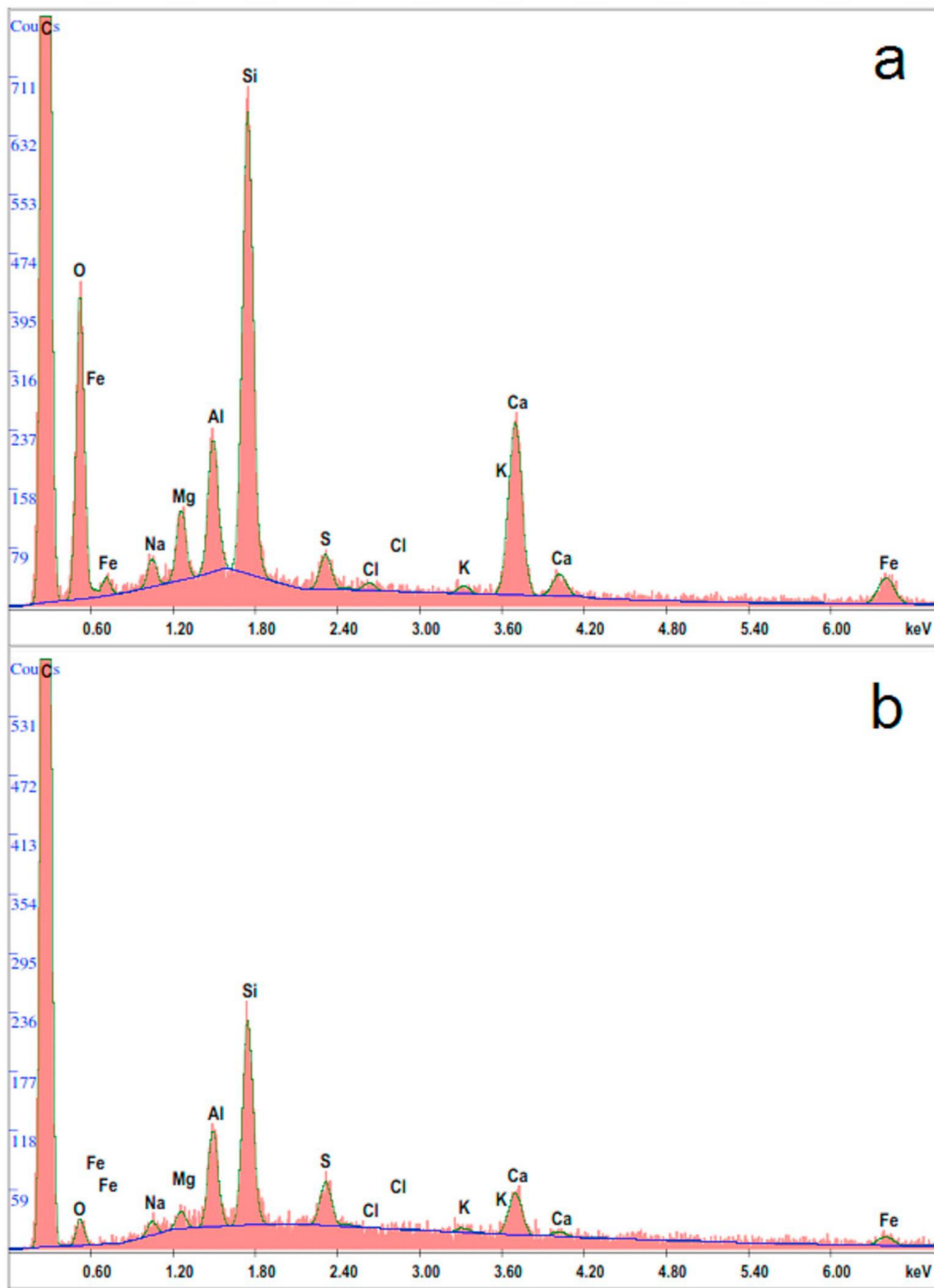


Fig. 4.3. SEM-EPMA spectra of Organosorb10 AA at two different positions indicated in Fig. 4.2C

Table 4.2 Characterization of granulated activated carbons

GAC type	Application for drug adsorption	Specific surface area	Total pore volume	Micropore volume	Mesopore volume	Particle size*
		(m ² g ⁻¹)	(cm ³ g ⁻¹)	(cm ³ g ⁻¹)	(cm ³ g ⁻¹)	
Organosorb11	no	1092± 6.5	0.552	0.513	0.039	0.6-2.36
Organosorb10	no	981± 6.1	0.491	0.454	0.037	0.42-1.7
Organosorb10 AA	before	1014 ± 6.8	0.634	0.364	0.270	0.42-1.7
	after	878 ± 6.7	0.564	0.364	0.202	not measured

Abbreviation GAC=granulated activated carbon.

* According to the specifications of Desotec HQ

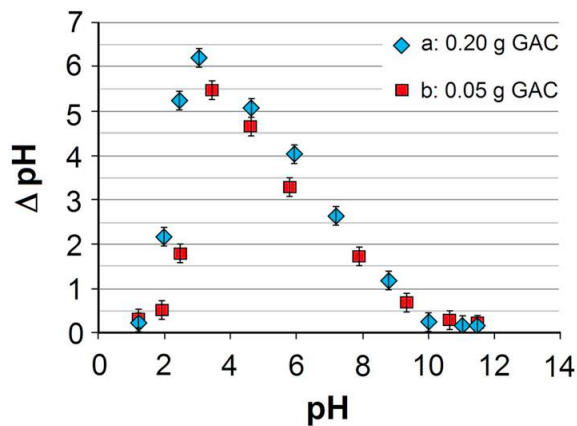


Fig. 4.4. Point of zero charge of Organosorb10 AA

4.2.2 Adsorption isotherms studies and modeling

The adsorption isotherms of DCL and NPR are illustrated in Fig. 4.5. Dots show the determined values, the line demonstrates the Langmuir equation fitted to the data. Applying GAC, the irreproducibility of the adsorbed amounts was considerably greater compared with data using PAC. For these measurements, the complete fraction of GAC was used and the irreproducibility was partly due to the imprecisely defined particle size ($d < 0.42\text{mm}$ in 7% and $d > 1.7\text{mm}$ in 10%). The other reason for the deviation of the adsorbed amounts is disintegration of granules during the experiment. Another difference between the adsorption studied on GAC and PAC was that maximal adsorbed amount (q_m) was considerably larger in the case of PAC. The experimentally measured and calculated maximal adsorbed amounts values expressed as both mmol g^{-1} and mg g^{-1} are summarized in Table 4.3. In the case of NPR, measured data were about two times larger than in the case of DCL applying GAC; nevertheless, the measured maximal adsorbed amounts were similar using PAC. Baccar et al. [194] studied adsorption of DCL and NPR on biochar in the presence of other acidic drugs. The determined maximal adsorbed amounts of DCL was comparable with our results, while those for NPR was the half. Bhadra et al. [232] compiled several q_m data measured by others for DCL on GAC. The values were between 11 and 487 mg g^{-1} ; usually, the lower ones were achieved on native AC, while the higher ones were due to surface modification. Certainly, the modified GACs were prepared only for laboratory use.

Results calculated from the several adsorption isotherm models applied in the present study are also summarized in Table 4.3. The calculated q_m values using the Langmuir model were in good agreement with the experimentally determined ones, the regression coefficient indicated a good fitting to the model ($R^2=0.964\text{--}0.998$). The separation factor (R_L) showed favorable adsorption ($0 < R_L < 1$). Nevertheless, the lower values in some cases were close to zero which could indicate an irreversible adsorption.

By applying the Freundlich model, the regression coefficient was below 0.9 (0.839–0.897) in the case of GAC. Thus, a worse fitting was obtained compared to the Langmuir model. Data obtained by PAC were not suitable to model the Freundlich isotherm because $\ln C_e$ vs. $\ln q_e$ did not result to be linear at low C_e values. At the second part of the curve ($\ln C_e > 0$), fitting was better but worse than in the case of the Langmuir model. At the same time, application of the Temkin model resulted in a worse fitting compared even to the Freundlich one and the predicted q_m values were not comparable with the experimental ones. The Dubinin-Radushkevich (D-R) model is usually applied to determine the activation energy of the adsorption processes. Fitting to the experimental

data was better than in the case of Freundlich and Temkin models but worse than for the Langmuir one. However, a good agreement was achieved between experimental and calculated q_m values. In the case of DCL adsorption onto PAC, only the first section of the curve could be used for modeling because of the non-linearity observed. The determined activation energies were 8.93, 6.62, 16.06 and 16.20 kJ mol^{-1} for the DCL-GAC, NPR-GAC, DCL-PAC and NPR-PAC combinations, respectively.

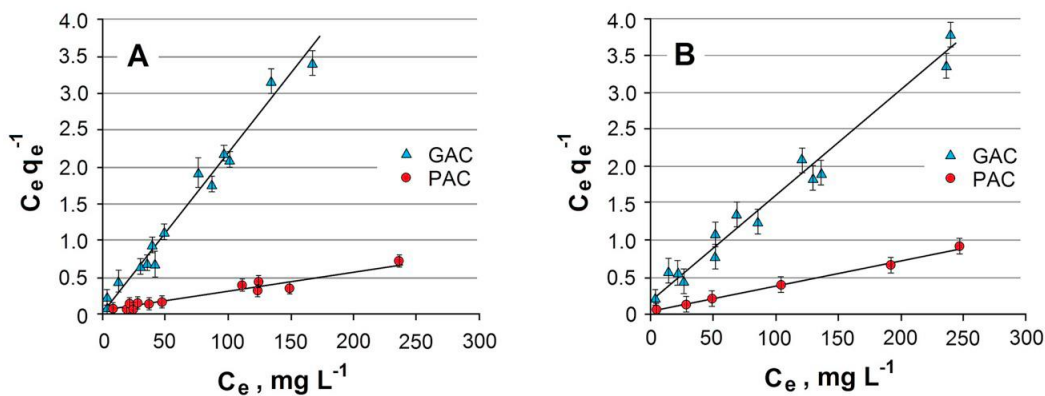


Fig. 5.

Fig. 4.5 Application of Langmuir isotherm (solid line) for the measured data (dots) of A) diclofenac, B) naproxen using granulated activated carbon (GAC) and pulverized GAC (PAC).

Finally, the model calculation with the Redlich–Peterson equation confirmed conformity with the Langmuir model because the β values were close to one (0.885–0.928) except for DCL in the case of adsorption onto GAC. In this latter case, the discrepancy can be explained by the quite big irreproducibility of the measured data. From the obtained results, it can be concluded that the adsorption process followed the Langmuir model.

4.2.3 Thermodynamic studies and modeling

Data of the adsorption isotherms at different temperatures are summarized in Table 4.4. Slight temperature dependence was observed in the experimentally determined q_m values. Using DCL and CRB, the adsorbed quantities measured at 25 °C was a little bit smaller than at the other two temperatures, while in case of NPR, the adsorbed quantities were larger. Among the q_m values determined at 35 and 45 °C, there were no considerable differences for any three compounds. The RSD values increased with the elevated temperatures. Due to the increasing error and the small differences among the measured the adsorbed quantities, there was impossible to reveal any reliable

trend in agreement with the measured data. Adsorption of DCL onto AC was studied at the same temperatures by de Franco et al. [211]. They have found a slight increase in the adsorption capacity as a function of temperature.

For modeling, those two adsorption isotherm equations were applied for which the best fittings were achieved at 25 °C using individual solutions, namely Langmuir and D-R models. The calculated q_m values for both models were in good agreement with the experimentally measured ones but again not any trends could be observed.

Although the D-R model resulted in very low regression coefficients, the activation energy could be calculated in this case. The best fitting was obtained for 25 °C and the calculated activation energies were between 5 and 7 kJ mol⁻¹ for each compound. Most probably, the lack of temperature dependence is the consequence of the low activation energies. Thus, a temperature value of 25 °C provides enough energy for the diffusion and adsorption of the investigated compounds.

Table 4.3 Comparison of adsorption parameters of DCL and NPR using different isotherm models

	Parameter	Compounds and types of activated carbons			
		DCL-GAC	DCL-PAC	NPR-GAC	NPR-PAC
Experimental	q_m mg g ⁻¹	49.5	323	82.0	281
	q_m mmol g ⁻¹	0.156	1.02	0.325	1.11
	RSD, %	6.8	2.2	6.0	0.3
Langmuir model	q_m mg g ⁻¹	46.55	318	77.30	280
	q_m mmol g ⁻¹	0.146	1.00	0.306	1.11
	b L mg ⁻¹	0.51	0.16	0.06	0.42
	R_L	0.007-0.282	0.020-0.549	0.057-0.784	0.008-0.324
	R^2	0.974	0.997	0.964	0.998
Freundlich model	K_F mg g ⁻¹ (Lmg) ^{1/n}	6.134	168,3 ^a	11.06	138.1 ^a
	n	2.19	8.67 ^a	2.72	6.92 ^a
	R^2	0.838	0.963 ^a	0.897	0.976 ^a
Tempkin model	K_T	1.012	14.85	1.269	144.4
	q_m mg g ⁻¹	10.01	41.15	12.96	28.02
	q_m mmol g ⁻¹	0.031	0.129	0.051	0.111
	R^2	0.888	0.966	0.824	0.986
Dubinin-Radushkevich model	q_m mg g ⁻¹	55.67	299.0 ^b	79.36	281.1
	q_m mmol g ⁻¹	0.175	0.940 ^b	0.316	1.114
	E kJ mol ⁻¹	8.93	16.06 ^b	6.62	16.20
	R^2	0.957	0.943 ^b	0.819	0.968
Redlich-Peterson model	K_{RP}	7.8	1650	4.3	1759
	α_{RP}	0.58	9.6	0.085	10.0
	β	0.706	0.885	0.928	0.909
	R^2	0.852	0.970	0.915	0.952

Main abbreviations: DCL=diclofenac, NPR=naproxen, GAC=granulated activated carbon, PAC=pulverized activated carbon, q_m = maximal adsorbed amount, RSD=relative standard deviation, R^2 =regression coefficient.

^a Second part of the adsorption curve ($\ln C_e > 0$).

^b First part of the adsorption curve

Table 4.4 Comparison of adsorption parameters in the mixture of three compounds using different isotherm models at various temperature

Model	Parameter	DCL			NPR			CRB		
		Temperature, °C								
		25	35	45	25	35	45	25	35	45
Experimental	q_m mg g ⁻¹	43.72	55.34	53.07	39.11	32.53	35.86	90.03	113.6	118.2
	q_m mmol g ⁻¹	0.137	0.174	0.167	0.155	0.129	0.149	0.381	0.481	0.500
	RSD, %	8.5	5.0	5.9	3.3	6.7	4.5	2.4	7.2	11.5
Langmuir	q_m mg g ⁻¹	47.39	59.52	55.25	45.25	34.72	32.57	107.5	110.0	105.3
	q_m mmol g ⁻¹	0.149	0.187	0.174	0.179	0.138	0.129	0.455	0.465	0.446
	b L mg ⁻¹	0.022	0.030	0.164	0.028	0.037	0.305	0.023	0.517	0.864
	R_L	0.476-0.132	0.400-0.100	0.109-0.020	0.417-0.107	0.351-0.083	0.062-0.011	0.465-0.127	0.037-0.006	0.023-0.004
	R^2	0.914	0.882	0.972	0.969	0.831	0.903	0.991	0.979	0.980
Dubinin-Radushkevich	q_m mg g ⁻¹	48.41	62.10	48.36	40.86	32.34	31.98	104.6	139.5	115.8
	q_m mmol g ⁻¹	0.152	0.195	0.152	0.162	0.12	0.127	0.480	0.590	0.490
	E kJ mol ⁻¹	5.76	6.82	*	6.94	7.30	*	5.13	10.08	15.89
	R^2	0.824	0.591	3.00E-05	0.848	0.264	0.116	0.899	0.447	0.405

Main abbreviations: CRB=carbamazepine, DCL=diclofenac, NPR=naproxen, R^2 =regression coefficient, RSD=relative standard deviation.

* Activation energy, E was not calculated due to the very low correlation coefficient

4.2.4 Kinetic studies and modeling

Results obtained for the kinetic studies are summarized in Table 4.5. The PFO rate constants were 0.076 min^{-1} , on average, for each pharmaceutical in the individual solutions. In the three-component systems, the adsorption rate constants were 0.114, 0.125 and 0.157 min^{-1} for DCL, NPR and CRB, respectively. The results are demonstrated in Fig. 4.6, as well, where the kinetic behavior of individual solutions was compared with the three-component ones. Although the reaction was monitored for 1 h, equilibrium was reached after 30 and 20 min in the individual and three-component solutions, respectively (see the last points of the curves in Fig. 4.6). The PFO model fits very well to the data ($R^2=0.999\text{--}0.981$) and even the predicted q_e values are in good agreement with the experimentally measured ones. For studying the effect of the particle size on the adsorption rate, experiments were repeated with a smaller GAC particle size. The obtained data could be characterized with the same linear fitting. Thus, the same pseudo-first order rate constants were obtained within an acceptable margin of error. Therefore, the two series of measurements were evaluated together. By applying PAC, adsorption rate was so intense that the compounds could not be detected in the three-component systems within 30 s. The increase in the adsorption rate constant by applying PAC can be explained by the higher availability of inner pores of GAC as a consequence of pulverization. At the same time, the use of GAC having different particle sizes did not influence the adsorption rate constant because the structure of granules was not destroyed.

For the deeper understanding of the adsorption kinetics, other models were also used for data evaluation. Unfortunately, both PSO and Elovich models provided worse fittings in terms of the regression coefficients and the error of fitting. The IPD model is usually applied to study those cases for which diffusion is expected to have a role in the adsorption process. According to this model [Table 4.1, Eq. (4.10)], the linear equation should be a straight line characterized by a slope indicated by k_{ip} when the intra-particle diffusion is the rate-determining step. Moreover, c_{ip} (intercept of the linear equation) should be zero if diffusion is the sole rate-limiting step of the adsorption [291, 294]. From the data presented in Table 4.5, it can be concluded that the intra-particle diffusion has a role in the adsorption of all studied compounds. In the case of CRB and NPR, the calculated intercepts were very close to zero both for the individual and three-component solutions. Values close to zero indicated that intra-particle diffusion was the only rate limiting step. Nevertheless, the negative values of the c_{ip} showed that fitting was not completely adequate. The measured values formed slight S-shape curves resulting in a small negative intercept after linearization. Adsorption of DCL in an individual solution resulted in $c_{ip}=0.675 \text{ mg g}^{-1}$. This value suggests that the intra-particle diffusion

has a role in the adsorption but it is not the sole rate-determining step. The adsorption process for DCL is even more complicated in the three-component solutions because the linearized model equation resulted in large negative intercept while removal of DCL from the system is delayed at the beginning due to the competition with the other two compounds.

The adsorption kinetics of the investigated drugs is usually modeled with PFO and PSO models [e.g. 194, 223, 232]. The calculated rate constants are not comparable because of the different experimental conditions. Comparison of single and multi-component solutions is usually not performed. Therefore, competition of compounds is usually not investigated in the literature. Our results clearly demonstrate that the target analytes can influence adsorption of each other.

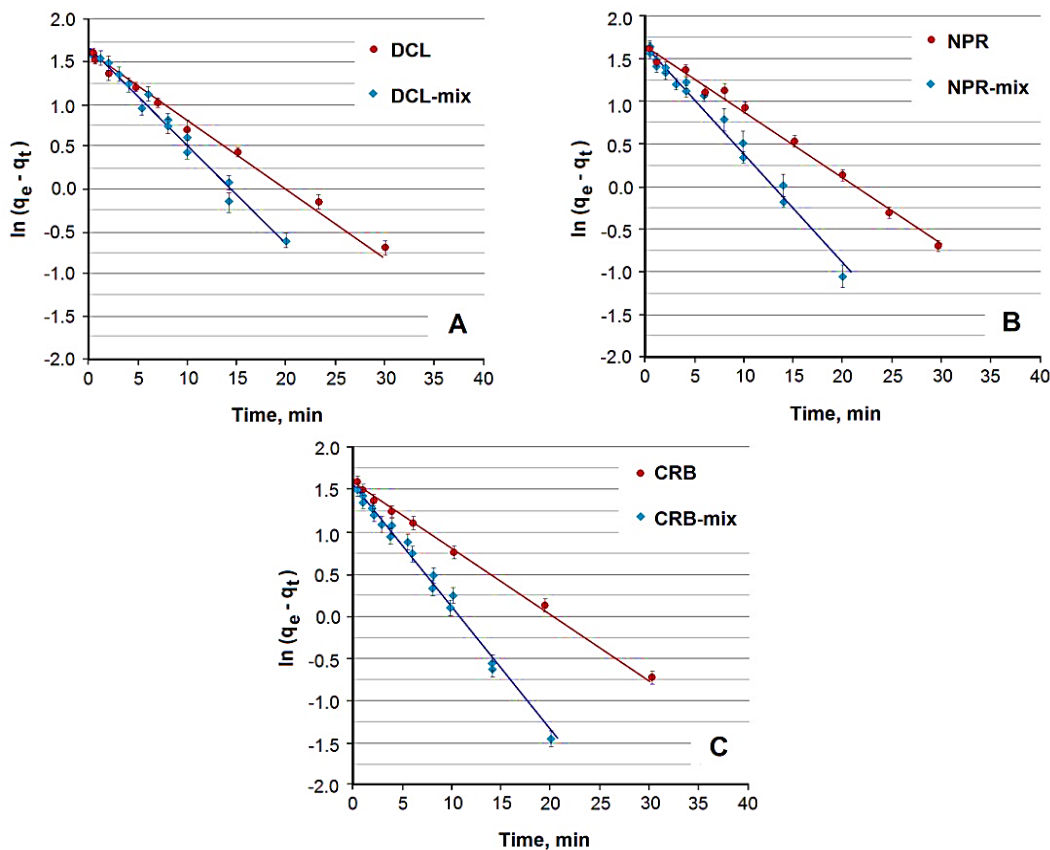


Fig. 4.6. Application of pseudo first-order kinetics model (solid line) for the measured data (dots). A) Diclofenac (DCL); B) naproxen (NPR) and C) carbamazepine (CRB) in individual as well as three-component system (abbreviated as *mix* in the figure legends).

Table 4.5 Kinetic parameters of adsorption in single and in three-component solutions evaluated by various kinetic models

Model		Single solutions			Mixture of three compounds		
		CRB	NPR	DCL	CRB	NPR	DCL
Experimental	$q_e \text{ mg g}^{-1}$	4.75	4.72	4.98	4.98	4.81	4.92
	$q_e \text{ mmol g}^{-1}$	0.020	0.019	0.016	0.021	0.019	0.019
	RSD, %	2.4	2.8	3.7	2.9	4.6	5.3
Pseudo first order	$q_e \text{ mg g}^{-1}$	4.77	5.07	4.47	5.05	5.23	5.42
	$q_e \text{ mmol g}^{-1}$	0.020	0.020	0.014	0.021	0.021	0.017
	$k_1 \text{ min}^{-1}$	0.076	0.075	0.076	0.157	0.125	0.114
	R^2	0.999	0.997	0.993	0.998	0.989	0.981
Pseudo second order	RSD %	1.65	2.75	3.55	1.94	3.60	4.82
	$q_e \text{ mg g}^{-1}$	5.57	5.93	5.46	5.49	7.42	12.73
	$q_e \text{ mmol g}^{-1}$	0.024	0.024	0.017	0.020	0.029	0.040
	$k_2 \text{ min}^{-1}$	0.021	0.013	0.028	0.040	0.011	0.002
Elovich	R^2	0.994	0.986	0.993	0.997	0.963	0.851
	RSD %	4.15	5.27	3.98	1.98	7.04	18.61
	$\alpha \text{ mg (g min)}^{-1}$	1.137	1.081	1.505	1.32	0.761	0.909
	$\beta \text{ g mg}^{-1}$	1.144	1.124	0.944	1.302	1.408	1.287
	R^2	0.980	0.963	0.989	0.982	0.966	0.937
	RSD %	9.07	8.90	4.70	4.62	6.74	9.07

continued

Intra-particle diffusion	$c_{ip} \text{ mg g}^{-1}$	0.008	-0.030	0.675	-0.063	-0.013	-1.096
	$k_{ip} \text{ mg (g min)}^{-0.5}$	1.289	0.794	0.583	1.162	0.928	1.326
	R^2	0.989	0.987	0.977	0.979	0.986	0.990
	RSD %	6.09	5.49	5.49	3.05	4.45	3.41

Main abbreviations: DCL=diclofenac, CRB=carbamazepine, NPR=naproxen, RSD=relative standard deviation; R^2 =regression coefficient.

4.2.5 Model solutions and secondary sewage water in semi open system

The adsorption characteristics of CRB could not be studied similarly to NPR and DCL due to its low water-solubility. To achieve this, I applied a different approach that permits study of adsorption of such compounds without addition of methanol (as a solubilizing agent), commonly applied for similar cases. In the semi-open system experiments, the liquid phase was renewed after each sampling with the three-component standard solution without removal of the GAC particles. In this way, GAC could be saturated gradually. The hereby proposed semi-open system permits sampling before the reactor is replenished with a new aliquot of the pharmaceutical standard solutions. Therefore, this procedure can be continued arbitrarily in time. This experimental design is suitable to study interaction of several compounds during adsorption in multi-component model systems. Furthermore, this method can be considered as a model for GAC-applying STPs working under batch conditions.

By applying the hereby developed method, single drug component systems were studied at first. Removal efficiency and the total adsorbed amounts of pharmaceuticals as a function of time are shown in Fig. 4.7A. The removal efficiency was defined as the ratio $q_t / (q_t + c_t) \times 100\%$ (where q_t is the total adsorbed amount onto GAC and c_t is the total amount of drugs introduced into the liquid phase until t time). At the termination of the experiment, the removal efficiency and the q_t were 68.9%, 63.0%, 52.5% and 26.0 mg g⁻¹ (0.103 mmol g⁻¹), 23.1 mg g⁻¹ (0.073 mmol g⁻¹), 16.3 mg g⁻¹ (0.069 mmol g⁻¹) for NPR, DCL and CRB, respectively. The order of adsorption efficiency was NPR > DCL > CRB. Nevertheless, the adsorbed amounts and the adsorption efficiency order were different for the three-component system (Fig. 4.7B). At the termination of the experiment, the removal efficiency and the q_t were 55.7%, 44.4%, 49.2% as well as 18.3 mg g⁻¹ (0.073 mmol g⁻¹), 12.9 mg g⁻¹ (0.041 mmol g⁻¹), 14.9 mg g⁻¹ (0.063 mmol g⁻¹) for NPR, DCL and CRB, respectively (Table 4.6). Thus, the following order could be established for the adsorption efficiency: NPR > CRB > DCL. The adsorbed amounts of the individual compounds decreased in the three-component system compared to the single component one by about 13%, 19% and 3% for NPR, DCL, CRB, respectively. Competition of other compounds on DCL adsorption was studied by Sotelo et al. [282] under batch conditions. According to their observation, adsorption of DCL decreased by 30% due to competition. In the present study, at the termination of the experiment, the sum of the adsorbed amount (0.177 mmol g⁻¹ = 0.073 + 0.041 + 0.063 for NPR, DCL and CRB, respectively), was 0.177 mmol g⁻¹ for the three component containing system and it is less with 28% than the adsorbed amounts for adsorbates in single systems together (0.245 mmol g⁻¹). In the next step, removal

efficiencies of the investigated drugs by GAC in the semi-open system were compared for MSW and SSW. First of all, the initial concentration of the target analytes in the SSW sample was determined and they were found to be 1.01, 0.04 and 1.63 ng L⁻¹ for CRB, NPR and DCL, respectively. Due to the low concentration of these compounds, SSW could be spiked with the three compounds of interest. The experiments were performed with large amounts of GAC for which competition among these drug molecules can be excluded. The results obtained using MSW can be seen in Fig. 4.8A and Table 4.6. It is clear from the results that 5 g GAC removed completely the drugs from the MSW. This amount of GAC was able to efficiently clean the MSW between 1.5 and 6 h, while the solution above GAC was replaced regularly with new aliquots of the untreated sample. In Fig. 4.8B–C–D, removal efficiencies from SSW as a function of time can be seen for CRB, NPR and DCL, respectively. All these results are compiled in Table 4.6. Applying 5 g of GAC, complete removal of the target analytes could be achieved starting from the first hour until the termination of the experiment. Nevertheless, adsorption efficiencies decreased by 5%, 3% and 3% for CRB, NPR and DCL, respectively, when a smaller amount (i.e., 2 g) of GAC was used. Similar experiments were performed by Bo et al. [230] under batch conditions using SSW but, in their case, complete removal of the contaminants was not achieved. On the basis of our results, it can be concluded that the semi-open system can serve as a model for an STP working under batch conditions because periodic and partial removal of SW above sludge during wastewater treatment can be applied. In the present work, sludge was substituted by GAC and the purified SSW was replenished by the untreated one.

In order to determine suitability of GAC utilization in STPs, it is important to clarify the desorption mechanism from the exhausted GAC. Thus, desorption was investigated at different pHs. According to the obtained data, the leaching extent of the adsorbate from the GAC was the largest in the case of CRB but <0.4% independently of the pH of the leaching solution. However, desorption was negligible in the case of the other two drugs; the concentration in the leaching solution was below the limit of quantification (LOQ). Thus, the adsorption can be considered practically irreversible.

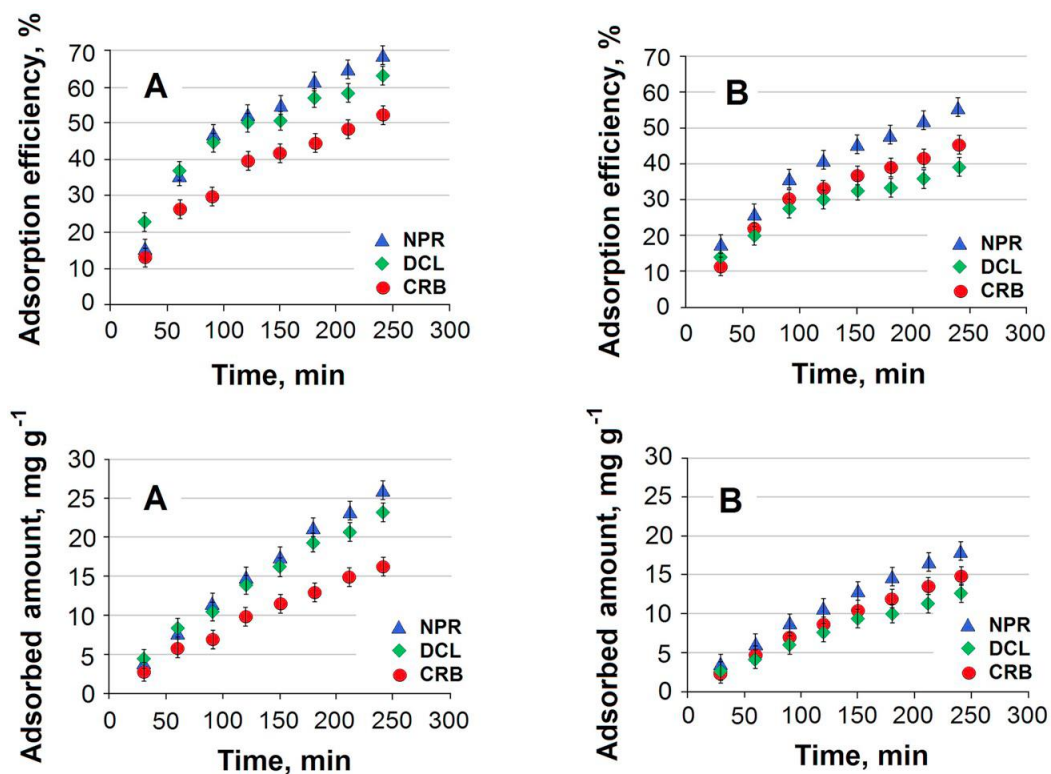


Fig. 4.7. Adsorption efficiencies and the total adsorbed amount for naproxen (NPR), diclofenac (DCL), and carbamazepine (CRB) as a function of time in a semi-open system for A) single component solution and B) three-component system

Table 4.6 Comparison of results obtained in a semi-open system: effect of sample type and amount of GAC on the adsorption efficiency and the adsorbed amount

Sample	Mass of GAC, g	t, h	Adsorption efficiency, %			Adsorbed amount, mmol g ⁻¹		
			CRB	NPR	DCL	CRB	NPR	DCL
MS single	0.1	4	52.5	68.9	63.0	0.069	0.103	0.073
MS mixture	0.1	4	49.2	55.7	44.4	0.063	0.073	0.041
MSW mixture	1	6	91.5	91.3	91.5	0.050	0.041	0.037
	5	6	99.8	100	100	0.011	0.010	0.008
SSW mixture	1	6	87.7	91.7	91.4	0.030	0.035	0.027
	2	6	95.1	97.1	97.0	0.023	0.027	0.019
	5	6	99.8	100	100	0.011	0.008	0.008

Abbreviations: CRB=carbamazepine, DCL=diclofenac, GAC=granulated activated carbon, MS=model solution, MSW=model sewage water, NPR=naproxen, SSW=secondary sewage water.

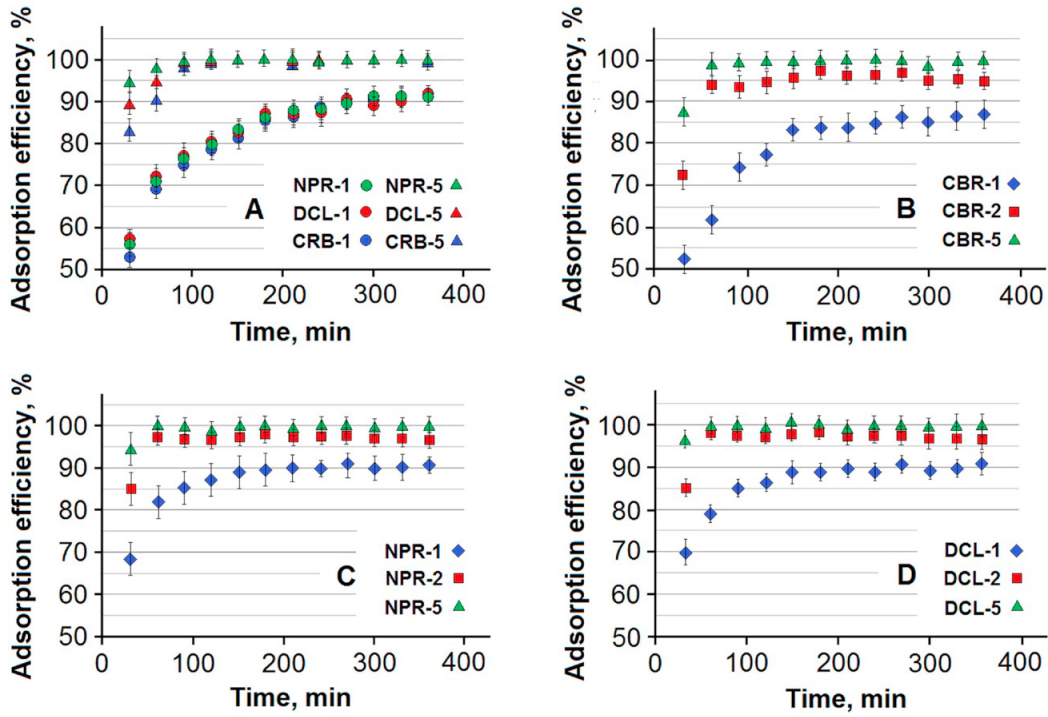


Fig. 4.8. Adsorption efficiencies for naproxen (NPR), diclofenac (DCL) and carbamazepine (CRB) as a function of time in a semi-open system applying model sewage water (A) and secondary sewage water (B, C, D) by using different amounts of granulated activated carbon (GAC). Figure legends: NPR-1, DCL-1, CRB-1; NPR-2, DCL-2, CRB-2 and NPR-5, DCL-5, CRB-5 correspond to sets of NPR, DCL and CRB using 1, 2 and 5 g of GAC, respectively.

4.2.6 Adsorption mechanism

The studied Organosorb10 AA contains non-polar pores of carbon matrix substituted with polar functional groups (carboxylic, silanol) on its surface as well as deeper, inside the granules. The non-polar part of pharmaceuticals can be bound to similar pores by Van der Waals forces and they should fit into the pores as much as possible depending on their molecular size and geometry. Besides that, the non-protonated polar part of compounds can be immobilized by the polar functional groups (silanol) of the carbon skeleton with H-bonds. Both the equilibrium and kinetic measurements demonstrated that adsorption of DCL can be characterized by the smallest q_m and rate constants compared with the others at 25 °C. Study of the adsorption process in three-component solution revealed that two effects, namely competition and enhancement arose among the compounds. In the semi-open system, decrease of the efficiency and adsorbed amount for each pharmaceutical is a clear sign of competition for the binding sites and it is also clear that adsorption of DCL was the least favorable. This can be explained with the characteristics of DCL (Table 4.7), namely, it cannot fit well into the non-polar pores. This can be derived from its nonplanar molecular geometry (spherical shape, spatial position and large fill space of chlorine atoms, position of the aromatic rings situated in different planes), lack of condensed aromatic rings, which would be advantageous for binding to the non-polar carbon skeleton. Therefore, free diffusion of DCL is limited and DCL can be substituted by other compounds in the case of competition. Diclofenac can be bound to the silanol groups by H-bonds through its deprotonated carboxylic group.

Adsorption of NPR was favored from both single and three-component aqueous solutions at 25 °C and its q_m value was the highest due to its size and molecular geometry. Naproxen can enter into the pores with its non-polar side by diffusion due to its elongated, flat shape and smaller size compared to DCL. It can be immobilized by the silanol groups similarly to DCL. When GAC was pulverized, the difference in MAC values for these two compounds disappeared because the structure of granules was destroyed and the inner pores became more accessible.

The CRB molecule has a similar molecular geometry to NPR but it has a slightly basic character. Being the least polar compound among all investigated drugs, it binds well to the non-polar carbon pores and with H-bonds to the silanol groups, as well. The rate-determining step for adsorption is the intra-particle diffusion for both aforementioned compounds. Protonation of N atom of CRB by the silanol groups can occur on the surface and, consequently, the positively charged CRB attracts the negatively charged compounds (NPR, DCL) forming multiple layers. Thus, presence of CRB in the three-component system accelerates adsorption (Section 4.2.4) because it

iswell-known that adsorption rate is always greater when adsorption is controlled by electrostatic interaction rather than if it is based only on Van der Waals forces. Therefore, increase of the adsorption rate constant in the three-component system can be attributed to the multiple layers of the adsorbed compounds. Nevertheless, adsorption of DCL is hampered at the beginning in the three-component system. Bhadra et al. [232] summarized the type of interactions proposed for adsorption of DCL under various conditions. Among these, similar type of interactions was listed, i.e., van der Waals, H-bound, electrostatic, hydrophobic, etc. like in the present work.

Adsorption of CRB from the three-component system was studied in aqueous and mixed water and methanol media. In the latter case, adsorption of CRB was more favorable while NPR could be removed at the largest extent from purely aqueous media. While q_m of DCL was similar in the aqueous phase and methanol-water system, q_m for NPR (which showed a real competition with CRB) decreased to the half. From these results, it can be concluded that adsorption can be influenced by methanol. Therefore, the two systems (aqueous and mixed water and methanol media) cannot be compared. Adsorption of CRB in a three-component system using commercial GAC in aqueous methanol systems was studied by Delgado et al. [223]. Although in the abovementioned study, the other two compounds were different from ours, an about three times larger adsorption capacity was observed in a methanol-water system compared to our value. Unfortunately, GAC was not characterized in terms of functional groups. Since contaminated water bases are naturally always aqueous systems, it is better to avoid use of organic solvents. Therefore, we emphasize, hereby, the relevance of the application of a semi-open system for studying adsorption of compounds having diverse and/or low water-solubility.

Table 4.7 Some relevant physico-chemical characteristics of the investigated active ingredients

Compound	pK _a	log K _{ow}	Characterization
DCL	4.0	4.51	Substitution of 1 st six-membered aromatic ring with carboxylic acid residue (polar character) Substitution of 2 nd six-membered aromatic ring with two chlorine atoms (non-polar character) Coupling of two six-membered aromatic rings by a flexible -NH group No molecular planarity Spherical molecular geometry
NPR	4.3	3.50	Substitution of 1 st aromatic ring with carboxylic acid residue (polar character) Substitution of 2 nd aromatic ring with an -OCH ₃ group (non-polar character) Condensed structure of two aromatic rings Planar molecule Elongated and flat molecular geometry
CRB	7	2.47	Coupling of two six-membered aromatic rings with a seven-membered one Molecular planarity Condensed aromatic ring structure Substitution of the seven-membered ring with non-polar, slightly basic urea residue Round and flat molecular geometry

Abbreviations: DCL=diclofenac, CRB=carbamazepine, K_a=acid dissociation constant; K_{ow}=n-octanol-water partition coefficient, NPR=naproxen.

4.3 Conclusions

Commercially available GACs (i.e., Organosorb10 AA) seem to be a promising adsorbent for removal of selected pharmaceuticals from aqueous matrices. Availability of the pores of granules was one of the main factors influencing adsorption. Among other factors, physicochemical characteristics of the investigated molecules (best fitting into the pores, flexibility of the molecular structure and the presence of condensed aromatic rings) were the most important ones. The adsorption and kinetic parameters can be different in the multi-component system from the single one according to the competition between the studied molecules. However in multi-component solutions, not only competition but interaction among the compounds having different chemical characteristics could be observed. Thus, the adsorption rate constant increased.

A semi-open system operating in batch mode with regular substrate supplementation to study adsorption of CRB as low-water soluble compound was set-up and successfully tested. Removal efficiency was nearly 100% from model sewage water (MSW) and secondary sewage water (SSW) spiked with CRB during several adsorption cycles using GAC. In this case, not only competition can be studied but the proposed method can be used as a model for STPs working under batch conditions. Applying GAC in STPs in batch mode, this carbonaceous material can be mixed with sewage water and the decontaminated SSW above the GAC can be partially removed periodically. However, by analyzing the exhausted GAC, it turned out that adsorption taking place in the mesopores and desorption was found to be practically irreversible. On the basis of our results, the exhausted GAC is not suitable for recycling but it can be treated during wastewater sludge treatment. From the results of the present work, it can be concluded that GACs were suitable adsorbents for removal of pharmaceuticals under batch conditions even from SSW.

Chapter 5

Removal of selected pharmaceuticals from aqueous matrices with activated carbon under flow conditions

5.1. Materials and methods

5.1.1 Chemicals

Chemicals and GAC were similar to those used for the batch experiments. Also the solutions were prepared the same way used in the batch experiments. The physico-chemical characterization of the applied GAC has been previously reported in Section 4.1.2.

5.1.2 Set-up of the flow system

The experimental set-up consisted of a 10 L glass container attached to an adsorption column packed with the studied GAC with the aid of Teflon tubing. During the adsorption experiments, several glass columns differing only in diameter and height were tested. At the bottom of the columns, sintered glass frits were built-in (Fig. 5.1). Moreover, the system was equipped with a pre-column for experiments involving SSW. The different amounts of GAC were soaked in deionized water for 24 h prior to the execution of the experiments. The mixtures were gently stirred until all air bubbles were purged out. Then the columns were filled with the suspension. The bed height was measured after each packing and then the mean was calculated. The applied column diameters and bed heights are given in Table 5.1. The GAC particles were transferred quantitatively into the columns with deionized water. The flow rate was set manually before each experiment by determining the time necessary for sampling 1 L of deionized water in adequate graduated cylinders. To control regularly the flow rate ($\pm 1\%$), two (in the case of pre-column system, three) glass stopcocks were used. The zero time of the experiment was fixed when the dead volume of deionized water required to set the flow rate flowed through the column.

The container was regularly replenished with the test solutions. Elution was achieved by the hydrostatic pressure. After each experiment, virgin GAC was used. Experiments were conducted at ambient temperature (24 ± 1 °C).

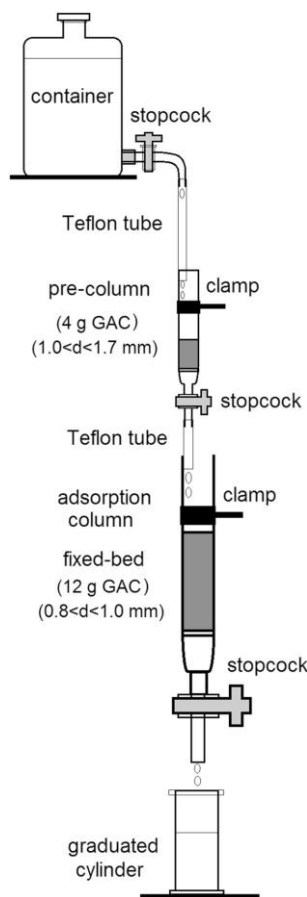


Fig. 5.1. Schematic representation of fixed-bed column system.

GAC: granulated activated carbon, d: particle size of GAC

5.1.3 Sampling of test solutions and model sewage water for HPLC-UV analysis

Effluent was taken in 1 L graduated cylinders. Generally, the last 1 mL of 1 L eluate was subjected to HPLC analysis (Section 4.1.3). After filtration through glass microfiber filter paper of 0.8 μm pore size, samples were stored at 5 $^{\circ}\text{C}$ prior to the HPLC analysis.

Model solutions were prepared with proper dilutions of NPR and DCL standards while the suitable amount of CRB was added in solid form to the two-component solutions and dissolved. The model solutions analyzed by HPLC-DAD-UV contained only these three components in 5 mg L^{-1} concentration. Normally, the pH of the model solutions was approximately 6. If necessary, pH was adjusted with some drops of either 0.1 mol L^{-1} NaOH or 0.1 mol L^{-1} HCl solutions added to the 10 L model solution volumes. Thus, the effect of the initial pH on the adsorption could be excluded.

Table 5.1 Summary of the breakthrough time (t_b), C/C_0^{-1} (%) values and adsorbed amounts by applying 20 L of outlet volume for the target compounds under different experimental conditions of the flow system

Mass of GAC (g) (column diameter: d mm bed height: h mm)	Particle size (mm)	Flow rate (mL min ⁻¹)	t_b (min)			C/C_0^{-1} (%)			Adsorbed amount (mg g ⁻¹)		
			CRB	NPR	DCL	CRB	NPR	DCL	CRB	NPR	DCL
2(d:8, h:160)	0.42-0.80	5	>4000	>4000	3762	3.45	0.80	5.13	48.3	49.6	47.4
2(d:8, h:160)	0.42-0.80	20	32.9	27.8	22.3	23.9	27.0	34.3	38.1	36.5	32.8
4(d:18, h:68)	0.80-1.0	40	22.3	21.6	15.6	19.9	25.6	33.7	20.0	18.6	16.6
4(d:18, h:68)	0.80-1.0	60	9.47	18.3	11.9	30.9	36.4	44.1	17.3	15.7	14.0
8(d:18, h:133)	0.80-1.0	40	<500	<500	109	3.66	4.13	9.74	12.0	12.0	11.3
8 ^a (d:18, h:133)	0.80-1.0	60	<333	<333	50.6	3.94	2.11	9.22	12.0	12.2	11.4
8(d:18, h:133)	0.80-1.0	60	303	134	29.8	5.04	7.46	12.5	11.9	11.6	11.0
8(d:18, h:133)	0.80-1.0	100	12.3	15.0	8.33	14.8	19.7	26.5	10.7	10.0	9.2
8(d:18, h:125)	0.42-0.80	60	39.8	135	26.9	8.87	6.67	11.3	11.4	11.7	11.1
8(d:18, h:187)	1.0-1.7	60	5.87	4.73	4.12	31.4	41.5	47.9	8.7	7.4	6.6
12(d:18, h:241)	0.80-1.0	60	>333	>333	>333	0.75	0.11	4.23	8.3	8.3	8.0
8 ^b (d:18, h:133)	0.80-1.0	60	277	206	35.9	5.42	7.40	12.0	11.8	11.6	11.1
8 ^c (d:18, h:133)	0.80-1.0	60	35.5	31.8	14.3	20.3	24.6	36.7	10.0	9.4	7.9
4 (d:12, h:140)	1.0-1.7	60	>333	>333	208	1.16	0.93	6.40	8.2	8.3	7.8
12 (d:18, h:241) ^c	0.80-1.0										

Abbreviations: C_0 : inlet concentration, C: outlet concentration, CRB: carbamazepine, DCL: diclofenac, NPR: naproxen, d: inner diameter of column, h: height of fixedbed. ^a For single component solutions; ^b Model sewage water; ^c Secondary sewage water.

Model sewage water (MSW) was prepared and analyzed by HPLC-UV in the same way as the model solutions but pH and specific electrical conductivity were set with NaHCO_3 and Na_2HPO_4 to be the same as those of SSW.

Generally, 20 samples were taken during one experiment. In the optimized case, the experiments were continued until 40 L treated water was eluted. If the analyte concentration change in the consecutive samples was $<5\%$, only every second or third sample was analyzed.

5.1.4 Investigation of secondary sewage water

The SSW bulk sample originated from the effluent stream of the STP (with GPS coordinates ($47^\circ 23' 31''$ N, $18^\circ 54' 16.3''$ E) of Érd, a settlement with 70,000 inhabitants, located near the capital city of Hungary. In this plant, conversion of wastewater into an effluent is achieved through a cyclic activated sludge treatment technology.

The initial SSW was characterized by specific electrical conductivity, pH and turbidity according to standard methods MSZ ISO 10523: 2003, MSZ EN 27888: 1998, MSZ EN ISO 7027: 2000, respectively. The concentration of anions (except for hydrogen carbonate and phosphate) and cations were determined by using a DIONEX ICS 5000+ ion-chromatography system (Thermo Scientific, USA). Hydrogen carbonate and phosphate concentrations were determined by titrimetric (MSZ 448 11-86) and spectrophotometric methods (MSZ EN ISO 6878: 2004), respectively. Total organic carbon (TOC) and total nitrogen (TN) concentrations were determined by applying a Multi N/C 3100 TC-TN analyzer (Analytik Jena, Germany) equipped with a non-dispersive infrared detector (for C) and a chemiluminescent detector (for N) according to the international standards being in force (EN ISO 5667-3:1995 and MSZ EN 12260:2004, respectively).

For study of the breakthrough curves, the SSW sample was used after spiking with the three compounds to obtain 5 mg L^{-1} concentration for DCL, NPR and CRB ($0.016, 0.020, 0.021 \text{ mmol L}^{-1}$). Initial and the effluent concentrations of the analytes were determined in the same way as described in Section 4.1.3. The initial pH was not changed. For the adsorption experiments, the column bed contained 8 g of GAC ($0.8 < d < 1.0 \text{ mm}$) and 60 mL min^{-1} flow rate was applied. The optimized set-up of the fixed-bed column system can be seen in Fig. 5.1. Pre-column was packed with 4 g of GAC ($1.0 < d < 1.7 \text{ mm}$) and the adsorption column contained 12 g of GAC ($0.8 < d < 1.0 \text{ mm}$), the flow rate was 60 mL min^{-1} . The other operating conditions were the same as in the case of the model solutions. Moreover, the physico-chemical characterization of two GAC-treated spiked SSW was also done as described above. These two additional 1 L samples were taken from the

effluent of the adsorption column corresponding to the $t=16.7-33.3$ min and $t=316.7-333.3$ min time intervals.

For another suitable aliquot of the SSW, concentration of each analyte was 1000-fold lower (i.e. $5 \mu\text{g L}^{-1}$). In this case, for the quantitative determination of the selected active ingredients in SSW, the effluent samples were filtered subsequently through Whatman™ 0.45 and $0.2 \mu\text{m}$ pore size nylon membrane filters. For pre-concentration of the investigated drugs, SPE was used according to Section 4.1.3.

Quantitative analysis of the compounds was achieved on a Bruker Elute UHPLC equipped with binary pump, autosampler and column oven – coupled to a Bruker Compact quadrupole–time of flight mass spectrometer (MS) (Bruker Daltonik GmbH, Bremen, Germany). For the chromatographic separation, Zorbax Eclipse XDB-C18 (50×4.6 mm i.d., $1.8 \mu\text{m}$ particle size) column was used, equipped with a 5 mm long guard column of the same type (Agilent Technologies Inc., USA). Mobile phase consisted of 0.2% (v/v) formic acid in ultra-pure water (eluent A) and acetonitrile (eluent B). The following gradient elution program was used: 10% B (initial conditions); 2 min, 10% B; 5 min, 50% B; 11 min, 99% B, 14 min, 99% B; 4 min post-run equilibration. The gradient elution method applied was similar to that reported by Campos-Mañas et al. [293].

By performing adsorption experiments at $5 \mu\text{g L}^{-1}$ spiked concentration level, five effluent samples each of 1 L were taken corresponding to the 0-16.7, 66.7-83.3, 150-166.7, 233.3-250 and 316.7-333.3 min time intervals; thus, at the end of each one 1, 5, 10, 15 and 20 L of SSW were conducted through the column, respectively. Sample volume was divided into two equal aliquots and analyte concentrations were determined after SPE by the UHPLC-MS method described above.

5.1.5 HPLC-UV and UHPLC-MS method performance

Assessment of the analytical performance of the LC-based methods applied, recovery and the relative standard deviation (RSD) were determined by spiking the MSW and SSW samples with standard solution at two concentration levels (Table 5.2). Recovery rates were determined with and without applying SPE in the case of the HPLC-UV method. For the UHPLC-MS method, recovery rates were taken from our previous work [180]. For the quantitative determination, a five point calibration was applied. The limit of quantification (LOQ) was considered to be the lowest point of the calibration curve. In the case of SPE, LOQ was calculated for the initial solutions taking into account the enrichment factor. For the mathematical calculations, the Adams-Bohart and the Thomas models were chosen.

Table 5.2 Analytical performance parameters of the applied liquid chromatography-based methods

	Comment	Compound		
		CRB	NPR	DCL
HPCL-UV method				
nominal concentration of MSW (mg L ⁻¹)				
Recovery, %	without SPE	1.00	1.00	1.00
(RSD, %)	by using SPE	98.9 (± 1.5)	99.5 (± 0.8)	99.8 (± 0.5)
spiked concentration of SSW (mg L ⁻¹)				
Recovery, %	without SPE	91.2 (± 4.5)	93.6 (± 4.5)	95.4 (± 3.7)
(RSD, %)	by using SPE	5.00	5.00	5.00
LOQ (µg L ⁻¹)	without enrichment	108.7 (± 6.2)	106.8 (± 5.9)	107.3 (± 6.4)
		88.8 (± 6.5)	91.7 (± 5.5)	93.4 (± 5.7)
UHPLC-MS method*				
spiked concentration of SSW (ng L ⁻¹)				
Recovery, %		100	–	100
(RSD, %)	by using SPE	86.9 (±5.5)	–	80.1 (±9.4)
spiked concentration of SSW (ng L ⁻¹)				
Recovery, %		1000	1000	1000
(RSD, %)	by using SPE	97.8 (±3.2)	79.4 (±6.4)	95.9(±11.8)
LOQ (ng L ⁻¹)	for the initial solution	10	250	25

Abbreviations: CRB: carbamazepine, DCL: diclofenac, LOQ: limit of quantification, MSW: model sewage water, NPR: naproxen, RSD: relative standard deviation, SPE: solid phase extraction, SSW: secondary sewage water.

* Ref. [180]

5.2 Results and discussion

5.2.1 HPLC method performance

The analytical performance parameters applied to the HPLC-UV method are summarized in Table 5.2. For MSW, good recovery and proper repeatability (i.e. low RSD values) were obtained. Nevertheless, the recovery rates decreased in about 5-10% by applying SPE. For the SSW matrix, the mean recovery rate by applying SPE was about 110% indicating coelution of unknown contaminants with the target compounds at a slight extent. At the same time, the mean recovery rate was approximately 90% without applying SPE. Due to the slight difference in the SPE recovery rates, the spiked SSW samples were further analyzed solely by HPLC-UV detection. The LOQ values were about thousand times lower than the spiked concentrations (Table 5.2). Therefore, the method was applicable even for investigation of spiked SSW.

For testing the optimized parameter sets of the fixed-bed column system at the environmentally realistic concentration level (i.e. $\mu\text{g L}^{-1}$), an UHPLC-MS method was chosen [22]. The analytical performance parameters for this case are also demonstrated in Table 5.2. By using this instrumental approach, application of SPE prior to LC-MS analysis was unavoidable since the matrix components of SSW should be removed. As it can be seen from the obtained data, the recovery rates were adequate at the $1 \mu\text{g L}^{-1}$ spike concentration level and the RSD values were acceptable. During the application of this UHPLC-MS method, an 1250-fold enrichment factor was applied, so the LOQ values reported for the target analytes in the present work are referred to the initial SSW.

5.2.2 Results obtained for model solutions

During the experiments, the main parameters of the breakthrough curves (t_b : breakthrough time, C/C_0^{-1} : outlet-to-inlet concentration, m_{20} : adsorbed amount at 20 L of inlet volume) were determined and evaluated. The breakthrough times were considered at $C/C_0^{-1} (\%) = 5\%$. Applying 8 g of GAC, the effect of flow rate was studied and the resulted data are shown in Table 5.1. The breakthrough curves at the highest flow rate (100 mL min^{-1}) are characterized by low t_b , i.e. 12.3; 15.0 and 8.33 min for CRB, NPR and DCL, respectively. The t_b increased drastically with decreasing the flow rate (at 60 mL min^{-1} , t_b 303, 134, 30.5 min for CRB, NPR and DCL, respectively). However, even at the lowest applied flow rate (40 mL min^{-1}), the column breakthrough occurred before the end of the experiment for one compound (DCL) for which the t_b was 109 min. Further reduction of the flow

rate would have been disadvantageous because it would have decreased the total flow capacity of the system. Therefore, the optimization continued by using different amounts of GAC after setting the flow rate to 60 mL min^{-1} . In Fig. 5.2, the above discussed results are demonstrated together with the calculated curves, the latter will be discussed in more detail in Section 5.2.4.

Effect of GAC mass can be seen in Fig. 5.3. At 12 g of GAC, the breakthrough time was not attained ($t_b > 333.3 \text{ min}$) until the termination of the experiments, namely after 20 L of inlet volume for each compound. This experiment was repeated until conducting 40 L of inlet volume through the column but the t_b was not reached ($t_b > 666.7 \text{ min}$). Further continuation was hindered by the gradual clogging of the column resulting in the decrease of the flow rate. Due to the above discussed reasons, 12 g GAC was considered to be the optimal column package mass. Investigation of the non-optimal case (e.g., 4 g of GAC) was necessary to obtain enough data beyond the t_b of the breakthrough curve for modeling purposes.

It was expected to further improve the adsorption efficiency through optimization of the GAC particle size. By using a suitable particle size, column package and flow rate can be increased without the risk of clogging. The effect of particle size is demonstrated in Table 5.1. Using small ($0.42 < d < 0.80 \text{ mm}$) and medium ($0.80 < d < 1.0 \text{ mm}$) GAC particle sizes, the main parameters of the breakthrough curves were similar within the error margin (which is about 4-6%) for all compounds. Application of large particles ($1.0 < d < 1.7 \text{ mm}$) decreased the adsorption efficiencies dramatically. The t_b decreased to 5.87, 4.73, 4.12 min, while C/C_0 (%) increased to 31.4, 41.5, 47.9 and m_{20} decreased to 8.7, 7.4 and 6.6 mg g^{-1} for CRB, NPR and DCL, respectively at the termination of experiment. At this particle size, the increased column void volume decreased the contact time of the dissolved analytes with the GAC surface. Particle size should be chosen as large as possible to avoid clogging during the adsorption process. Therefore, the optimal particle size was considered to be 0.8-1.0 mm for the further experiments.

The breakthrough curves were compared for the single (Fig. 5.4A) and three-component model solutions (Fig. 5.4B). In the individual solutions, the order of adsorption efficiency was $\text{NPR} > \text{CRB} > \text{DCL}$. In the three-component solution, this order was identical at the beginning, but after a certain time, the adsorption order changed to $\text{CRB} > \text{NPR} > \text{DCL}$, and this order remained until the end of the experiment. The same phenomenon occurred under all conditions; while NPR was the most adsorbed compound in the single solution, adsorption of CRB prevailed in the three-component solution demonstrating a competition among the compounds for the surface sites. Similar phenomena was experienced under batch conditions in Chapter 4. Breakthrough time decreased

considerably in the three components system ($t_b > 303, 134, 29.8$ min in the mixture, while $t_b > 333, > 333, 50.6$ min in the single solutions for CRB, NPR, DCL, respectively). However, there is no difference between single or three-component solutions in the total adsorbed amounts, as it is $0.140 \text{ mmol g}^{-1}$ in the single solutions, while $0.137 \text{ mmol g}^{-1}$ in three-component solutions (Table 5.1).

The parameters of the breakthrough curves are summarized in Table 5.1 under other circumstances applied, as well. All the C/C_0^{-1} (%) and m_{20} values corresponded to 20 L of outlet volume. The C/C_0^{-1} (%) < 5% could be reached using lower amounts of GAC (i.e. 2 g) for all compounds as well as when the flow rate was low enough. Exhaustion time (t_{ex}) and, consequently the saturation adsorption capacity (SAC) had never been reached under the applied conditions even at 40 L of outlet volume.

5.2.3 Comparison of adsorption for sewage water with model solutions

The MSW provided somewhat different adsorption characteristics (Table 5.1, row 13) compared to the model solution (Table 5.1, row 6) due to the higher initial pH and specific electrical conductivity values. The higher pH was advantageous for adsorption of the two acidic drugs; breakthrough occurred later (206 and 35.9 min in MSW as well as 135 and 27.9 min in model solution for NPR and DCL, respectively) but it was disadvantageous for the slightly basic CRB; for the latter, breakthrough occurred earlier (277 and 303 min in MSW and model solution, respectively). Nevertheless, differences in the final C/C_0^{-1} (%) values were 7.5, 4.0, 0.8% comparing MS with MSW for CRB, DCL, NPR respectively.

Comparison of the breakthrough curves registered for SSW with those for MSW is demonstrated in Fig. 5.5. The SSW provided remarkably different breakthrough curves from those obtained for the MSW (Fig. 5.5. a, b). The t_b were 35.5, 31.8, 14.3 min, the C/C_0^{-1} (%) values at 20 L of outflow volume were higher by about 15, 17 and 25% compared to the MSW for CRB, NPR and DCL, respectively (Table 5.1, 13th row). Decrease of the adsorption efficiencies is due to the TOC content of SSW, since other organic compounds can also be adsorbed on the GAC.

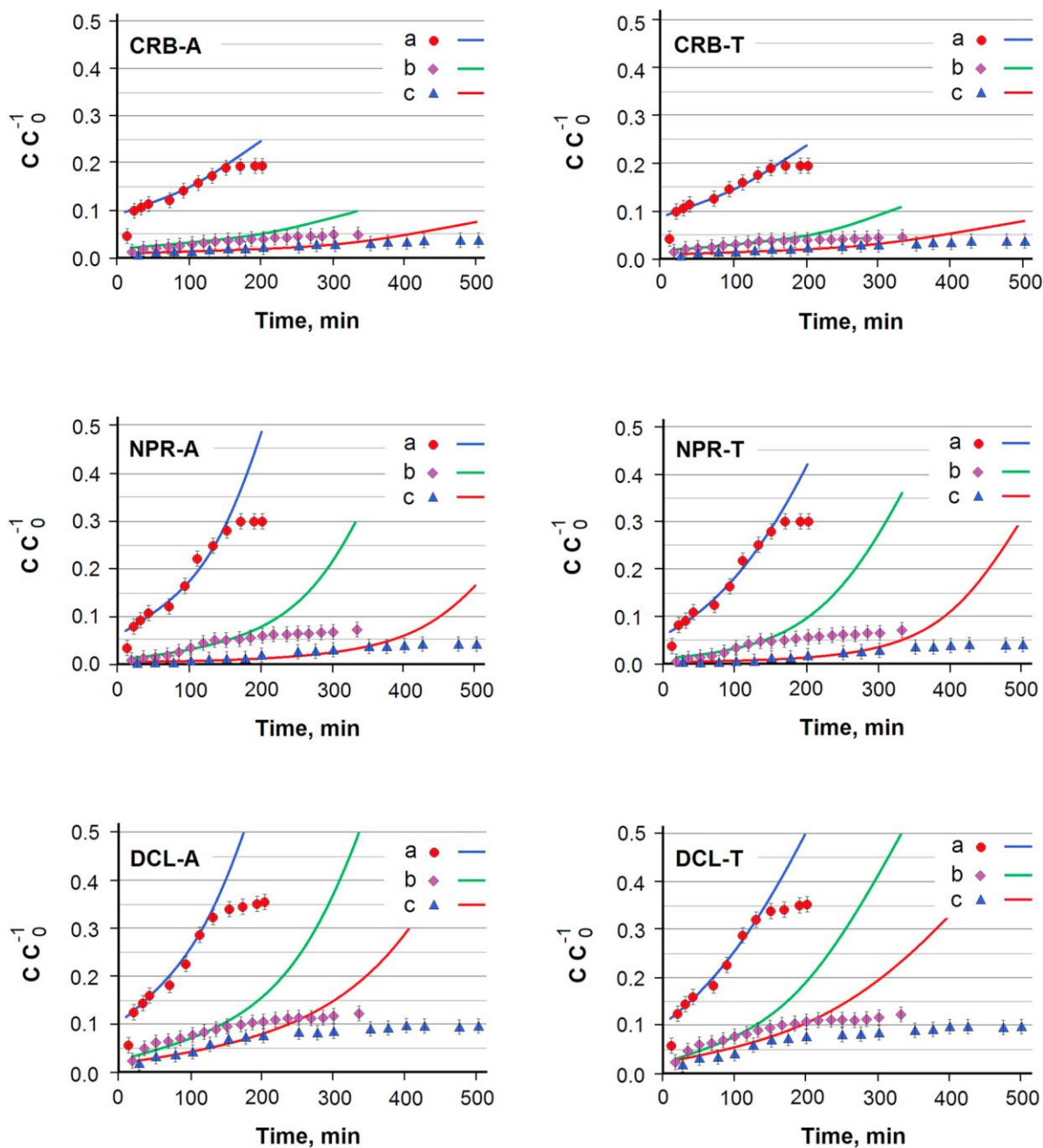


Fig. 5.2. Effect of the flow rate on the column breakthrough curve as a function of time in the three-component solutions. Flow rates applied were as follows: a) 40 mL min⁻¹, b) 60 mL min⁻¹, c) 100 mL min⁻¹. Other parameters: concentration of target compounds: 5 mg L⁻¹, mass of carbon: 8.0 g, particle size: 0.8–1.0 mm. Dots symbolize the experimental data, lines mean the model calculations. Abbreviations: CRB-A, NPR-A, DCL-A measured values and calculated data using Adams-Bohart model for carbamazepine, naproxen, diclofenac, respectively; CRB-T, NPR-T, DCL-T experimental and calculated data using Thomas model for carbamazepine, naproxen, diclofenac, respectively.

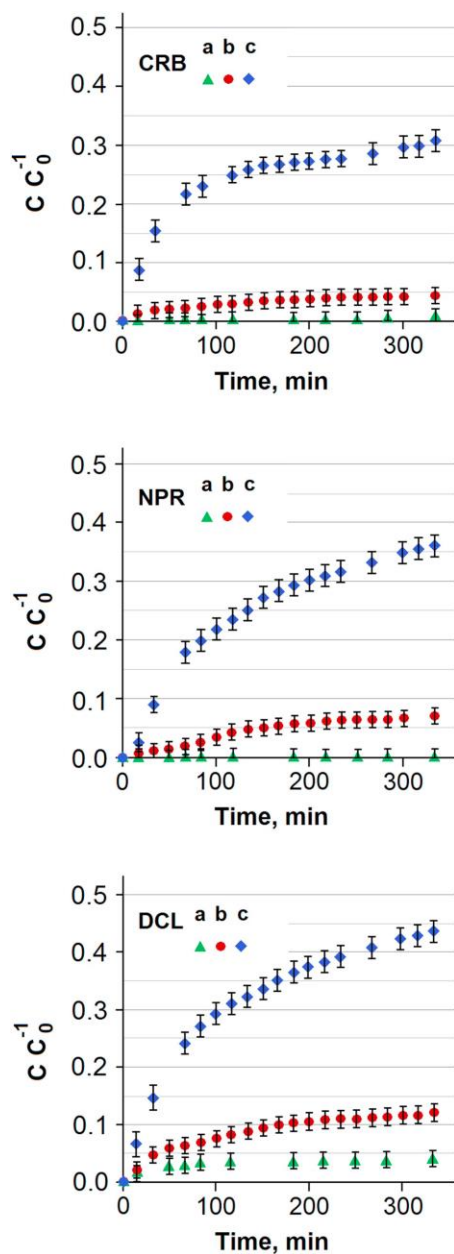


Fig. 5.3. Effect of GAC mass on the column breakthrough curve as a function of time in the three-component solutions. Amounts of GAC were as follows: a) 12.0, b) 8.0 c) 4.0 g. Other parameters: concentration of target compounds: 5 mg L^{-1} , particle size: 0.8–1.0 mm, flow rate: 60 mL min^{-1} . Abbreviations: CRB: carbamazepine, DCL: diclofenac, NPR: naproxen.

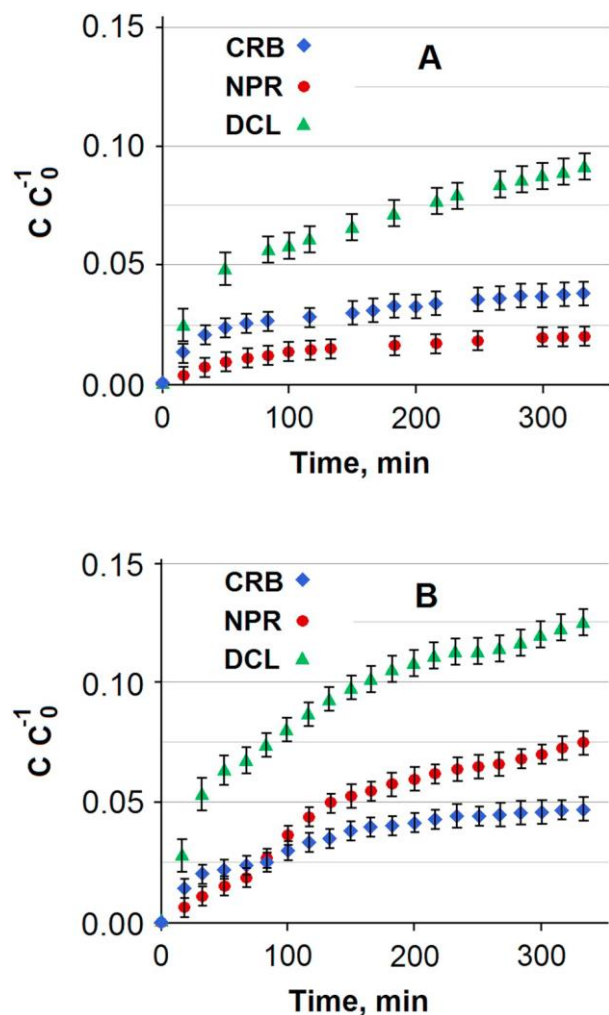


Fig. 5.4. Comparison of the breakthrough curves as a function of time. A) Individual, B) three-component solutions. Other parameters: concentration of target compounds: 5 mg L^{-1} , particle size: 0.8–1.0 mm, flow rate: 60 mL min^{-1} . Abbreviations: CRB: carbamazepine, DCL: diclofenac, NPR: naproxen.

The model calculations (see also Section 5.2.4) predicted a quite large GAC amount for the sufficient removal of the target analytes from SSW and it was clear that probability of column clogging would increase by applying these amounts due to the sample matrix components and turbidity of the SSW. Furthermore, from the point of view of the industrial application, filtration prior to adsorption should be solved in the most cost-effective way decreasing the steps of water purification. Therefore, the applied GAC mass was divided into two portions. Thus, 4 g ($1.0 < d < 1.7$ mm) of it was packed in a pre-column for removal of the solid and suspended matrix components. However, only the relatively large particle sized GAC was able to operate as filter without clogging. Another portion of GAC (12 g) with the mean particle size comprised between 0.8 and 1.0 mm were used to pack the adsorption column. This latter fraction was already used successfully for investigation of model solutions. In spite of the fact that the Thomas model predicted larger amounts of GAC for removal of DCL (i.e. 12+4 g), more than 12 g of GAC bed would not be applicable in the present configuration of the flow system because the flow rate cannot be maintained constant during the whole process even by using a peristaltic pump. The obtained results can be seen in Fig. 5.5.c and Table 5.1. The CRB and NPR were removed successfully and the C/C_0^{-1} (%) values were $< 5\%$ until the termination of the experiment, while the t_b was 208 min in the case of DCL, which is about the 60% of the adsorption time applied.

The physico-chemical characterization of the initial SSW sample is summarized in the first column of Table 5.3. The total organic carbon (TOC), total nitrogen (TN) and pH were 8.5, 5.4 mg L⁻¹ and 7.72, respectively. Concentration of the target compounds, i.e. CRB, NPR and DCL were 5.4, 5.3 and 5.4 mg/L, respectively after spiking with standard solutions to set as a nominal value of 5 mg L⁻¹ for each. Among the cations and anions, Na⁺ and HCO₃⁻ were present in the largest concentration.

As a consequence of the adsorption on GAC, the other physico-chemical parameters of SSW also changed. Thus, turbidity and TOC decreased. However, concentration of the inorganic ions did not change considerably.

Although the inlet concentration was in agreement with literary data, flow rate applied in the present work was 5-10 times (5-100 mL min⁻¹) and the bed height was 2-20 times (7-24 cm) higher compared to some recent reports [180]. The attempt to simulate operating conditions for industrial water treatment technologies increases the potential of the proposed procedure to improve the removal efficiency of persistent organic micropollutants. Therefore, we opted for lowering 1000-fold the inlet concentration level for each analyte and to conduct adsorption experiments with the

most promising parameter set obtained for model solutions. In this case, the initial analyte concentration in SSW was not negligible compared to the spike level (i.e. $5 \mu\text{g L}^{-1}$). Mean concentrations in the SSW samples after spiking were 0.038 , 0.032 and $0.017 \mu\text{mol L}^{-1}$ for CRB, DCL and NPR, respectively. Results of the adsorption process are demonstrated in Fig. 5.6. In this case, 1 L volume of samples was taken, therefore the mean concentration values can be assigned only to time intervals. As it can be seen in Fig. 5.6, C/C_0 (%) values $\leq 20\%$ except for the last data sets. Thus, efficiency of our proposed procedure on fixed-bed column would be approximately 80% even at an industrial scale application.

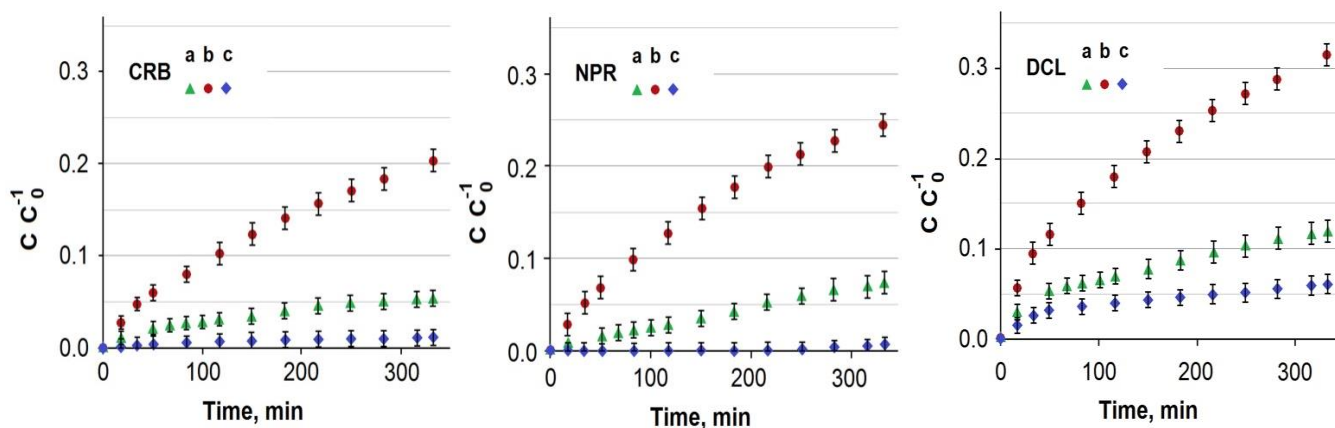


Fig. 5.5 Comparison of the breakthrough curves for a) model sewage water and b) secondary sewage water by using 8 g GAC as well as for c) secondary sewage water using 4+12 g GAC as a function of time in the three-component solutions. Other parameters: concentration of target compounds: 5 mg L^{-1} , particle size: 0.8-1.0 mm, flow rate: 60 mL min^{-1}
 Abbreviations: CRB: carbamazepine, DCL: diclofenac, NPR: naproxen, GAC: granulated activated carbon.

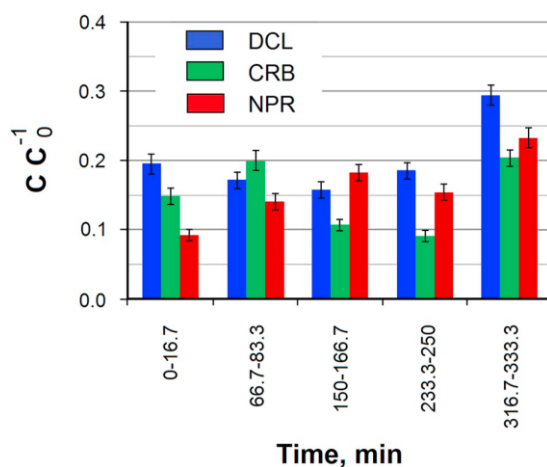


Fig. 6. Determined concentration of compounds in secondary sewage water at different time intervals. Other parameters: 4+12 g granulated activated carbon (GAC), spiked concentration of target compounds $5 \mu\text{g L}^{-1}$, particle size: 1.0–1.7mm in pre-column, 0.8–1.0mm in adsorption column, flow rate: 60 mL min^{-1} . Abbreviations: DCL: diclofenac, CRB: carbamazepine, NPR: naproxen.

Table 5.3 Physico-chemical characterization of secondary sewage water before and after treatment by adsorption on GAC

Parameter	Initial SSW effluent	Treated SSW effluent	
	determined concentration after spiking to obtain 5 mg L ⁻¹ (± RSD, %)	determined concentration at t, sampling time (min)	
		t=16.7- 33.3	t=316.7-333
CRB (mg L ⁻¹)	5.4 (± 0.3)	0.02	0.06
NPR (mg L ⁻¹)	5.3 (± 0.3)	< 0.01	0.04
DCL (mg L ⁻¹)	5.4 (± 0.3)	0.14	0.31
pH	7.72	7.85	7.82
specific electric conductivity (µS cm ⁻¹)	900	590	600
turbidity (NTU)	7.3	<1	<1
TOC (mg L ⁻¹)	8.5	3.9	5.3
TN (mg L ⁻¹)	22	16	20
Na ⁺ (mg L ⁻¹)	199	181	182
NH ₄ ⁺ (mg L ⁻¹)	<0.1	<0.1	<0.1
Mg ²⁺ (mg L ⁻¹)	28	24	25
K ⁺ (mg L ⁻¹)	25	25	25
Ca ²⁺ (mg L ⁻¹)	39	36	35
Cl ⁻ (mg L ⁻¹)	187	172	173
SO ₄ ²⁻ (mg L ⁻¹)	68	61	64
NO ₃ ⁻ (mg L ⁻¹)	99	72	91
NO ₂ ⁻ (mg L ⁻¹)	<0.01	<0.01	<0.01
PO ₄ ³⁻ (mg L ⁻¹)	0.8	0.3	0.7
HCO ₃ ⁻ (mg L ⁻¹)	562	533	562

5.2.4 Modeling of fixed-bed experiments

Results of model calculation with the two generally used mathematical models can be seen in Fig. 5.2 (lines). For the calculation, k_A and N_0 in the case of Adams-Bohart and k_T and q_0 in the case of Thomas model were used as fitting parameters. The other parameters were varied according to the experimental value. In both cases, the models could describe the experimental values only partially. These models cannot follow the very initial and the end parts of experimental data. It is observable that the curves obtained by connecting the measured data break down compared to the calculated ones. From data of the present study, classical S-shaped breakthrough curves with the used GAC could never be obtained. A possible explanation for this is that the applied GAC contain silicates, as it was explained in Chapter 4, possessing a good swelling ability. Therefore, pore size is not constant during the adsorption procedure.

Since any of these two models in the exponential form were not adequate for modeling the complete adsorption process, yet linearization of the Thomas model using those experimental data that gave the best linear fitting proved to be suitable for further model calculation of the intermediate section of the curves. The Thomas model was preferred because we have demonstrated, by performing batch experiments, that the adsorption process of the target compounds could be described by the Langmuir isotherm which is the basic requirement for the application of that model. The adsorption kinetics fulfilled both pseudo first and pseudo second order reactions. The third criteria, namely that there should be no axial dispersion in the adsorption column can be approximated with small column diameter and large height which was accomplished in our case (Table 5.1). In this way, axial dispersion can be minimized at least for a certain part of the breakthrough curves.

Results of the mathematical model calculations are summarized in Table 5.4. For modeling, only that part of the breakthrough curves can be used for which enough experimentally measured data are available after the breakthrough had been attained for each studied compound. Finally, experimental data (series of C/C_0^{-1}) chosen in the case of the model solutions were as follows: 8 g of GAC was and flow rate of 100 mL min^{-1} . After the 1st calculation, the parameter values of the model (i.e. q_0 , k_T) could be calculated. The q_0 values provide the theoretical SAC. The calculated data were higher for each case than the measured ones (Table 5.1, 8th row) because SAC had been never reached during the experiment. During the 2nd calculation, the parameter values obtained in the first case were used to optimize the conditions. Flow rate was set to 60 mL min^{-1} as well as C_0

was set as 5 mg L^{-1} , C/C_0 as 0.05 and t as 333 min (this time is necessary for the outflow of 20 L solution). In this way, amounts of GAC necessary to fulfill the fixed parameters could be calculated. These values were 7.35, 9.90, 11.6 g for CRB, NPR and DCL, respectively. By repeating the experiment with the fixed set of parameters (60 mL min^{-1} , 5 mg L^{-1} , 333 min) and using 12 g GAC (instead of the largest calculated mass), C/C_0 (%) < 5% indicating that breakthrough did not occur (see also Section 5.2.2 and Table 5.1, 12th row).

For modeling of the breakthrough curve for SSW, flow rate was set to 60 mL min^{-1} , GAC mass was 8 g and the spiked concentrations were 5 mg L^{-1} (Table 5.1, 13th row). The model calculation was repeated in the same way as for the model solution. With the first calculation, the values of q_0 and k_T were determined while, in the second one, the required amount of GAC was estimated using the calculated parameters and fixing the others as aforementioned. Thus, the GAC amounts necessary to avoid the column breakthrough during the adsorption were 13.8, 14.7 and 18.3 g for CRB, NPR and DCL, respectively (Table 5.4). The calculated amounts were larger than those applicable in order to avoid clogging (i.e. 12 g). Therefore, it was reasonable to divide the mass of GAC into two parts as mentioned before. The results were already summarized in Section 5.2.3.

From both the adsorption experiments and calculation it turned out that removal of DCL - among the three target analytes - was the biggest challenge. This behavior cannot only be explained with the acidic character of DCL since the other acidic drug studied (NPR) could be extracted without any difficulty. As we demonstrated with our previous batch experiments, shape and size of the target molecules must be taken into account, as well, during adsorption within GAC pores.

Table 5.4 Summarization of model calculations by using the Thomas model

	First model calculation (applied data)		Abbreviation of target compound	Second model calculation (applied data)			Calculated data, 2 nd Mass of GAC (g)
	Mass of GAC (g)	Flow rate (mL min ⁻¹)		Calculated data, 1 st		Flow rate (mL min ⁻¹)	
				q ₀ (mg g ⁻¹)	k _T (L mg ⁻¹ min ⁻¹)		
Three- component model solution (5 mg L ⁻¹ for each compound)	8	100	CRB	24.7	1.17E-3	0.9 96	7.35
			NPR	14.2	2.32E-3	0.9 91	9.90
			DCL	12.5	2.10E-3	0.9 93	11.6
Spiked secondary sewage water (5 mg L ⁻¹ for each compound)		60	CRB	10.5	2.10E-3	0.9 94	13.8
			NPR	10.3	1.87E-3	0.9 88	14.7
			DCL	9.59	1.63E-3	0.9 92	18.3

Abbreviations: CRB: carbamazepine, DCL: diclofenac, NPR: naproxen, GAC: granulated activated carbon, k_T: rate parameter, q₀: maximal adsorption capacity, R²: regression coefficient.

5.3 Conclusions

In the present work, a commercially available GAC was applied successfully for removal of selected drugs from secondary sewage water. From this point of view, not only the effect of the flow rate and mass of carbon bed proved to be important but also the particle size of column package. Operational conditions for the laboratory-scale experiments were chosen in such a way that they would be closer to the applied industrial technologies. Design of fixed-bed column system was performed by mathematical model calculations.

For the successful removal of these drugs by adsorption, it is important a further fine tuning of the parameters obtained under laboratory conditions, as sewage water matrix decreased adsorption efficiency considerably compared to the model solutions. However, application of sewage water seems to be inevitable for the design of fixed-bed column systems. Nevertheless, clarification of the theoretical background for the batch system (adsorption isotherm, kinetics, adsorption capacity and other parameters of the applied adsorbent) and investigation of the model solutions have a high importance as well, particularly from the point of view of modeling. Mathematical modeling can predict properly the optimal parameters of the adsorption process only after clarification of the most important theoretical parameters. Nevertheless, even the best mathematical model can be used only as an estimation of the flow parameters if the adsorbent changes its characteristics during the adsorption process.

Chapter 6

Summary

Adsorption of diclofenac (DCL), naproxen (NPR) and carbamazepine (CRB) from aqueous matrices onto a commercial granulated activated carbon (GAC) has been studied. Model individual, three-component aqueous solutions, model sewage water (MSW) and secondary sewage water (SSW) were studied. Data obtained for DCL and NPR were evaluated by different adsorption isotherm models. Best fitting was reached using Langmuir equation model. Experimental maximal adsorbed amounts were 0.16 and 0.33 mmol g⁻¹ for DCL and NPR, respectively, which increased to 1.02 mmol g⁻¹ and 1.11 mmol g⁻¹ applying pulverized activated carbon. Activation energy calculated at different temperatures was between 5-9 KJ mol⁻¹ for each compound in the three-component systems. By modeling adsorption kinetics, best fitting was obtained by applying the pseudo first order model. Calculated rate constant was about 0.076 min⁻¹ for each compound in individual solutions. However, the obtained values for three-component solutions were 0.16, 0.13 and 0.11 min⁻¹ for CRB, NPR and DCL, respectively. According to model calculations, intra-particle diffusion has a role in adsorption and it is the sole rate determining step for CRB and NPR. Applying a semi-open system, removal efficiency was nearly 100% from MSW and SSW during several cycles. This semi-open system allowed to study i) adsorption of low water-solubility CRB, ii) adsorption of NRP, CRB and DCL at a concentration level similar to that in real samples iii) comparison of drug removal from MSW/SSW, and iv) modeling for sewage water treatment plants. Under flow conditions, effects of GAC amount (4-12 g), flow rate (40-100 mL min⁻¹), and GAC particle size (0.42-0.82, 0.82-1.0 and 1.0-1.7 mm) on the breakthrough curves were investigated. For each column bed, an adequate flow rate could be chosen for which the outlet-to-inlet concentration ratio <0.05 for 20 L outflow volume. Above 1 mm particle size, increase in the void volume decreased adsorption efficiency by 30-40%. Adsorption order changed from NPR>CRB>DCL to CRB>NPR>DCL for the individual and three-component model solutions, respectively. For SSW, adsorption order remained the same but its efficiency decreased by 15, 17 and 25% compared to the MSW for CRB, NPR and DCL, respectively, by applying the same conditions. Nevertheless, removal efficiency in the optimal case for SSW was ≥95% and ≥80% at mg L⁻¹ and µg L⁻¹ concentration levels, respectively. Adsorption process was simulated for MSW and SSW by the Adams-Bohart and Thomas models.

Chapter 7

New Results

T1. By applying nitrogen physisorption measurements, the commercially available Organosorb10 AA activated carbon with a mesopore volume of $0.27 \text{ cm}^3 \text{ g}^{-1}$, that is approximately one order of magnitude larger than those of Organosorb10 and Organosorb11, is recommended for adsorption of selected pharmaceutically active ingredients, namely diclofenac (DCL), naproxen (NPR) and carbamazepine (CRB) from aqueous matrices.

T2. By applying Organosorb10 AA in granulated (GAC) and pulverized (PAC) forms, 0.16 and 0.33 mmol g^{-1} maximal adsorbed amounts were achieved for DCL and NPR onto GAC, respectively, which increased to 1.02 mmol g^{-1} and 1.11 mmol g^{-1} when PAC was used.

T3. A semi-open system operating in batch mode with regular substrate supplementation to study adsorption of CRB as low-water soluble compound was set-up and successfully tested. By applying this system, removal efficiency was nearly 100% from model sewage water (MSW) and secondary sewage water (SSW) spiked with CRB during several substrate supplements using GAC.

T4. Adsorption onto GAC followed the Langmuir model with the best fitting in all cases ($R^2=0.974$ - 0.998). Maximal capacity (q_m) values derived from this model were in agreement with the maximum adsorbed amounts per adsorbent unit. Only a slight temperature dependence was observed in the experimentally determined q_m values. The determined activation energies using Dubinin-Radushkevich model for the adsorption process were 8.93 , 6.62 , 16.06 and $16.20 \text{ KJ mol}^{-1}$ applying DCL-GAC, NPR-GAC, DCL-PAC and NPR-PAC, respectively. According to the model calculations performed, intra-particle diffusion is the sole rate-determining step for adsorption of CRB and NPR.

T5. Adsorption followed pseudo first order kinetics with mean rate constants of 0.076 min^{-1} for each investigated pharmaceutical in the individual solutions. However, in the three-component systems,

the adsorption rate constants were 0.114, 0.125 and 0.157 min^{-1} for DCL, NPR and CRB, respectively, due to the interaction among their molecules.

T6. In the case of secondary sewage water spiked with 5 mg L^{-1} for each compound, 60 mL min^{-1} flow rate, 20 L outlet volume and 0.05 C/C_0 value, breakthrough did not occur using 13.8, 14.7 and 18.3 g GAC ($0.8 < d < 1.0$) amount for CRB, NPR and DCL, respectively. Breakthrough time (t_b) increased drastically with decreasing the flow rate (e.g. to 40 mL min^{-1}) and increasing bed height (e.g. to 187 mm), but decreased with an increase of the particle size.

T7. Due to the higher initial pH and specific electrical conductivity values, MSW provided somewhat different adsorption characteristics (t_b : 277, 206, 35.9 min for CRB, NPR and DCL, respectively) compared to the model solution (t_b : >333, 135 and 27.9 min for CRB, NPR and DCL, respectively) due to the higher organic carbon content of SSW. The desirable 90-95% removal efficiency for the investigated drugs in the flow system was achieved with the following parameter sets for precolumn and adsorption column: diameter of 12 mm, height of 140 mm, particle size of 1-1.7 mm, GAC mass of 4 g as well as diameter of 18 mm, height of 241 mm, GAC mass of 12 g, particle size of 0.8-1.0 mm; flow rate of 60 mL min^{-1} , respectively.

SCI publications constituting the basis of the present dissertation

1. Varga, M., ELAbadsa, M., Tatár, E., Mihucz, V.G. (2019). Removal of selected pharmaceuticals from aqueous matrices with activated carbon under batch conditions. *Microchemical Journal*, 148, 661–672.
2. ELAbadsa, M., Varga, M., Mihucz, V.G. (2019). Removal of selected pharmaceuticals from aqueous matrices with activated carbon under flow conditions. *Microchemical Journal*, 150, 104079.

Acknowledgments

First of all, I praise God for blessings and guidance in fulfilling this goal. I am grateful for the assistance and encouragement of numerous people during this study and wish to sincerely thank them.

My sincere gratitude goes to the head of the group, Prof. Gyula Zárny for his great help, direction and guidance. He supported me from the very beginning throughout my PhD studies.

I would like to express my sincerest gratitude to my supervisor, Dr. Viktor G. Mihucz, for his guidance, advices, constructive suggestions and support that helped me throughout all my research work.

I also owe thanks to Dr. Margit Varga for her continuous support, patience and guidance and her great help in the experimental part and preparation of my publications.

I would like to express my deep gratitude to Dr. Enikő Tatár for her help throughout all my stay in Hungary. She has offered her time to help me in my hardest days. Actually, there are no words that could describe what she has done for me.

Last but not least, special gratitude to my parents, my beloved Israa, my beloved sons Osama and Ahmed, and beloved daughter Shaima who have been a great source of motivation and inspiration to me.

References

- [1] Bu, Q., Wang, B., Huang, J., Deng, S., Yu, G. (2013). Pharmaceuticals and personal care products in the aquatic environment in China: A review. *Journal of Hazardous Materials*, 262, 189-211.
- [2] European Federation of Pharmaceutical Industry and Associations (EFPIA), 2018, *The Pharmaceutical Industry in Figures Key Data 2018*.
- [3] OECD. (2014). *Health at a Glance: Europe 2014*. OECD publishing 2. Paris: OECD.
- [4] Fekadu, S., Alemayehu, E., Dewil, R., Van der Bruggen, B. (2019). Pharmaceuticals in freshwater aquatic environments: A comparison of the African and European challenge. *Science of the Total Environment*, 654, 324-337.
- [5] López-Pacheco, I., Silva-Núñez, A., Salinas-Salazar, C., Arévalo-Gallegos, A., Lizarazo-Holguin, L., Barceló, D., Parra-Saldívar, R. (2019). Anthropogenic contaminants of high concern: Existence in water resources and their adverse effects. *Science of the Total Environment*, 690, 1068-1088.
- [6] Wang, J., Wang, S. (2016). Removal of pharmaceuticals and personal care products (PPCPs) from wastewater: A review. *Journal of Environmental Management*, 182, 620-640.
- [7] Comber, S., Gardner, M., Sörme, P., Ellor, B. (2019). The removal of pharmaceuticals during wastewater treatment: Can it be predicted accurately? *Science of the Total Environment*, 676, 222-230.
- [8] Pohl, J., Ahrens, L., Carlsson, G., Golovko, O., Norrgren, L., Weiss, J., Örn, S. (2019). Embryotoxicity of ozonated diclofenac, carbamazepine, and oxazepam in zebrafish (*Danio rerio*). *Chemosphere*, 225, 191-199.
- [9] Bilal, M., Adeel, M., Rasheed, T., Zhao, Y., Iqbal, H. (2019). Emerging contaminants of high concern and their enzyme-assisted biodegradation – A review. *Environment International*, 124, 336-353.
- [10] Rasheed, T. Bilal, M., Nabeel, F., Adeel, M., Iqbal, H. (2019). Environmentally-related contaminants of high concern: Potential sources and analytical modalities for detection, quantification, and treatment. *Environment International*, 122, 52-66.

- [11] Fang, W., Peng, Y., Muir, D., Lin, J., Zhang, X. (2019). A critical review of synthetic chemicals in surface waters of the US, the EU and China. *Environment International*, 131, 104994.
- [12] Kötke, D., Gandrass, J., Xie, Z., Ebinghaus, R. (2019). Prioritised pharmaceuticals in German estuaries and coastal waters: Occurrence and environmental risk assessment. *Environmental Pollution*, 113161, 113-161.
- [13] Sehonova, P., Plhalova, L., Blahova, J., Doubkova, V., Prokes, M., Tichy, F., Svobodova, Z. (2017). Toxicity of naproxen sodium and its mixture with tramadol hydrochloride on fish early life stages. *Chemosphere*, 188, 414-423.
- [14] Decision 2015/495/EU, 2015. Commission implementing decision (EU) 2015/495 of March 2015 establishing a watch list of substances for Union-wide monitoring in the field of water policy pursuant to Directive 2008/105/EC of the European Parliament and of the Council. *Off. J. Eur. Union L78*, 40-42.
- [15] Sousa, J., Ribeiro, A., Barbosa, M., Ribeiro, C., Tiritan, M., Pereira, M., Silva, A. (2019). Monitoring of the 17 EU Watch List contaminants of emerging concern in the Ave and the Sousa Rivers. *Science of the Total Environment*, 649, 1083-1095.
- [16]. Gusmaroli, L., Buttiglieri, G., Petrovic, M. (2019). The EU watch list compounds in the ebro delta region: Assessment of sources, river transport, and seasonal variations. *Environmental Pollution* 253, 606-615.
- [17] Xie, H., Hao, H., Xu, N., Liang, X., Gao, D., Xu, Y., Wong, M. (2019). Pharmaceuticals and personal care products in water, sediments, aquatic organisms, and fish feeds in the Pearl River Delta: Occurrence, distribution, potential sources, and health risk assessment. *Science of the Total Environment*, 659, 230-239.
- [18] Jiang, X., Qu, Y., Liu, L., He, Y., Li, W., Huang, J., Yu, G. (2019). PPCPs in a drinking water treatment plant in the Yangtze River Delta of China: Occurrence, removal and risk assessment. *Front. Environ. Sci. Eng*, 13(2), 27.
- [19] Loraine, G., Pettigrove, M. (2006). Seasonal variations in concentrations of pharmaceuticals and personal care products in drinking water and reclaimed wastewater in Southern California. *Environmental Science and Technology*, 40(3), 687-695.

- [20] Balakrishna, K., Rath, A., Praveenkumarreddy, Y., Guruge, K., Subedi, B. (2017). A review of the occurrence of pharmaceuticals and personal care products in Indian water bodies. *Ecotoxicology and Environmental Safety*, 137, 113-120.
- [21] Loos, R., Carvalho, R., António, D., Comero, S., Locoro, G., Tavazzi, S., Gawlik, B. (2013). EU-wide monitoring survey on emerging polar organic contaminants in wastewater treatment plant effluents. *Water Research*, 47(17), 6475-6487.
- [22] D. Krakkó., V. Licul-Kucera., Gy. Zárny., V. G. Mihucz. (2019). Single-run ultra-high performance liquid chromatography for quantitative determination of ultra-traces of ten popular active pharmaceutical ingredients by quadrupole time-of-flight mass spectrometry after offline preconcentration by solid phase extraction from drinking and river waters as well as treated wastewater, *Microchem. J.* 148, 108-119.
- [23] http://www.neak.gov.hu/felso_menu/szakmai_oldalak/publikus_forgalmi_adatok/gyogyszer_forgalmi_adatok
- [24] Sophia A., C., Lima, E. (2018). Removal of emerging contaminants from the environment by adsorption. *Ecotoxicology and Environmental Safety*, 150, 1-17.
- [25] Al-Khateeb, L., Hakami, W., Salam, M. (2017). Removal of non-steroidal anti-inflammatory drugs from water using high surface area nanographene: Kinetic and thermodynamic studies. *Journal of Molecular Liquids*, 241, 733-741.
- [26] Pires, B. C., do Nascimento, T. A., Dutra, F. V. A., Borges, K. B. (2019). Removal of a non-steroidal anti-inflammatory by adsorption on polypyrrole/ multiwalled carbon nanotube composite—Study of kinetics and equilibrium in aqueous medium. *Colloids and Surfaces A: Physicochemical and Engineering Aspects*, 578, 123583.
- [27] Wang, Y., Huang, H., Wei, X. (2018). Influence of wastewater pre-coagulation on adsorptive filtration of pharmaceutical and personal care products by carbon nanotube membranes, *Chemical Engineering Journal*, 333, 66-75.
- [28] Lu, F., Astruc, D. (2018). Nanomaterials for removal of toxic elements from water, *Coordination Chemistry Reviews*, 356, 147-164.
- [29] Aschermann, G., Neubert, L., Zietzschmann, F., Jekel, M. (2019). Impact of different DOM size fractions on the desorption of organic micropollutants from activated carbon. *Water Research*, 161, 161-170.

- [30] Inyang, M., Dickenson, E. (2015). The potential role of biochar in the removal of organic and microbial contaminants from potable and reuse water: A review. *Chemosphere*, 134, 232-240.
- [31] Dalahmeh, S., Ahrens, L., Gros, M., Wiberg, K., Pell, M. (2018). Potential of biochar filters for onsite sewage treatment: Adsorption and biological degradation of pharmaceuticals in laboratory filters with active, inactive and no biofilm. *Science of the Total Environment*, 612, 192-201.
- [32] Borvendég, J. (2008). *Gyógyszer Kompendium*, CMPMedica Információs Kft, Budapest, 2008.
- [33] Mazák, K. *Pharmaceutical chemistry – The quality control of medicinal compounds and pharmaceutical preparations*, Semmelweis Kiadó és Multimédia Stúdió, 201.
- [34] Gyires, K., Fürst, Z. (2011). *A farmakológia alapjai*.
- [35] Camacho-Muñoz, D., Petrie, B., Lopardo, L., Proctor, K., Rice, J., Youdan, J., Kasprzyk-Hordern, B. (2019). Stereoisomeric profiling of chiral pharmaceutically active compounds in wastewaters and the receiving environment – A catchment-scale and a laboratory study. *Environment International*, 127, 558-572.
- [36] Kwok, E., Atkinson, R. (1995). Estimation of hydroxyl radical reaction rate constants for gas-phase organic compounds using a structure-reactivity relationship: An update. *Atmospheric Environment*, 29(14), 1685-1695.
- [37] Finn A et al; *Acta Technol Legis Med* 4: 33-44 (1986) .
- [38] US EPA; Estimation Program Interface (EPI) Suite. Ver. 4.1. Jan, 2011. Available from, as of Oct 26, 2011:
<http://www.epa.gov/oppt/exposure/pubs/episuitedi.htm>
- [39] Yalkowsky, S.H., He, Yan. (2003). *Handbook of Aqueous Solubility Data: An Extensive Compilation of Aqueous Solubility*. 962-356 Sangster 1994.
- [40] US EPA; Estimation Program Interface (EPI) Suite. Ver. 4.0. Jan, 2009. Available from, as of April 22, 2009:
<http://www.epa.gov/oppt/exposure/pubs/episuitedi.htm>
- [41] US EPA; Estimation Program Interface (EPI) Suite. Ver.3.12. Nov 30, 2004. Available from, as of Jun 7, 2007: <http://www.epa.gov/oppt/exposure/pubs/episuitedi.htm> at 25 °C (est)

- [42] Jones, O., Voulvoulis, N., Lester, J. (2002). Aquatic environmental assessment of the top 25 English prescription pharmaceuticals. *Water Research*, 36(20), 5013-5022.
- [43] US EPA; Estimation Program Interface (EPI) Suite. Ver.3.12. Nov 30, 2004. Available from, as of Jun 7, 2007: <http://www.epa.gov/oppt/exposure/pubs/episuitedi.htm>
- [44] Mlunguza, N., Ncube, S., Nokwethemba Mahlambi, P., Chimuka, L., Madikizela, L. (2019). Adsorbents and removal strategies of non-steroidal anti-inflammatory drugs from contaminated water bodies. *Journal of Environmental Chemical Engineering*, 7(3). 103142.
- [45] Rosenfeld, P. E., Feng, L. G. H. (2011). Emerging Contaminants. *Risks of Hazardous Wastes*, 215-222.
- [46] A.B. Boxall, M.A. Rudd, B.W. Brooks, D.J.Caldwell, K. Choi, S. Hickmann, E. Innes, K.Ostapyk, J.P. Staveley, T. Verslycke, G.T. Ankley, K.F. Beazley, S.E. Belanger, J.P. Berninger, P.Carriquiriborde, A. Coors, P.C. Deleo, S.D. Dyer, J.F. Ericson, F. Gagne, J.P. Giesy, T. Gouin, L.Hallstrom, M.V. Karlsson, D.G. Larsson, J.M.Lazorchak, F. Mastrocco, A. Mclaughlin, M.E.Mcmaster, R.D. Meyerhoff, R. Moore, J.L. Parrott, J.R. Snape, R. MurraySmith, M.R. Servos, P.K.Sibley, J.O. Straub, N.D. Szabo, E. Topp, G.R.Tetreault, V.L. Trudeau., G. Van der Kraak. (2012). Pharmaceuticals and Personal Care Products in the Environment: What Are the Big Questions? *Environmental Health Perspectives*, 120(9), 1221-1229.
- [47] Zhang, Y., Geißen, S., Gal, C. (2008). Carbamazepine and diclofenac: Removal in wastewater treatment plants and occurrence in water bodies. *Chemosphere*, 73(8), 1151-1161.
- [48] Palmiotto, M., Castiglioni, S., Zuccato, E., Manenti, A., Riva, F., Davoli, E. (2018). Personal care products in surface, ground and wastewater of a complex aquifer system, a potential planning tool for contemporary urban settings. *Journal of Environmental Management*, 214, 76-85.
- [49] International Pharmaceutical Federation (FIP). *Green pharmacy practice: Taking responsibility for the environmental impact of medicines* (2015).
- [50] Sui, Q. Cao, X., Lu, S., Zhao, W., Qiu, Z., Yu, G. (2015). Occurrence, sources and fate of pharmaceuticals and personal care products in the groundwater: A review. *Emerging Contaminants*, 1(1), 14-24.

- [51] Kasprzyk-Hordern, B., Dinsdale, R., Guwy, A. (2009). The removal of pharmaceuticals, personal care products, endocrine disruptors and illicit drugs during wastewater treatment and its impact on the quality of receiving waters. *Water Research*, 43(2), 363-380.
- [52] Tambosi, J., Yamanaka, L., José, H., De, R., Peralta, F., Moreira, M., Schröder, H. (2010). recent research data on the removal of pharmaceuticals from sewage treatment plants (STP). *Quim. Nova*, 33, 411-420.
- [53] Na, T., Kang, T., Lee, K., Hwang, S., Jung, H., Kim, K. (2019). Distribution and ecological risk of pharmaceuticals in surface water of the Yeongsan river, Republic of Korea. *Ecotoxicology and Environmental Safety*, 181, 180-186.
- [54] Grenni, P., Patrolecco, L., Ademollo, N., Di Lenola, M., Barra Caracciolo, A. (2018). Assessment of gemfibrozil persistence in river water alone and in co-presence of naproxen. *Microchemical Journal*, 136, 49-55.
- [55] Heberer, T. (2002). Fate and removal of pharmaceutical residues in aquatic environment: a review of recent research data. *Toxicol Lett*, 131, 5-17.
- [56] Jones, O., Voulvoulis, N., Lester, J. (2005). Human pharmaceuticals in wastewater treatment processes. *Critical Reviews in Environmental Science and Technology*, 35, 4, 401-427.
- [57] Li, B., Zhang, T., Xu, Z., Fang, H. (2009). Rapid analysis of 21 antibiotics of multiple classes in municipal wastewater using ultra performance liquid chromatography-tandem mass spectrometry. *Analytica Chimica Acta*, 645 (1-2), 64-72.
- [58] Morasch, B., Bonvin, F., Reiser, H., Grandjean, D., De Alencastro, L., Perazzolo, C., Kohn, T. (2010). Occurrence and fate of micropollutants in the Vidy Bay of Lake Geneva, Switzerland. Part II: Micropollutant removal between wastewater and raw drinking water. *Environmental Toxicology and Chemistry*, 29(8), 1658-1668.
- [59] Cooper, E., Siewicki, T., Phillips, K. (2008). Preliminary risk assessment database and risk ranking of pharmaceuticals in the environment. *Science of the Total Environment*, 398(1-3), 26-33.
- [60] Ebele, A., Abou-Elwafa Abdallah, M., Harrad, S. (2017). Pharmaceuticals and personal care products (PPCPs) in the freshwater aquatic environment. *Emerging Contaminants*, 3(1), 1-16.

- [61] Kümmerer, K. (2008). *Pharmaceuticals in the environment : sources, fate, effects, and risks*. Springer-Verlag, Berlin Heidelberg. 2008. ISBN: 978-3-540-74663-8.
- [62] Michael, I., Rizzo, L., McArdell, C., Manaia, C., Merlin, C., Schwartz, T., Fatta-Kassinos, D. (2013). Urban wastewater treatment plants as hotspots for the release of antibiotics in the environment: A review. *Water Research*, 47(3), 957-995.
- [63] Sun, Q., Lv, M., Hu, A., Yang, X., Yu, C. (2014). Seasonal variation in the occurrence and removal of pharmaceuticals and personal care products in a wastewater treatment plant in Xiamen, China. *Journal of Hazardous Materials*, 277, 69-75.
- [64] Afonso-Olivares, C., Sosa-Ferrera, Z., Santana-Rodríguez, J. (2017). Occurrence and environmental impact of pharmaceutical residues from conventional and natural wastewater treatment plants in Gran Canaria (Spain). *Science of the Total Environment*, 599-600, 934-943.
- [65] Tran, N., Chen, H., Do, T., Reinhard, M., Ngo, H., He, Y., Gin, K. (2016). Simultaneous analysis of multiple classes of antimicrobials in environmental water samples using SPE coupled with UHPLC-ESI-MS/MS and isotope dilution. *Talanta*, 159, 163-173.
- [66] Gumbi, B., Moodley, B., Birungi, G., Ndungu, P. (2017). Detection and quantification of acidic drug residues in South African surface water using gas chromatography-mass spectrometry. *Chemosphere*, 168, 1042-1050.
- [67] Vystavna, Y., Frkova, Z., Celle-Jeanton, H., Diadin, D., Huneau, F., Steinmann, M., Loup, C. (2018). Priority substances and emerging pollutants in urban rivers in Ukraine: Occurrence, fluxes and loading to transboundary European Union watersheds. *Science of the Total Environment*, 637-638, 1358-1362.
- [68] Kleywegt, S., Payne, M., Raby, M., Filippi, D., Ng, C., Fletcher, T. (2019). The final discharge: Quantifying contaminants in embalming process effluents discharged to sewers in ontario, Canada. *Environmental Pollution*, 252, 1476- 1482.
- [69] Luo, Y., Guo, W., Ngo, H., Nghiem, L., Hai, F., Zhang, J., Wang, X. (2014). A review on the occurrence of micropollutants in the aquatic environment and their fate and removal during wastewater treatment. *Science of the Total Environment*, 473-474, 619-641.
- [70] Archer, E., Petrie, B., Kasprzyk-Hordern, B., Wolfaardt, G. (2017). The fate of pharmaceuticals and personal care products (PPCPs), endocrine disrupting

- contaminants (EDCs), metabolites and illicit drugs in a WWTW and environmental waters. *Chemosphere*, 174, 437-446.
- [71] Dalahmeh, S., Björnberg, E., Elenström, A.-K., Niwagaba, C. B., Komakech, A. J. (2019). Pharmaceutical pollution of water resources in Nakivubo wetlands and Lake Victoria, Kampala, Uganda. *Science of The Total Environment*, 136347.
- [72] Vieno, N., Härkki, H., Tuhkanen, T., Kronberg, L. (2007). Occurrence of pharmaceuticals in river water and their elimination in a pilot-scale drinking water treatment plant. *Environmental Science and Technology*, 41(14), 5077-5084.
- [73] Sim, W., Lee, J., Lee, E., Shin, S., Hwang, S., Oh, J. (2011). Occurrence and distribution of pharmaceuticals in wastewater from households, livestock farms, hospitals and pharmaceutical manufactures. *Chemosphere*, 82(2), 179-186.
- [74] OECD. (2013). Strategies for Grouping Chemicals to Fill Data Gaps to Assess Acute Aquatic Toxicity Endpoints.
- [75] Rivera-Jaimes, J., Postigo, C., Melgoza-Alemán, R., Aceña, J., Barceló, D., López de Alda, M. (2018). Study of pharmaceuticals in surface and wastewater from Cuernavaca, Morelos, Mexico: Occurrence and environmental risk assessment. *Science of the Total Environment*, 613-614, 1263-1274.
- [76] Krall, A., Elliott, S., Erickson, M., Adams, B. (2018). Detecting sulfamethoxazole and carbamazepine in groundwater: Is ELISA a reliable screening tool? *Environmental Pollution*, 234, 420-428.
- [77] Pereira, C., Maranhão, L., Cortez, F., Pusceddu, F., Santos, A., Ribeiro, D., Guimarães, L. (2016). Occurrence of pharmaceuticals and cocaine in a Brazilian coastal zone. *Science of the Total Environment*, 548-549, 148-154.
- [78] Veras, T., Luiz Ribeiro de Paiva, A., Duarte, M., Napoleão, D., da Silva Pereira Cabral, J. (2019). Analysis of the presence of anti-inflammatories drugs in surface water: A case study in Beberibe river - PE, Brazil. *Chemosphere*, 222, 961- 969.
- [79] Letsinger, S., Kay, P., Rodríguez-Mozaz, S., Villagrassa, M., Barceló, D., Rotchell, J. (2019). Spatial and temporal occurrence of pharmaceuticals in UK estuaries. *Science of the Total Environment*, 678, 74-84.

- [80] Xie, Z., Lu, G., Yan, Z., Liu, J., Wang, P., Wang, Y. (2017). Bioaccumulation and trophic transfer of pharmaceuticals in food webs from a large freshwater lake. *Environmental Pollution*, 222, 356-366.
- [81] Brumovský, M., Bečanová, J., Kohoutek, J., Borghini, M., Nizzetto, L. (2017). Contaminants of emerging concern in the open sea waters of the Western Mediterranean. *Environmental Pollution*, 229, 976-983.
- [82] B. Björlenius., M. Ripszám., P. Haglund., R.H. Lindberg., M. Tysklind., J. Fick, (2018) Pharmaceutical residues are widespread in Baltic Sea coastal and offshore waters – Screening for pharmaceuticals and modelling of environmental concentrations of carbamazepine, *Science of the Total Environment* 633 1496-1509.
- [83] Deo, R. (2014). Pharmaceuticals in the Surface Water of the USA: A Review. *Current Environmental Health Reports*, 1(2), 113-122.
- [84] Wang, Z., Zhang, X., Huang, Y., Wang, H. (2015). Comprehensive evaluation of pharmaceuticals and personal care products (PPCPs) in typical highly urbanized regions across China. *Environmental Pollution*, 204, 223-232.
- [85] Biel-Maeso, M., Baena-Nogueras, R., Corada-Fernández, C., Lara-Martín, P. (2018). Occurrence, distribution and environmental risk of pharmaceutically active compounds (PhACs) in coastal and ocean waters from the Gulf of Cadiz (SW Spain). *Science of the Total Environment*, 612, 649-659.
- [86] Pablos, M., Rodríguez, J., García-Hortigüela, P., Fernández, A., Beltrán, E., Torrijos, M., Fernández, C. (2018). Sublethal and chronic effects of reclaimed water on aquatic organisms. Looking for relationships between physico-chemical characterisation and toxic effects. *Science of the Total Environment*, 640-641, 1537-1547.
- [87] Vörösmarty, C. J., McIntyre, P. B., Gessner, M. O., Dudgeon, D., Prusevich, A., Green, P., Davies, P. M. (2010). Global threats to human water security and river biodiversity. *Nature*, 467(7315), 555-561.
- [88] Hughes, S., Kay, P., Brown, L. (2013). Global synthesis and critical evaluation of pharmaceutical data sets collected from river systems. *Environmental Science and Technology*, 47(2), 661-677.
- [89] Raquel N. Carvalho, Lidia Ceriani, Alessio Ippolito and Teresa Lettieri. Development of the First Watch List under the Environmental Quality Standards Directive, Directive

- 2008/105/EC, as Amended by Directive 2013/39/EU, in the Field of Water Policy (2015).
- [90] Fent, K. (2015). Progestins as endocrine disrupters in aquatic ecosystems: Concentrations, effects and risk assessment. *Environment International*, 84, 115-130.
- [91] Niemuth, N., Klaper, R. (2015). Emerging wastewater contaminant metformin causes intersex and reduced fecundity in fish. *Chemosphere*, 135, 38-45.
- [92] Sanderson, H., Johnson, D., Reitsma, T., Brain, R., Wilson, C., Solomon, K. (2004). Ranking and prioritization of environmental risks of pharmaceuticals in surface waters. *Regulatory Toxicology and Pharmacology*, 39(2), 158-183.
- [93] Rizzo, L., Manaia, C., Merlin, C., Schwartz, T., Dagot, C., Ploy, M., Fatta-Kassinos, D. (2013). Urban wastewater treatment plants as hotspots for antibiotic resistant bacteria and genes spread into the environment: A review. *Science of the Total Environment*, 447, 345-360.
- [94] Schmidt, S., Winter, J., Gallert, C. (2012). Long-term effects of antibiotics on the elimination of chemical oxygen demand, nitrification, and viable bacteria in laboratory-scale wastewater treatment plants. *Archives of Environmental Contamination and Toxicology*, 63(3), 354-364.
- [95] da Silva Santos, N., Oliveira, R., Lisboa, C., Moniz e Pinto, J., Sousa-Moura, D., Camargo, N., Domingues, I. (2018). Chronic effects of carbamazepine on zebrafish: Behavioral, reproductive and biochemical endpoints. *Ecotoxicology and Environmental Safety*, 164, 297-304.
- [96] Pi, N., Ng, J., Kelly, B. (2017). Bioaccumulation of pharmaceutically active compounds and endocrine disrupting chemicals in aquatic macrophytes: Results of hydroponic experiments with *Echinodorus horemanii* and *Eichhornia crassipes*. *Science of the Total Environment*, 601-602, 812-820.
- [97] US EPA, 2014. Technical overview of ecological risk assessment/risk characterization, pesticides. *Environ. Prot.* 1-8.
- [98] Hoeger, B., Köllner, B., Dietrich, D., Hitzfeld, B. (2005). Water-borne diclofenac affects kidney and gill integrity and selected immune parameters in brown trout (*Salmo trutta f. fario*). *Aquatic Toxicology*, 75(1), 53-64.

- [99] Saravanan, M., Hur, J., Arul, N., Ramesh, M. (2014). Toxicological effects of clofibrac acid and diclofenac on plasma thyroid hormones of an Indian major carp, *Cirrhinus mrigala* during short and long-term exposures. *Environmental Toxicology and Pharmacology*, 38(3), 948-958.
- [100] Cleuvers, M. (2004). Mixture toxicity of the anti-inflammatory drugs diclofenac, ibuprofen, naproxen, and acetylsalicylic acid. *Ecotoxicology and Environmental Safety*, 59(3), 309-315.
- [101] Shao, Y., Chen, Z., Hollert, H., Zhou, S., Deutschmann, B., Seiler, T. (2019). Toxicity of 10 organic micropollutants and their mixture: Implications for aquatic risk assessment. *Science of the Total Environment*, 666, 1273-1282.
- [102] Huerta-Fontela, M., Galceran, M., Ventura, F. (2011). Occurrence and removal of pharmaceuticals and hormones through drinking water treatment. *Water Research*, 45(3), 1432-1442.
- [103] Mutiyar, P., Gupta, S., Mittal, A. (2018). Fate of pharmaceutical active compounds (PhACs) from River Yamuna, India: An ecotoxicological risk assessment approach. *Ecotoxicology and Environmental Safety*, 150, 297-304.
- [104] Valdés, M., Amé, M., Bistoni, M., Wunderlin, D. (2014). Occurrence and bioaccumulation of pharmaceuticals in a fish species inhabiting the Suquía River basin (Córdoba, Argentina). *Science of the Total Environment*, 472, 389-396.
- [105] Liu, J., Lu, G., Xie, Z., Zhang, Z., Li, S., Yan, Z. (2015). Occurrence, bioaccumulation and risk assessment of lipophilic pharmaceutically active compounds in the downstream rivers of sewage treatment plants. *Science of the Total Environment*, 511, 54-62.
- [106] Ruhí, A., Acuña, V., Barceló, D., Huerta, B., Mor, J., Rodríguez-Mozaz, S., Sabater, S. (2016). Bioaccumulation and trophic magnification of pharmaceuticals and endocrine disruptors in a Mediterranean river food web. *Science of the Total Environment*, 540, 250-259.
- [107] Bean, T., Rattner, B., Lazarus, R., Day, D., Burket, S., Brooks, B., Bowerman, W. (2018). Pharmaceuticals in water, fish and osprey nestlings in Delaware River and Bay. *Environmental Pollution*, 232, 533-545.

- [108] Balbi, T., Montagna, M., Fabbri, R., Carbone, C., Franzellitti, S., Fabbri, E., Canesi, L. (2018). Diclofenac affects early embryo development in the marine bivalve *Mytilus galloprovincialis*. *Science of the Total Environment*, 642, 601-609.
- [109] Pompei, C., Campos, L., da Silva, B., Fogo, J., Vieira, E. (2019). Occurrence of PPCPs in a Brazilian water reservoir and their removal efficiency by ecological filtration. *Chemosphere*, 226, 210-219.
- [110] Paíga, P., Santos, L., Delerue-Matos, C. (2017). Development of a multi-residue method for the determination of human and veterinary pharmaceuticals and some of their metabolites in aqueous environmental matrices by SPE-UHPLC–MS/MS. *Journal of Pharmaceutical and Biomedical Analysis*, 135, 75-86.
- [111] Schmidt, S., Hoffmann, H., Garbe, L., Schneider, R. (2018). Liquid chromatography–tandem mass spectrometry detection of diclofenac and related compounds in water samples. *Journal of Chromatography A*, 1538, 112-116.
- [112] Česen, M., Ahel, M., Terzić, S., Heath, D., Heath, E. (2019). The occurrence of contaminants of emerging concern in Slovenian and Croatian wastewaters and receiving Sava river. *Science of the Total Environment*, 650, 2446-2453.
- [113] Barra Caracciolo, A., Patrolecco, L., Grenni, P., Di Lenola, M., Ademollo, N., Rauseo, J., Sperlagh, B. (2019). Chemical mixtures and autochthonous microbial community in an urbanized stretch of the River Danube. *Microchemical Journal*, 147, 985-994.
- [114] Brunsch, A. F., Langenhoff, A. A. M., Rijnaarts, H. H. M., Ahring, A., ter Laak, T. L. (2019). In situ removal of four organic micropollutants in a small river determined by monitoring and modelling. *Environmental Pollution*, 252, 758-766.
- [115] Reis-Santos, P., Pais, M., Duarte, B., Caçador, I., Freitas, A., Vila Pouca, A., Fonseca, V. (2018). Screening of human and veterinary pharmaceuticals in estuarine waters: A baseline assessment for the Tejo estuary. *Marine Pollution Bulletin*, 135, 1079-1084.
- [116] Mijangos, L., Ziarrusta, H., Ros, O., Kortazar, L., Fernández, L., Olivares, M., Etxebarria, N. (2018). Occurrence of emerging pollutants in estuaries of the Basque Country: Analysis of sources and distribution, and assessment of the environmental risk. *Water Research*, 147, 152-163.

- [117] White, D., Lapworth, D. J., Civil, W., Williams, P. (2019). Tracking changes in the occurrence and source of pharmaceuticals within the River Thames, UK; from source to sea. *Environmental Pollution*, 249, 257-266.
- [118] Palli, L., Spina, F., Varese, G., Vincenzi, M., Aragno, M., Arcangeli, G., Gori, R. (2019). Occurrence of selected pharmaceuticals in wastewater treatment plants of Tuscany: An effect-based approach to evaluate the potential environmental impact. *International Journal of Hygiene and Environmental Health*, 222(4), 717-725.
- [119] Marsik, P., Rezek, J., Židková, M., Kramulová, B., Tauchen, J., Vaněk, T. (2017). Non-steroidal anti-inflammatory drugs in the watercourses of Elbe basin in Czech Republic. *Chemosphere*, 171, 97-105.
- [120] Ali, A., Sydnese, L., Alarif, W., Al-Lihaibi, S., Aly, M., Aanrud, S., Kallenborn, R. (2019). Diclofenac and two of its photooxidation products in the marine environment: Their toxicology and occurrence in Red Sea coastal waters. *Environmental Chemistry and Ecotoxicology*, 1, 19-25.
- [121] Kumar, R., Sarmah, A., Padhye, L. (2019). Fate of pharmaceuticals and personal care products in a wastewater treatment plant with parallel secondary wastewater treatment train. *Journal of Environmental Management*, 233, 649-659.
- [122] Ashfaq, M., Nawaz Khan, K., Saif Ur Rehman, M., Mustafa, G., Faizan Nazar, M., Sun, Q., Yu, C. (2017). Ecological risk assessment of pharmaceuticals in the receiving environment of pharmaceutical wastewater in Pakistan. *Ecotoxicology and Environmental Safety*, 136, 31-39.
- [123] González-Alonso, S., Merino, L., Esteban, S., López de Alda, M., Barceló, D., Durán, J., Valcárcel, Y. (2017). Occurrence of pharmaceutical, recreational and psychotropic drug residues in surface water on the northern Antarctic Peninsula region. *Environmental Pollution*, 229, 241-254.
- [124] Kibuye, F., Gall, H., Elkin, K., Ayers, B., Veith, T., Miller, M., Elliott, H. (2019). Fate of pharmaceuticals in a spray-irrigation system: From wastewater to groundwater. *Science of the Total Environment*, 654, 197-208.
- [125] Ma, R., Qu, H., Wang, B., Wang, F., Yu, Y., Yu, G. (2019). Simultaneous enantiomeric analysis of non-steroidal anti-inflammatory drugs in environment by chiral LC-

- MS/MS: A pilot study in Beijing, China. *Ecotoxicology and Environmental Safety*, 174, 83-91.
- [126] Ngubane, N., Naicker, D., Ncube, S., Chimuka, L., Madikizela, L. (2019). Determination of naproxen, diclofenac and ibuprofen in Umgeni estuary and seawater: A case of northern Durban in KwaZulu–Natal Province of South Africa. *Regional Studies in Marine Science*, 29.100675.
- [127] Lancheros, J., Madera-Parra, C., Caselles-Osorio, A., Torres-López, W., Vargas-Ramírez, X. (2019). Ibuprofen and Naproxen removal from domestic wastewater using a Horizontal Subsurface Flow Constructed Wetland coupled to Ozonation. *Ecological Engineering*, 135, 89-97.
- [128] Ekpeghere, K., Lee, J., Kim, H., Shin, S., Oh, J. (2017). Determination and characterization of pharmaceuticals in sludge from municipal and livestock wastewater treatment plants. *Chemosphere*, 168, 1211-1221.
- [129] He, K., Yonetani, T., Asada, Y., Echigo, S., Itoh, S. (2019). Simultaneous determination of carbamazepine-N-glucuronide and carbamazepine phase I metabolites in the wastewater by liquid chromatography-tandem mass spectrometry. *Microchemical Journal*, 145, 1191-1198.
- [130] Durán-Álvarez, J., Prado, B., González, D., Sánchez, Y., Jiménez-Cisneros, B. (2015). Environmental fate of naproxen, carbamazepine and triclosan in wastewater, surface water and wastewater irrigated soil - Results of laboratory scale experiments. *Science of the Total Environment*, 538, 350-362.
- [131] Yuan, X., Li, S., Hu, J., Yu, M., Li, Y., Wang, Z. (2019). Experiments and numerical simulation on the degradation processes of carbamazepine and triclosan in surface water: A case study for the Shahe Stream, South China. *Science of the Total Environment*, 655, 1125-1138.
- [132] Avetta, P., Fabbri, D., Minella, M., Brigante, M., Maurino, V., Minero, C., Vione, D. (2016). Assessing the phototransformation of diclofenac, clofibric acid and naproxen in surface waters: Model predictions and comparison with field data. *Water Research*, 105, 383-394.
- [133] Clara, M., Strenn, B., Kreuzinger, N. (2004). Carbamazepine as a possible anthropogenic marker in the aquatic environment: Investigations on the behaviour of

- Carbamazepine in wastewater treatment and during groundwater infiltration. *Water Research*, 38(4), 947-954.
- [134] Vernouillet, G., Eullaffroy, P., Lajeunesse, A., Blaise, C., Gagné, F., Juneau, P. (2010). Toxic effects and bioaccumulation of carbamazepine evaluated by biomarkers measured in organisms of different trophic levels. *Chemosphere*, 80(9), 1062-1068.
- [135] Oliveira, P., Almeida, Â., Calisto, V., Esteves, V., Schneider, R., Wrona, F., Freitas, R. (2017). Physiological and biochemical alterations induced in the mussel *Mytilus galloprovincialis* after short and long-term exposure to carbamazepine. *Water Research*, 117, 102-114.
- [136] Boillot, C., Martinez Bueno, M., Munaron, D., Le Dreau, M., Mathieu, O., David, A., Gomez, E. (2015). In vivo exposure of marine mussels to carbamazepine and 10-hydroxy-10,11-dihydro-carbamazepine: Bioconcentration and metabolization. *Science of the Total Environment*, 532, 564-570.
- [137] Gomes, T., Fernandes Sales Junior, S., Saint'Pierre, T., Correia, F., Hauser-Davis, R., Saggiaro, E. (2019). Sublethal psychotropic pharmaceutical effects on the model organism *Danio rerio*: Oxidative stress and metal dishomeostasis. *Ecotoxicology and Environmental Safety*, 171, 781-789.
- [138] Ericson, H., Thorsén, G., Kumblad, L. (2010). Physiological effects of diclofenac, ibuprofen and propranolol on Baltic Sea blue mussels. *Aquatic Toxicology*, 99(2), 223-231.
- [139] Oviedo-Gómez, D., Galar-Martínez, M., García-Medina, S., Razo-Estrada, C., Gómez-Oliván, L. (2010). Diclofenac-enriched artificial sediment induces oxidative stress in *Hyalella azteca*. *Environmental Toxicology and Pharmacology*, 29(1), 39-43.
- [140] Cunha, S., Pena, A., Fernandes, J. (2017). Mussels as bioindicators of diclofenac contamination in coastal environments. *Environmental Pollution*, 225, 354-360.
- [141] Lee, J., Ji, K., Lim Kho, Y., Kim, P., Choi, K. (2011). Chronic exposure to diclofenac on two freshwater cladocerans and Japanese medaka. *Ecotoxicology and Environmental Safety*, 74(5), 1216-1225.
- [142] Thibaut, R., Porte, C. (2008). Effects of fibrates, anti-inflammatory drugs and antidepressants in the fish hepatoma cell line PLHC-1: Cytotoxicity and interactions with cytochrome P450 1A. *Toxicology in Vitro*, 22(5), 1128-1135.

- [143] Isidori, M., Lavorgna, M., Nardelli, A., Parrella, A., Previtera, L., Rubino, M. (2005). Ecotoxicity of naproxen and its phototransformation products. *Science of the Total Environment*, 348(1-3), 93-101.
- [144] Falaki, F. (2019). Sample Preparation Techniques for Gas Chromatography. In F. Falaki, *Gas Chromatography - Derivatization, Sample Preparation, Application*. Peter Kusch, IntechOpen.,
- [145] Shen, J., Ding, T., Zhang, M. (2019). Analytical techniques and challenges for removal of pharmaceuticals and personal care products in water. *Pharmaceuticals and Personal Care Products: Waste Management and Treatment Technology*, 239-257.
- [146] Casado, J., Santillo, D., Johnston, P. (2018). Multi-residue analysis of pesticides in surface water by liquid chromatography quadrupole-Orbitrap high resolution tandem mass spectrometry. *Analytica Chimica Acta*, 1024, 1-17.
- [147] Kim, C., Ryu, H., Chung, E., Kim, Y. (2018). Determination of 18 veterinary antibiotics in environmental water using high-performance liquid chromatography-q-orbitrap combined with on-line solid-phase extraction. *Journal of Chromatography B: Analytical Technologies in the Biomedical and Life Sciences*, 1084, 158-165.
- [148] Lakade, S., Borrull, F., Furton, K., Kabir, A., Marcé, R., Fontanals, N. (2018). Novel capsule phase microextraction in combination with liquid chromatography-tandem mass spectrometry for determining personal care products in environmental water. *Analytical and Bioanalytical Chemistry*, 410(12), 2991-3001.
- [149] Caban, M., Kumirska, J., Bialk-Bielinska, A., Stepnowski, P. (2015). Analytical Techniques for Determining Pharmaceutical Residues in Drinking Water – State of Art and Future Prospects. *Current Analytical Chemistry*, 12(3), 237-248.
- [150] Furey, A., Moriarty, M. (2011). In defence of dependability and reliability: LC-UV/DAD. *Pharmaceutical Methods*, 2(4), 209-210.
- [151] Arany, E., Láng, J., Somogyvári, D., Láng, O., Alapi, T., Ilisz, I., Hernádi, K. (2014). Vacuum ultraviolet photolysis of diclofenac and the effects of its treated aqueous solutions on the proliferation and migratory responses of *Tetrahymena pyriformis*. *Science of the Total Environment*, 468-469, 996-1006.
- [152] Gul, S., Sultana, N., Saeed Arayne, M., Shamim, S., Akhtar, M. (2012). New Method for Optimization and Simultaneous Determination of Sparfloxacin and Non Steroidal

- Anti-Inflammatory Drugs: Its In-Vitro Application. *American Journal of Analytical Chemistry*, 03(04), 328-337.
- [153] Roscher, J., Vogel, M., Karst, U. (2016). Identification of ultraviolet transformation products of diclofenac by means of liquid chromatography and mass spectrometry. *Journal of Chromatography A*, 1457, 59-65.
- [154] Caldas, S. S., Rombaldi, C., de Oliveira Arias, J. L., Marube, L. C., Primel, E. G. (2016). Multi-residue method for determination of 58 pesticides, pharmaceuticals and personal care products in water using solvent demulsification dispersive liquid-liquid microextraction combined with liquid chromatography-tandem mass spectrometry. *Talanta*, 146, 676-688.
- [155] Guedes-Alonso, R., Santana-Viera, S., Sosa-Ferrera, Z., Santana-Rodríguez, J. (2015). Molecularly imprinted solid-phase extraction coupled with ultra high performance liquid chromatography and fluorescence detection for the determination of estrogens and their metabolites in wastewater. *Journal of Separation Science*, 38(22), 3961-3968.
- [156] Lakade, S., Borrull, F., Furton, K., Kabir, A., Fontanals, N., Marcé, R. (2015). Comparative study of different fabric phase sorptive extraction sorbents to determine emerging contaminants from environmental water using liquid chromatography-tandem mass spectrometry. *Talanta*, 144, 1342-1351.
- [157] Lee, J., Lee, S., Oh, J. (2013). Analysis of nine nitrosamines in water by combining automated solid-phase extraction with high-performance liquid chromatography-atmospheric pressure chemical ionisation tandem mass spectrometry. *International Journal of Environmental Analytical Chemistry*, 93(12), 1261-1273.
- [158] Aparicio, I., Martín, J., Santos, J., Malvar, J., Alonso, E. (2017). Stir bar sorptive extraction and liquid chromatography-tandem mass spectrometry determination of polar and non-polar emerging and priority pollutants in environmental waters. *Journal of Chromatography A*, 1500, 43-52.
- [159] Togola, A., Budzinski, H. (2007). Analytical development for analysis of pharmaceuticals in water samples by SPE and GC-MS. *Analytical and Bioanalytical Chemistry*, 388(3), 627-635.

- [160] Yilmaz, B., Ciltas, U. (2015). Determination of diclofenac in pharmaceutical preparations by voltammetry and gas chromatography methods. *Journal of Pharmaceutical Analysis*, 5(3), 153-160.
- [161] Nödler, K., Licha, T., Bester, K., Sauter, M. (2010). Development of a multi-residue analytical method, based on liquid chromatography-tandem mass spectrometry, for the simultaneous determination of 46 micro-contaminants in aqueous samples. *Journal of Chromatography A*, 1217(42), 6511-6521.
- [162] Carmona, E., Andreu, V., Picó, Y. (2017). Multi-residue determination of 47 organic compounds in water, soil, sediment and fish-Turia River as case study. *Journal of Pharmaceutical and Biomedical Analysis*, 146, 117-125.
- [163] Pugajeva, I., Rusko, J., Perkons, I., Lundanes, E., Bartkevics, V. (2017). Determination of pharmaceutical residues in wastewater using high performance liquid chromatography coupled to quadrupole-Orbitrap mass spectrometry. *Journal of Pharmaceutical and Biomedical Analysis*, 133, 64-74.
- [164] Valls-Cantenys, C., Scheurer, M., Iglesias, M., Sacher, F., Brauch, H., Salvadó, V. (2016). A sensitive multi-residue method for the determination of 35 micropollutants including pharmaceuticals, iodinated contrast media and pesticides in water. *Analytical and Bioanalytical Chemistry*, 408(22), 6189-6200.
- [165] Madikizela, L., Chimuka, L. (2017). Simultaneous determination of naproxen, ibuprofen and diclofenac in wastewater using solid-phase extraction with high performance liquid chromatography. *Water SA*, 43(2), 264-274.
- [166] Brozinski, J., Lahti, M., Meierjohann, A., Oikari, A., Kronberg, L. (2013). The anti-inflammatory drugs diclofenac, naproxen and ibuprofen are found in the bile of wild fish caught downstream of a wastewater treatment plant. *Environmental Science and Technology*, 47(1), 342-348.
- [167] Mallick, S., Chattopadhyay, H., De, A., Datta, S. (2017). A comparative study of two separate analytical techniques for the simultaneous determination of diclofenac sodium and diacerein from combined dosage form. *Brazilian Journal of Pharmaceutical Sciences*, 53(2).

- [168] Montemurro, N., Postigo, C., Chirón, S., Barcelò, D., Pérez, S. (2019). Analysis and fate of 14 relevant wastewater-derived organic pollutants in long-term exposed soil. *Analytical and Bioanalytical Chemistry*.
- [169] Rashid, A., Wang, Y., Li, Y., Yu, C., Sun, Q. (2019). Simultaneous analysis of multiclass contaminants of emerging concern in sediments by liquid chromatography with tandem quadrupole mass spectrometry. *Environmental Toxicology and Chemistry*, 38(7), 1409-1422.
- [170] Miossec, C., Lanceleur, L., Monperrus, M. (2019). Multi-residue analysis of 44 pharmaceutical compounds in environmental water samples by solid-phase extraction coupled to liquid chromatography-tandem mass spectrometry. *Journal of Separation Science*, 42(10), 1853-1866.
- [171] Campos-Mañas, M., Plaza-Bolaños, P., Sánchez-Pérez, J., Malato, S., Agüera, A. (2017). Fast determination of pesticides and other contaminants of emerging concern in treated wastewater using direct injection coupled to highly sensitive ultra-high performance liquid chromatography-tandem mass spectrometry. *Journal of Chromatography A*, 1507, 84-94.
- [172] Yilmaz, B., Sahin, H., Erdem, A. (2014). Determination of naproxen in human plasma by GC-MS. *Journal of Separation Science*, 37(8), 997-1003.
- [173] Kotowska, U., Kapelewska, J., Sturgulewska, J. (2014). Determination of phenols and pharmaceuticals in municipal wastewaters from Polish treatment plants by ultrasound-assisted emulsification-microextraction followed by GC-MS. *Environmental Science and Pollution Research*, 21(1), 660-673.
- [174] Rodrigues, J., Albino, S., Silva, S., Cravo, A., Cardoso, V., Benoliel, M., Almeida, C. (2019). Development of a Multiresidue Method for the Determination of 24 Pharmaceuticals in Clams by QuEChERS and Liquid Chromatography-Triple Quadrupole Tandem Mass Spectrometry. *Food Analytical Methods*.
- [175] Díaz, A., Peña-Alvarez, A. (2017). A Simple Method for the Simultaneous Determination of Pharmaceuticals and Personal Care Products in River Sediment by Ultrasound-Assisted Extraction Followed by Solid-Phase Microextraction Coupled with Gas Chromatography–Mass Spectrometry. *Journal of Chromatographic Science*, 55(9), 946-953.

- [176] Javid, A., Nasser, S., Mesdaghinia, A., Hossein Mahvi, A., Alimohammadi, M., Mehdiavaz Aghdam, R., Rastkari, N. (2013). Performance of photocatalytic oxidation of tetracycline in aqueous solution by TiO₂ nanofibers. *Journal of Environmental Health Sciences, Engineering*, 11(1), 24.
- [177] Safari, G., Hoseini, M., Seyedsalehi, M., Kamani, H., Jaafari, J., Mahvi, A. (2014). Photocatalytic degradation of tetracycline using nanosized titanium dioxide in aqueous solution. *International Journal of Environmental Science and Technology*, 12(2), 603-616.
- [178] Safari, G., Nasser, S., Mahvi, A., Yaghmaeian, K., Nabizadeh, R., Alimohammadi, M. (2015). Optimization of sonochemical degradation of tetracycline in aqueous solution using sono-activated persulfate process. *Journal of Environmental Health Science and Engineering*, 13(1).
- [179] Bagheri, A., Mahvi, A., Nabizadeh, R., Dehghani, M., Mahmoudi, B., Akbari-Adergani, B., Yaghmaeian, K. (2017). Rapid destruction of the non-steroidal anti-inflammatory drug Diclofenac using advanced Nano-Fenton process in aqueous solution. *edica Mediterranea*, 33(5), 879-883.
- [180] Ahmed, M. J., Hameed, B. H. (2018). Removal of emerging pharmaceutical contaminants by adsorption in a fixed-bed column: A review. *Ecotoxicology and Environmental Safety*, 149, 257-266.
- [181] Ali, I., Gupta, V. (2007). Advances in water treatment by adsorption technology. *Nature Protocols*, 1(6), 2661-2667.
- [182] Premarathna, K., Rajapaksha, A., Adassoriya, N., Sarkar, B., Sirimuthu, N., Cooray, A., Vithanage, M. (2019). Clay-biochar composites for sorptive removal of tetracycline antibiotic in aqueous media. *Journal of Environmental Management*, 238, 315-322.
- [183] De Carvalho Eufrásio Pinto, M., Gonçalves, R., Dos Santos, R., Araújo, E., Perotti, G., Dos Santos Macedo, R., Tronto, J. (2016). Mesoporous carbon derived from a biopolymer and a clay: Preparation, characterization and application for an organochlorine pesticide adsorption. *Microporous and Mesoporous Materials*, 225, 342-354.

- [184] Rakić, V., Rac, V., Krmar, M., Otman, O., Auroux, A. (2015). The adsorption of pharmaceutically active compounds from aqueous solutions onto activated carbons. *Journal of Hazardous Materials*, 282, 141-149.
- [185] De Ridder, D., Verberk, J., Heijman, S., Amy, G., Van Dijk, J. (2012). Zeolites for nitrosamine and pharmaceutical removal from demineralised and surface water: Mechanisms and efficacy. *Separation and Purification Technology*, 89, 71-77.
- [186] Zheng, S., Li, X., Zhang, X., Wang, W., Yuan, S. (2017). Effect of inorganic regenerant properties on pharmaceutical adsorption and desorption performance on polymer anion exchange resin. *Chemosphere*, 182, 325-331.
- [187] Worch, E., Eckhard, A. (2012). *Adsorption Technology in Water Treatment*.
- [188] Nam, S., Jung, C., Li, H., Yu, M., Flora, J., Boateng, L., Yoon, Y. (2015). Adsorption characteristics of diclofenac and sulfamethoxazole to graphene oxide in aqueous solution. *Chemosphere*, 136, 20-26.
- [189] Cai, N., Larese-Casanova, P. (2014). Sorption of carbamazepine by commercial graphene oxides: A comparative study with granular activated carbon and multiwalled carbon nanotubes. *Journal of Colloid and Interface Science*, 426, 152-161.
- [190] Mohammadi Nodeh, M., Radfard, M., Zardari, L., Rashidi Nodeh, H. (2018). Enhanced removal of naproxen from wastewater using silica magnetic nanoparticles decorated onto graphene oxide; parametric and equilibrium study. *Separation Science and Technology (Philadelphia)*, 53(15), 2476-2485.
- [191] Zambianchi, M., Durso, M., Liscio, A., Treossi, E., Bettini, C., Capobianco, M., Melucci, M. (2017). Graphene oxide doped polysulfone membrane adsorbers for the removal of organic contaminants from water. *Chemical Engineering Journal*, 326, 130-140.
- [192] Jauris, I., Matos, C., Saucier, C., Lima, E., Zarbin, A., Fagan, S., Zanella, I. (2016). Adsorption of sodium diclofenac on graphene: A combined experimental and theoretical study. *Physical Chemistry Chemical Physics*, 18(3), 1526-1536.
- [193] Ncibi, M., Sillanpää, M. (2017). Optimizing the removal of pharmaceutical drugs Carbamazepine and Dorzolamide from aqueous solutions using mesoporous activated carbons and multi-walled carbon nanotubes. *Journal of Molecular Liquids*, 238, 379-388.

- [194] Baccar, R., Sarrà, M., Bouzid, J., Feki, M., Blánquez, P. (2012). Removal of pharmaceutical compounds by activated carbon prepared from agricultural by-product. *Chemical Engineering Journal*, 211-212, 310-317.
- [195] Song, J., Bhadra, B., Jhung, S. (2017). Contribution of H-bond in adsorptive removal of pharmaceutical and personal care products from water using oxidized activated carbon. *Microporous and Mesoporous Materials*, 243, 221-228.
- [196] Wilhelm, S., Henneberg, A., Köhler, H., Rault, M., Richter, D., Scheurer, M., Triebkorn, R. (2017). Does wastewater treatment plant upgrading with activated carbon result in an improvement of fish health? *Aquatic Toxicology*, 192, 184-197.
- [197] Rigobello, E., Dantas, A., Di Bernardo, L., Vieira, E. (2013). Removal of diclofenac by conventional drinking water treatment processes and granular activated carbon filtration. *Chemosphere*, 92(2), 184-191.
- [198] Al-Ghouti, M. A., Da'ana, D., Abu-Dieyeh, M., Khraisheh, M. (2019). Adsorptive removal of mercury from water by adsorbents derived from date pits. *Scientific Reports*, 9(1).
- [199] Hiew, B., Lee, L., Lee, X., Gan, S., Thangalazhy-Gopakumar, S., Lim, S., Yang, T. (2019). Adsorptive removal of diclofenac by graphene oxide: Optimization, equilibrium, kinetic and thermodynamic studies. *Journal of the Taiwan Institute of Chemical Engineers*, 98, 150-162.
- [200] Husein, D., Hassanien, R., Al-Hakkani, M. (2019). Green-synthesized copper nano-adsorbent for the removal of pharmaceutical pollutants from real wastewater samples. *Heliyon*, 5(8).
- [201] Katsigiannis, A., Noutsopoulos, C., Mantziaras, J., Gioldasi, M. (2015). Removal of emerging pollutants through Granular Activated Carbon. *Chemical Engineering Journal*, 280, 49-57.
- [202] Jung, C., Boateng, L., Flora, J., Oh, J., Braswell, M., Son, A., Yoon, Y. (2015). Competitive adsorption of selected non-steroidal anti-inflammatory drugs on activated biochars: Experimental and molecular modeling study. *Chemical Engineering Journal*, 264, 1-9.
- [203] Stoykova, M., Koumanova, B. (2013). adsorptive removal of carbamazepine from wastewaters by activated charcoals .

- [204] Mestre, A., Pires, J., Nogueira, J., Carvalho, A. (2007). Activated carbons for the adsorption of ibuprofen. *Carbon*, 45(10), 1979-1988.
- [205] Torrellas, S., García Lovera, R., Escalona, N., Sepúlveda, C., Sotelo, J., García, J. (2015). Chemical-activated carbons from peach stones for the adsorption of emerging contaminants in aqueous solutions. *Chemical Engineering Journal*, 279, 788-798.
- [206] Sharma, P. K., Wankat, P. C. (2010). Solvent Recovery by Steamless Temperature Swing Carbon Adsorption Processes. *Industrial, Engineering Chemistry Research*, 49(22), 11602-11613.
- [207] Ali, S., El-Shafey, E., Al-Busafi, S., Al-Lawati, H. (2019). Adsorption of chlorpheniramine and ibuprofen on surface functionalized activated carbons from deionized water and spiked hospital wastewater. *Journal of Environmental Chemical Engineering*, 7(1).
- [208] Saucier, C., Adebayo, M., Lima, E., Cataluña, R., Thue, P., Prola, L., Dotto, G. (2015). Microwave-assisted activated carbon from cocoa shell as adsorbent for removal of sodium diclofenac and nimesulide from aqueous effluents. *Journal of Hazardous Materials*, 289, 18-27.
- [209] Ahmed, M., Zhou, J., Ngo, H., Guo, W., Chen, M. (2016). Progress in the preparation and application of modified biochar for improved contaminant removal from water and wastewater. *Bioresource Technology*, 214, 836-851.
- [210] Yu, F., Li, Y., Han, S., Ma, J. (2016). Adsorptive removal of antibiotics from aqueous solution using carbon materials. *Chemosphere*, 153, 365-385.
- [211] de Franco, M., de Carvalho, C., Bonetto, M., de Pelegrini Soares, R., Féris, L. (2018). Diclofenac removal from water by adsorption using activated carbon in batch mode and fixed-bed column: Isotherms, thermodynamic study and breakthrough curves modeling. *Journal of Cleaner Production*, 181, 145-154.
- [212] Patel, H. (2019). Fixed-bed column adsorption study: a comprehensive review. *Applied Water Science*, 9(3).
- [213] Yang, Y., Ok, Y., Kim, K., Kwon, E., Tsang, Y. (2017). Occurrences and removal of pharmaceuticals and personal care products (PPCPs) in drinking water and water/sewage treatment plants: A review. *Science of the Total Environment*, 596-597, 303-320.

- [214] Gautam, R., Chattopadhyaya, M. (2016). Kinetics and Equilibrium Isotherm Modeling: Graphene-Based Nanomaterials for the Removal of Heavy Metals From Water. *Nanomaterials for Wastewater Remediation*, 79-109.
- [215] Khezami, L., Chetouani, A., Taouk, B., Capart, R. (2005). Production and characterization of activated carbon from wood components in powder: Cellulose, lignin, xylan. *Powder Technology*, 157(1-3), 48-56.
- [216] Theydan, S. K., Ahmed, M. J. (2012). Optimization of preparation conditions for activated carbons from date stones using response surface methodology. *Powder Technology*, 224, 101-108.
- [217] Snyder, S. A., Adham, S., Redding, A. M., Cannon, F. S., DeCarolis, J., Oppenheimer, J., Yoon, Y. (2007). Role of membranes and activated carbon in the removal of endocrine disruptors and pharmaceuticals. *Desalination*, 202(1-3), 156-181.
- [218] Pal, P. (2017). Physicochemical Treatment Technology. *Industrial Water Treatment Process Technology*, 145-171.
- [219] Sotelo, J. L., Rodríguez, A., Álvarez, S., García, J. (2012). Removal of caffeine and diclofenac on activated carbon in fixed bed column. *Chemical Engineering Research and Design*, 90(7), 967-974.
- [220] Jedynek, K., Szczepanik, B., Rędzia, N., Słomkiewicz, P., Kolbus, A., Rogala, P. (2019). Ordered Mesoporous Carbons for Adsorption of Paracetamol and Non-Steroidal Anti-Inflammatory Drugs: Ibuprofen and Naproxen from Aqueous Solutions. *Water*, 11(5), 1099.
- [221] Delgado, L. F., Charles, P., Glucina, K., Morlay, C. (2012). The removal of endocrine disrupting compounds, pharmaceutically activated compounds and cyanobacterial toxins during drinking water preparation using activated carbon—A review. *Science of The Total Environment*, 435-436, 509-525.
- [222] Dickenson, E. R. V., Drewes, J. E. (2010). Quantitative structure property relationships for the adsorption of pharmaceuticals onto activated carbon. *Water Science and Technology*, 62(10), 2270-2276.
- [223] Delgado, N.Y., Capparelli, A.L., Marino, D.J., Navarro, A.F., Peñuela, G.A., Ronco, A.E. (2016) Adsorption of pharmaceuticals and personal care products on granular activated carbon. *J. Surf. Eng. Mater. Adv. Technol*, 6 183-200.

- [224] Kårelid, V., Larsson, G., Björleinius, B. (2017). Pilot-scale removal of pharmaceuticals in municipal wastewater: Comparison of granular and powdered activated carbon treatment at three wastewater treatment plants. *Journal of Environmental Management*, 193, 491-502.
- [225] Yu, Z., Peldszus, S., Huck, P. M. (2008). Adsorption characteristics of selected pharmaceuticals and an endocrine disrupting compound—Naproxen, carbamazepine and nonylphenol—on activated carbon. *Water Research*, 42(12), 2873-2882.
- [226] Lach, J., Szymonik A. (2019). Adsorption of Naproxen Sodium from Aqueous Solutions on Commercial Activated Carbons. *Journal of Ecological Engineering*, 20 (10), 241-251.
- [227] Gao, N., Bo L., Liu, J., Zhao, P., Feng, Q., Tan; N. (2016). Adsorption characteristics of granular activated carbon to typical pharmaceuticals in water, *Chinese Journal of Environmental Engineering*, 08.
- [228] Larous, S., Meniai, A.-H. (2016). Adsorption of Diclofenac from aqueous solution using activated carbon prepared from olive stones. *International Journal of Hydrogen Energy*, 41(24), 10380-10390.
- [229] Chang, E., Wan, J., Kim, H., Liang, C., Dai, Y., Chiang, P. (2015). Adsorption of selected pharmaceutical compounds onto activated carbon in dilute aqueous solutions exemplified by acetaminophen, diclofenac, and sulfamethoxazole. *Scientific World Journal*, 2015.
- [230] Bo, L., Gao, N., Liu, J., Gao, B. (2015). The competitive adsorption of pharmaceuticals on granular activated carbon in secondary effluent. *Desalination and Water Treatment*, 1-7.
- [231] Sabio, E., Zamora, F., Gañan, J., González-García, C.M., González, J.F. (2006). Adsorption of p-nitrophenol on activated carbon fixed-bed. *Water Res.* 40, 3053-60.
- [232] Bhadra, B. N., Seo, P. W., Jhung, S. H. (2016). Adsorption of diclofenac sodium from water using oxidized activated carbon. *Chemical Engineering Journal*, 301, 27-34.
- [233] Ahmed, M. J. (2017). Adsorption of non-steroidal anti-inflammatory drugs from aqueous solution using activated carbons: Review. *Journal of Environmental Management*, 190, 274-282.

- [234] Gautam, R., Rawat, V., Banerjee, S., Sanroman, M., Soni, S., Singh, S., Chattopadhyaya, M. (2015). Synthesis of bimetallic Fe-Zn nanoparticles and its application towards adsorptive removal of carcinogenic dye malachite green and Congo red in water. *Journal of Molecular Liquids*, 212, 227-236.
- [235] Fallou, H., Cimetière, N., Giraudet, S., Wolbert, D., Le Cloirec, P. (2016). Adsorption of pharmaceuticals onto activated carbon fiber cloths – Modeling and extrapolation of adsorption isotherms at very low concentrations. *Journal of Environmental Management*, 166, 544-555.
- [236] Chen, D., Xie, S., Chen, C., Quan, H., Hua, L., Luo, X., Guo, L. (2017). Activated biochar derived from pomelo peel as a high-capacity sorbent for removal of carbamazepine from aqueous solution. *RSC Advances*, 7(87), 54969-54979.
- [237] Yu, Z., Peldszus, S., Huck, P. M. (2008). Adsorption characteristics of selected pharmaceuticals and an endocrine disrupting compound—Naproxen, carbamazepine and nonylphenol—on activated carbon. *Water Research*, 42(12), 2873-2882.
- [238] Akhtar, J., Amin, N., Shahzad, K. (2016). A review on removal of pharmaceuticals from water by adsorption. *Desalination and Water Treatment*, 57(27), 12842-12860.
- [239] Lin, S., Juang, R. (2009. 3). Adsorption of phenol and its derivatives from water using synthetic resins and low-cost natural adsorbents: A review. *Journal of Environmental Management*, 90(3), 1336-1349.
- [240] Robberson, K., Waghe, A., Sabatini, D., Butler, E. (2006). Adsorption of the quinolone antibiotic nalidixic acid onto anion-exchange and neutral polymers. *Chemosphere*, 63(6), 934-941.
- [241] Scordino, M., Di Mauro, A., Passerini, A., Maccarone, E. (2003). Adsorption of Flavonoids on Resins: Hesperidin. *Journal of Agricultural and Food Chemistry*, 51(24), 6998-7004.
- [242] Soto, M., Moure, A., Domínguez, H., Parajó, J. (2017). Batch and fixed bed column studies on phenolic adsorption from wine vinasses by polymeric resins. *Journal of Food Engineering*, 209, 52-60.
- [243] Baker, H., Massadeh, A., Younes, H. (2009). Natural Jordanian zeolite: Removal of heavy metal ions from water samples using column and batch methods. *Environmental Monitoring and Assessment*, 157(1-4), 319-330.

- [244] Cejka, J., van Bekkum, H., Corma, A., Schueth, F. (2007). Introduction to zeolite science and practice, Studies in Surface Science and Catalysis, 168, third ed.
- [245] Akimkhan., A. M. (2012). Structural and Ion-Exchange Properties of Natural Zeolite, Ion Exchange Technologies, Ayben Kilislioğlu, IntechOpen.
- [246] Martucci, A., Pasti, L., Marchetti, N., Cavazzini, A., Dondi, F., Alberti, A. (2012). Adsorption of pharmaceuticals from aqueous solutions on synthetic zeolites. Microporous and Mesoporous Materials, 148(1), 174-183.
- [247] Townsend, R.P., Coker, E.N. (2001) Ion exchange in zeolites. Stud. Surf. Sci. Catal. 137, 467–524.
- [248] Ötker, H., Akmehmet-Balcioğlu, I. (2005). Adsorption and degradation of enrofloxacin, a veterinary antibiotic on natural zeolite. Journal of Hazardous Materials, 122(3), 251-258.
- [249] Lee, B. (2012) Removal of antibiotics from contaminated waters using natural zeolite. City University of New York (CUNY) CUNY Academic Works.
- [250] Behera, S., Oh, S., Park, H. (2012). Sorptive removal of ibuprofen from water using selected soil minerals and activated carbon. International Journal of Environmental Science and Technology, 9(1), 85-94.
- [251] Blasioli, S., Martucci, A., Paul, G., Gigli, L., Cossi, M., Johnston, C. T., Braschi, I. (2014). Removal of sulfamethoxazole sulfonamide antibiotic from water by high silica zeolites: A study of the involved host–guest interactions by a combined structural, spectroscopic, and computational approach. Journal of Colloid and Interface Science, 419, 148-159.
- [252] Al-rimawi, F., Daana, M., Khamis, M., Karaman, R., Khoury, H., Qurie, M. (2018). Removal of Selected Pharmaceuticals from Aqueous Solutions Using Natural Jordanian Zeolite. Arabian Journal for Science and Engineering.
- [253] Salem Attia, T. M., Hu, X. L., Yin, D. Q. (2013). Synthesized magnetic nanoparticles coated zeolite for the adsorption of pharmaceutical compounds from aqueous solution using batch and column studies. Chemosphere, 93(9), 2076-2085.
- [254] Rossner, A., Snyder, S., Knappe, D. (2009). Removal of emerging contaminants of concern by alternative adsorbents. Water Research, 43(15), 3787-3796.

- [255] Knappe, D.R.U., Rossner, A.; Snyder, S.A., Strickland, C. (2007). Alternative Adsorbents for the Removal of Polar Organic Contaminants. American Water Works Association Research Foundation: Denver, Colorado.
- [256] Braschi, I., Blasioli, S., Gigli, L., Gessa, C. E., Alberti, A., Martucci, A. (2010). Removal of sulfonamide antibiotics from water: Evidence of adsorption into an organophilic zeolite Y by its structural modifications. *Journal of Hazardous Materials*, 178(1-3), 218-225.
- [257] Cabrera-Lafaurie, W. A., Román, F. R., Hernández-Maldonado, A. J. (2014). Removal of salicylic acid and carbamazepine from aqueous solution with Y-zeolites modified with extraframework transition metal and surfactant cations: Equilibrium and fixed-bed adsorption. *Journal of Environmental Chemical Engineering*, 2(2), 899-906.
- [258] Suna, K., Shia, Y., Wang, X., Li, Z. (2017). Sorption and retention of diclofenac on zeolite in the presence of cationic surfactant. *J. Hazard. Mater.* 323, 584-592.
- [259] Treybal, R.E. (1981). *Mass-Transfer Operations*, 3rd Ed. McGraw-Hill, Tokyo.
- [260] Shahbeig, H., Bagheri, N., Ghorbanian, S., Hallajisani, A., Poorkarimi, S. (2013). A new adsorption isotherm model of aqueous solutions on granular activated carbon,” *World Journal of Modelling and Simulation*, vol. 9, no. 4, pp. 243-254.
- [261] Ringot, D., Lerzy, B., Chaplain, K., Bonhoure, J., AUCLAIR, E., LARONDELLE, Y. (2007). In vitro biosorption of ochratoxin A on the yeast industry by-products: Comparison of isotherm models. *Bioresource Technology*, 98(9), 1812-1821.
- [262] Dubinin, M. M., Zaverina, E. D., Radushkevich, L. V. (1947). Sorption and Structure of Active Carbons I. Adsorption of Organic Vapors, *Zhurnal Fizicheskoi Khimii*, 21, 1351-1362.
- [263] Günay, A., Arslankaya, E., Tosun, I. (2007). Lead removal from aqueous solution by natural and pretreated clinoptilolite: Adsorption equilibrium and kinetics. *Journal of Hazardous Materials*, 146(1-2), 362-371.
- [264] Qiu, H., Lv, L., Pan, B., Zhang, Q., Zhang, W., Zhang, Q. (2009). Critical review in adsorption kinetic models. *Journal of Zhejiang University: Science A*, 10(5), 716-724.
- [265] Ho, Y., McKay, G. (1999). Pseudo-second order model for sorption processes.

- [266] Gerente, C., Lee, V., Le Cloirec, P., McKay, G. (2007). Application of chitosan for the removal of metals from wastewaters by adsorption - Mechanisms and models review. *Critical Reviews in Environmental Science and Technology*, 37(1), 41-127.
- [267] Zhao, Y., Liu, F., Qin, X. (2017). Adsorption of diclofenac onto goethite: Adsorption kinetics and effects of pH. *Chemosphere*, 180, 373-378.
- [268] Domínguez-Vargas, J., Gonzalez, T., Palo, P., Cuerda-Correa, E. (2013). Removal of Carbamazepine, Naproxen, and Trimethoprim from Water by Amberlite XAD-7: A Kinetic Study. *Clean - Soil, Air, Water*, 41(11), 1052-1061.
- [269] Khazri, H., Ghorbel-Abid, I., Kalfat, R., Trabelsi-Ayadi, M. (2017). Removal of ibuprofen, naproxen and carbamazepine in aqueous solution onto natural clay: equilibrium, kinetics, and thermodynamic study. *Applied Water Science*, 7(6), 3031-3040.
- [270] İlbay, Z., Şahin, S., Kerkez., Bayazit, S. (2015). Isolation of naproxen from wastewater using carbon-based magnetic adsorbents. *International Journal of Environmental Science and Technology*, 12(11), 3541-3550.
- [271] Zhang, Z., Li, Y., Chen, H., Zhang, X., Li, H. (2018). The systematic adsorption of diclofenac onto waste red bricks functionalized with iron oxides. *Water (Switzerland)*, 10 (10).
- [272] Swarzewicz, M., Sobczak, J., Paździoch, W. (2013). Removal of carbamazepine from aqueous solution by adsorption on fly ash-amended soil. *Water Science and Technology*, 67(6), 1396-1402.
- [273] Thomas, J.M., Thomas, W.J., 1997. Principle and practice of heterogeneous catalysis. VCH, Weinheim.
- [274] Gubernak, M., Zapala, W., Tyrpien, K., Kaczmarski, K. (2004). Analysis of Amylbenzene Adsorption Equilibria on Different RP-HPLC. *Journal of Chromatographic Science*, 42(9), 457-463.
- [275] Rudzinski, W., Panczyk, T. (2000). Kinetics of isothermal adsorption on energetically heterogeneous solid surfaces: A new theoretical description based on the statistical rate theory of interfacial transport. *Journal of Physical Chemistry B*, 104(39), 9149-9162.
- [276] Shaarani, F., Hameed, B. (2010). Batch adsorption of 2,4-dichlorophenol onto activated carbon derived from agricultural waste. *Desalination*, 255(1-3), 159-164.

- [277] Robati, D. (2013). Pseudo-second-order kinetic equations for modeling adsorption systems for removal of lead ions using multi-walled carbon nanotube . *Journal of Nanostructure in Chemistry*, 3(1), 55.
- [278] Lima, E., Hosseini-Bandegharai, A., Moreno-Piraján, J., Anastopoulos, I. (2019). A critical review of the estimation of the thermodynamic parameters on adsorption equilibria. Wrong use of equilibrium constant in the Van't Hoof equation for calculation of thermodynamic parameters of adsorption. *Journal of Molecular Liquids*, 273, 425-434.
- [279] Lawal, I. A., Moodley, B. (2018). Fixed-Bed and Batch Adsorption of Pharmaceuticals from Aqueous Solutions on Ionic Liquid-Modified Montmorillonite. *Chemical Engineering., Technology*, 41(5), 983-993.
- [280] Sancho, J. L. S., Rodríguez, A. R., Torrellas, S. Á., Rodríguez, J. G. (2012). Removal of an emerging pharmaceutical compound by adsorption in fixed bed column. *Desalination and Water Treatment*, 45(1-3), 305-314.
- [281] Han, R., Wang, Y., Zou, W., Wang, Y., Shi, J. (2007). Comparison of linear and nonlinear analysis in estimating the Thomas model parameters for methylene blue adsorption onto natural zeolite in fixed-bed column. *Journal of Hazardous Materials*, 145(1-2), 331-335.
- [282] Sotelo, J. L., Ovejero, G., Rodríguez, A., Álvarez, S., Galán, J., García, J. (2014). Competitive adsorption studies of caffeine and diclofenac aqueous solutions by activated carbon. *Chemical Engineering Journal*, 240, 443-453.
- [283] Sotelo, J. L., Ovejero, G., Rodríguez, A., Álvarez, S., García, J. (2013). Adsorption of Carbamazepine in Fixed Bed Columns: Experimental and Modeling Studies. *Separation Science and Technology*, 48(17), 2626-2637.
- [284] Marzbali, M., Esmaili, M. (2017). Fixed bed adsorption of tetracycline on a mesoporous activated carbon: Experimental study and neuro-fuzzy modeling. *Journal of Applied Research and Technology*, 15(5), 454-463.
- [285] Benstoem, F., Nahrstedt, A., Boehler, M., Knopp, G., Montag, D., Siegrist, H., Pinnekamp, J. (2017). Performance of granular activated carbon to remove micropollutants from municipal wastewater—A meta-analysis of pilot- and large-scale studies. *Chemosphere*, 185, 105-118.

- [286] Deng, H., Li, Y., Wu, L., Ma, X. (2017). The novel composite mechanism of ammonium molybdophosphate loaded on silica matrix and its ion exchange breakthrough curves for cesium. *Journal of Hazardous Materials*, 324, 348-356.
- [287] Fadzil, F., Ibrahim, S., Hanafiah, M. (2016). Adsorption of lead(II) onto organic acid modified rubber leaf powder: Batch and column studies. *Process Safety and Environmental Protection*, 100, 1-8.
- [288] Mastral, A., Garcia, T., Murillo, R., Callen, M., Lopez, J., Navarro, M. (2002). Effects of CO₂ on the phenanthrene adsorption capacity of carbonaceous materials. *Energy and Fuels*, 16(2), 510-516.
- [289] Babaei, A. A., Kakavandi, B., Rafiee, M., Kalantarhormizi, F., Purkaram, I., Ahmadi, E., Esmaeili, S. (2017). Comparative treatment of textile wastewater by adsorption, Fenton, UV-Fenton and US-Fenton using magnetic nanoparticles-functionalized carbon (MNPs@C). *Journal of Industrial and Engineering Chemistry*, 56, 163-174.
- [290] Ahmadi, M., Hazrati Niari, M., Kakavandi, B. (2017). Development of maghemite nanoparticles supported on cross-linked chitosan (γ -Fe₂O₃@CS) as a recoverable mesoporous magnetic composite for effective heavy metals removal. *Journal of Molecular Liquids*, 248, 184-196.
- [291] Salimi, J., Kakavandi, B., Babaei, A. A., Takdastan, A., Alavi, N., Neisi, A., Ayoubi-Feiz, B. (2016). Modeling and optimization of nonylphenol removal from contaminated water media using a magnetic recoverable composite by artificial neural networks. *Water Science and Technology*, 75(8), 1761-1775.
- [292] Tylová, T., Flieger, M., Olšovská, J. (2013). Determination of antibiotics in influents and effluents of wastewater-treatment-plants in the Czech Republic – development and application of the SPE and a UHPLC-ToFMS method. *Analytical Methods*, 5(8), 2110.
- [293] Campos-Mañas, M. C., Plaza-Bolaños, P., Sánchez-Pérez, J. A., Malato, S., Agüera, A. (2017). Fast determination of pesticides and other contaminants of emerging concern in treated wastewater using direct injection coupled to highly sensitive ultra-high performance liquid chromatography-tandem mass spectrometry. *Journal of Chromatography A*, 1507, 84-94.

- [294] Kalanry, R.R., Jafari, A.J., Esrafil, A., Kakavandi, B., Gholizadeh, A., Azari, A. (2015). Optimization and evaluation of reactive dye adsorption on magnetic composite of activated carbon and iron oxide. *Desalination and Water Treatment*, 57, 6411-6422.
- [295] Kinney, C.A., Furlong, E.T., Werner, S.L., and Cahill, J.D., 2006, Presence and distribution of wastewater-derived pharmaceuticals in soil irrigated with reclaimed water: *Environmental Toxicology and Chemistry*, v. 25, no. 2, p. 317-326,
- [296] Al-rimawi Fuad, Daana, M., Khamis, M., Karaman, R., Khoury, H., & Qurie, M. (2018). Removal of Selected Pharmaceuticals from Aqueous Solutions Using Natural Jordanian Zeolite. *Arabian Journal for Science and Engineering*.

EÖTVÖS LORÁND UNIVERSITY
DECLARATION FORM
for disclosure of a doctoral dissertation

I. The data of the doctoral dissertation:

Name of the author: **ELAbadsa Mohammed**

MTMT-identifier: **10072485**

Title and subtitle of the doctoral dissertation: **Removal of selected pharmaceuticals from aqueous matrices with activated carbon**

DOI-identifier⁷²: **10.15476/ELTE.2020.049**

Name of the doctoral school: **Doctoral School of Environmental Sciences**

Name of the doctoral programme: **Environmental Chemistry Doctoral Programme**

Name and scientific degree of the supervisor: **Dr. Viktor Gábor Mihucz, associate professor**

Workplace of the supervisor: **Department of Analytical Chemistry, Institute of Chemistry ELTE – Eötvös Loránd University**

II. Declarations

1. As the author of the doctoral dissertation,⁷³

a) I agree to public disclosure of my doctoral dissertation after obtaining a doctoral degree in the storage of ELTE Digital Institutional Repository. I authorize the administrator of the Department of Doctoral, Habilitational and International Affairs of the Dean's Office of the Faculty of Science to upload the dissertation and the abstract to ELTE Digital Institutional Repository, and I authorize the administrator to fill all the declarations that are required in this procedure.

b) I request to defer public disclosure to the University Library and the ELTE Digital Institutional Repository until the date of announcement of the patent or protection. For details, see the attached application form;⁷⁴

c) I request in case the doctoral dissertation contains qualified data pertaining to national security, to disclose the doctoral dissertation publicly to the University Library and the ELTE Digital Institutional Repository ensuing the lapse of the period of the qualification process;⁷⁵

d) I request to defer public disclosure to the University Library and the ELTE Digital Institutional Repository, in case there is a publishing contract concluded during the doctoral procedure or up until the award of the degree. However, the bibliographical data of the work shall be accessible to the public. If the publication of the doctoral dissertation will not be carried out within a year from the award of the degree subject to the publishing contract, I agree to the public disclosure of the doctoral dissertation and abstract to the University Library and the ELTE Digital Institutional Repository.⁷⁶

2. As the author of the doctoral dissertation, I declare that

- a) the doctoral dissertation and abstract uploaded to the ELTE Digital Institutional Repository are entirely the result of my own intellectual work and as far as I know, I did not infringe anyone's intellectual property rights.;
- b) the printed version of the doctoral dissertation and the abstract are identical with the doctoral dissertation files (texts and diagrams) submitted on electronic device.
3. As the author of the doctoral dissertation, I agree to the inspection of the dissertation and the abstract by uploading them to a plagiarism checker software.

Budapest, 2020 April 15th

.....

Mohammed ELAbadsa

⁷² *Filled by the administrator of the faculty offices.*

⁷³ *The relevant part shall be underlined.*

⁷⁴ *Submitting the doctoral dissertation to the Disciplinary Doctoral Council, the patent or protection application form and the request for deferment of public disclosure shall also be attached.*

⁷⁵ *Submitting the doctoral dissertation, the notarial deed pertaining to the qualified data shall also be attached.*

⁷⁶ *Submitting the doctoral dissertation, the publishing contract shall also be attached.*